KTH Engineering Sciences

Consensus and Pursuit-Evasion in Nonlinear Multi-Agent Systems

JOHAN THUNBERG

Doctoral Thesis
Stockholm, Sweden 2014

TRITA-MAT-A 2014:04
ISRN KTH/MAT/A–14/04-SE
ISBN 978-91-7595-073-0

Optimization and Systems Theory
Department of Mathematics
Royal Institute of Technology
Se: 100 44 Stockholm, Sweden

Akademisk avhandling som med tillstånd av Kungl Tekniska Högskolan framlägges till offentlig granskning för avläggande av teknologie doktorsexamen, fredagen den 11 April 2014 klockan 10.00 i rum F3, Lindstedtsvägen 26, Kungl Tekniska Högskolan, Stockholm.

© Johan Thunberg, 2014

Print: Universitetsservice US AB

Abstract

Within the field of multi-agent systems theory, we study the problems of consensus and pursuit-evasion. In our study of the consensus problem, we first provide some theoretical results and then consider the problem of consensus on $SO(3)$ or attitude synchronization.

In Chapter 2, for agents with states in $\mathbb{R}^m$, we present two theorems along the lines of Lyapunov's second method that, under different conditions, guarantee asymptotic state consensus in multi-agent systems where the interconnection topologies are switching. The first theorem is formulated by using the states of the agents in the multi-agent system, whereas the second theorem is formulated by using the pairwise states for pairs of agents in the multi-agent system.

In Chapter 3, the problem of consensus on $SO(3)$ for a multi-agent system with directed and switching interconnection topologies is addressed. We provide two different types of kinematic control laws for a broad class of local representations of $SO(3)$. The first control law consists of a weighted sum of pairwise differences between positions of neighboring agents, expressed as coordinates in a local representation. The structure of the control law is well known in the consensus community for being used in systems of agents in the Euclidean space, and here we show that the same type of control law can be used in the context of consensus on $SO(3)$. In a later part of this chapter, based on the kinematic control laws, we introduce torque control laws for a system of rigid bodies in space and show that the system reaches consensus when these control laws are used.

Chapter 4 addresses the problem of consensus on $SO(3)$ for networks of uncalibrated cameras. Under the assumption that each agent uses a camera in order to measure its rotation, we prove convergence to the consensus set for two types of kinematic control laws, where only conjugate rotation matrices are available for the agents. In these conjugate rotations, the rotation matrix can be seen as distorted by the (unknown) intrinsic parameters of the camera. For the conjugate rotations we introduce distorted versions of well known local parameterizations of $SO(3)$ and show consensus by using control laws that are similar to the ones in Chapter 3, with the difference that the distorted local representations are used instead.

In Chapter 5, we study the output consensus problem for homogeneous systems of agents with linear continuous time-invariant dynamics. We derive control laws that solve the problem, while minimizing a cost functional of the control signal. Instead of considering a fixed communication topology for the system, we derive the optimal control law without any restrictions on the topology. We show that for all linear output controllable homogeneous systems, the optimal control law uses only relative information but requires the connectivity graph to be complete and in general requires measurements of the state errors. We identify cases where the optimal control law is only based on output errors.

In Chapter 6, we address the multi-pursuer version of the visibility pursuit-evasion problem in polygonal environments. By discretizing the problem and applying a Mixed Integer Linear Programming (MILP) framework, we are able to address problems requiring so-called recontamination and also impose additional constraints, such as connectivity between the pursuers. The proposed MILP formulation is less conservative than solutions based on graph discretizations of the environment, but still somewhat more conservative than the original underlying problem. It is well known that MILPs, as well as multi-pursuer pursuit-evasion problems, are NP-hard. Therefore we apply an iterative Receding Horizon Control (RHC) scheme, where a number of smaller MILPs are solved over shorter planning horizons. The proposed approach is illustrated by a number of solved examples.

Keywords: Multi-agent systems, consensus, attitude synchronization, nonlinear control, optimization, pursuit-evasion.

Sammanfattning

I denna avhandling betraktar vi konsensusproblem och avsökningsproblem i multiagent system. I vår studie av konsensusproblemet så presenterar vi först några teoretiska resultat, varefter vi studerar konsensusproblemet på $SO(3)$ där rotationsmatriser ska synkroniseras.

För agenter med tillsånd i $\mathbb{R}^m$ och där kommunikationen mellan agenterna är tidsberoende, presenterar vi i Kapitel 2, två teorem i linje med Lyapunovs andra metod som garanterar asymptotisk konsensus för tillstånden när tiden går mot oändligheten. De två teoremen kompletterar varandra såtillvida att det första är formulerat för de individuella tillstånden för agenterna, medan det andra är formulerat för par av individuella tillstånd för agenterna.

I Kapitel 3 betraktar vi konsensusproblemet på $SO(3)$, där kommunikationstopologierna är tidsberoende. För en stor klass av lokala representationer av $SO(3)$, presenterar vi två kinematiska styrlagar som löser problemet under olika antaganden. Den första styrlagen består av en viktad summa av parvisa differenser mellan positioner för agenter som är grannar med varandra. Denna typ av styrlag är vanligt förekommande inom konsensusfältet för system av agenter med tillstånd i det Euklidiska rummet. Här visar vi att denna typ av styrlag kan användas för att nästan globalt lösa konsensusproblemet på $SO(3)$. I den senare delen av detta kapitel så introducerar vi andra ordningens dynamik och löser konsensusproblemet för en viss typ av tidsbeorende kommunikation.

I Kapitel 4 betraktar vi konsensusproblemet på $SO(3)$ för nätverk av okalibrerade kameror. Under antagandet att alla agenter mäter sina rotationer genom att använda kameror, bevisar vi att systemet når konsensus för två typer av kinematiska styrlagar där endast de konjugerade rotationsmatriserna är tillgängliga för agenterna. Dessa konjugerade rotationsmatriser kan ses som förvrängda rotationsmatriser.

I Kapitel 5 studerar vi konsensusproblemet för homogena system av agenter med kontinuerlig tidsinvariant linjär dynamik. Vi formulerar en styrlag som löser problemet och samtidigt minimerar en kostnadsfunktion formulerad för styrlagen. Istället för att anta en viss kommunikationstopologi och sedan lösa problemet för denna topologi, så hittar vi den optimala styrlagen utan några restriktioner på topologin. Vi visar att om agenternas dynamik är sådan att utsignalen kan styras till godtyckligt värde så använder agenterna bara relativ information i styrlagen, dock måste kommunikationsgrafen vara fullständig.

I Kapitel 6 betraktar vi fallet med flera jägare ("pursuers") i ett avsökningsproblem i polygonmiljöer. Målet är att skapa en sökstrategi för ett minimalt antal robotar eller jägare som ska hitta en inkräktare på området, där inkräktaren känner till robotarnas positioner och kan röra sig godtyckligt fort. Genom att diskretisera problemet och lösa ett linjärt heltalsoptimeringsproblem, kan vi betrakta och lösa problem där sökstrategin kräver att redan avsökta områden måste sökas av igen. Vi kan också formulera krav på kommunikationen mellan agenterna. Sökstrategin för det nya diskreta problemet är en konservativ lösning till det ursprungliga problemet, men lösningen är inte lika konservativ som grafbaserade lösningsmetoder. Det är välkänt att heltalsoptimeringproblem är NP-svåra, därför använder vi oss av en iterativ lösningsmetod där vi i varje iteration löser ett delproblem för ett par tidssteg framåt i tiden.

Nyckelord: Multi-agent system, konsensus, konsensus för rotationsmatriser, ickelinjär styrning, optimering, avsökningsproblem.

Acknowledgments

First and foremost, I would like to express my gratitude to Professor Xiaoming Hu. As an advisor and co-author you have been excellent with your open door policy, your mathematical expertise and not the least your patience. Working with you has been a privilege, but not only working. You have a good sense of humor and during lunches you have been a great collocutor where the discussions have ranged from the small, domestic politics, to the large, foreign politics. I have always felt your wholehearted support.

The second person I would like to thank is my co-advisor, Associate Professor Petter Ögren. During my time at the Swedish Defence Research Agency (FOI) you and Doctor John Robinson were the ones who convinced me to follow the academic path. The material in Chapter 6 is a result of our collaboration. I regard you not only as a great advisor and researcher but also as a good friend.

Chapter 3 is a result of collaboration with Wenjung Song and Professor Yiguang Hong at Academy of Mathematics and Systems Science, Chinese Academy of Sciences in Beijing and Professor Eduardo Montijano at Centro Universitario de la Defensa in Zaragoza. Wenjung Song, collaborating with you was easy. Many of the results for the torque control laws in Chapter 3 were the outcome of our collaboration. Professor Yiguang Hong, during the autumn months I spent in Beijing, you were a great advisor and host, I felt very welcome. Professor Eduardo Montijano, I regard you as a great collaborator, with your sense for details and presentation. With your positive and outgoing persona you shed light in the Swedish winter darkness during your stay in Stockholm.

Several colleagues have contributed to the proofreading of the thesis. In addition to acknowledging my advisor Professor Xiaoming Hu, I would in particular like to thank Johan Markdahl, André Laestadius and Assistant Professor Johan Karlsson. Thank you for the time you spent and your constructive critique.

I would also like to thank the faculty members at the department. Thank you Professor Xiaoming Hu, Professor Anders Lindquist, Professor Anders Forsgren, Professor Krister Svanberg, Associate Professor Per Enqvist and Assistant Professor Johan Karlsson. You all contributed to the inspiring atmosphere that surrounded me during these years.

Furthermore, I would like to thank my colleagues of the present and the past for inspiring discussions. You are Johan Markdahl, André Laestadius, Göran Svensson, Hildur Æsa Oddsdóttir, Tove Odland, Yuecheng Yang, Henrik Svärd, Doctor Anders Möller, Doctor Albin Fredriksson, Doctor Ramsus Bokrantz, Doctor Corentin Briat, Doctor Mikael Fallgren and not the least Doctor David Alireza Anisi who was my advisor during my master's thesis project. In particular, I would also like to thank my office mates Doctor Anders Möller and Göran Svensson, you were both great office mates.

I want to thank my friends, especially Magnus and Thomas. Thank you guys for being such good friends, through all these years I have never questioned our friendship. I would like to thank my sister Linnea and my brother Peter for being there for me and express my deepest appreciation to my mother and my father for your unconditional support. Finally, thank you Hanna for moving from the rolling fields of canola in Scania to Stockholm, thank you for all the time we spend together.

Stockholm, March 2014

Johan Thunberg

Table of Contents

Abstract **iii**

Acknowledgments **vii**

Table of Contents **ix**

Reader's guide **xiii**

1 Introduction **1**
1.1 Convergence tools for consensus 2
1.2 Consensus on $SO(3)$ or attitude synchronization 3
1.3 Optimal output consensus control 7
1.4 Multi-robot pursuit-evasion 7
1.5 Bibliography 9

2 Convergence tools for consensus **13**
2.1 Preliminaries 14
2.1.1 Dynamics 15
2.1.2 Connectivity 17
2.1.3 Some special functions, sets and operators 18
2.1.4 Stability 19
2.2 Main results 22
2.3 Examples and interpretations 23
2.3.1 Non-convexity 23
2.3.2 Convexity 24
2.3.3 Nonlinear scaling 29
2.3.4 Avoiding discontinuities 30
2.3.5 Consensus on $SO(3)$ using the Axis-Angle Representation 30
2.3.6 Consensus on $SO(3)$ for networks of cameras using the epipoles . 31

2.3.7 Stabilization 34
2.4 Proofs 35
2.5 Bibliography 49

3 Consensus on $SO(3)$ or attitude synchronization for switching topologies 51
3.1 Preliminaries 53
3.2 Formulation and control design 57
3.3 Results for the first control law 59
3.4 Results for the second control law 61
3.5 Torque control laws 65
3.5.1 Static topologies 65
3.5.2 Dynamic topologies with continuous system dynamics 72
3.6 Formation control 74
3.7 Illustrative examples 75
3.8 Bibliography 78

4 Consensus on $SO(3)$ for networks of uncalibrated cameras using the conjugate rotations 81
4.1 Preliminaries 83
4.1.1 Camera model 83
4.1.2 Distorted rotations and conjugate rotations 84
4.1.3 Local distorted representations 85
4.1.4 Kinematics 87
4.2 Control design and results 88
4.2.1 Stability 88
4.2.2 Local consensus 89
4.2.3 Almost global consensus 94
4.3 Bibliography 95

5 Optimal output consensus control for systems of agents with continuous linear dynamics 97
5.1 Preliminaries 98
5.2 Finite time consensus 101
5.3 Extension to the asymptotic consensus problem 106
5.4 Bibliography 109

6 A mixed integer linear programming approach to pursuit-evasion problems with optional connectivity constraints 111
6.1 Problem formulation 112
6.2 Proposed solution 113
6.2.1 Discretization of the free space environment 113
6.2.2 MILP formulation 115
6.3 Reducing the computation times using RHC and relaxation 117
6.3.1 An RHC solution to the pursuit-evasion problem 118

6.3.2 Relaxation of the MILP problem 118
6.4 Decomposition of large environments 119
6.5 Connectivity constrained search 119
6.6 Simulation examples 120
6.7 Bibliography 129

Reader's guide

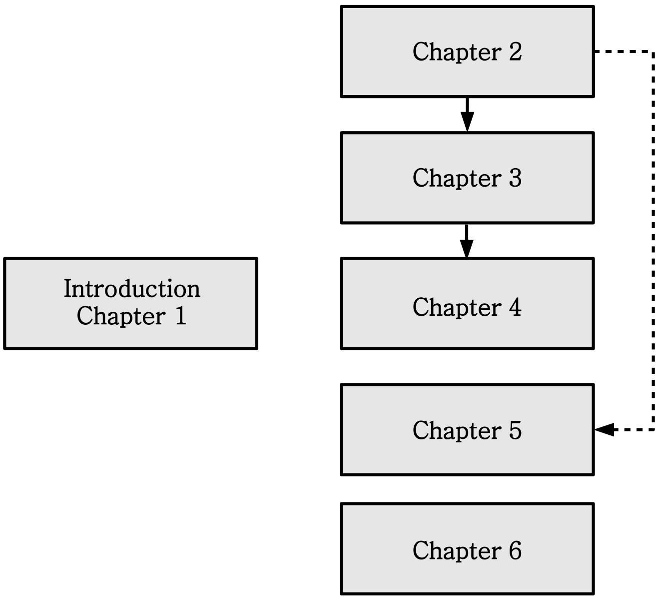

Figure 1: Illustration of the dependence between the chapters.

Except for reading the chapters in consecutive order, there are some alternative paths. In Figure 1, the dependence between the Chapters is illustrated. Chapter 6 is independent from the other chapters, but the results in Chapter 3-5 are dependent on the results in Chapter 2. The reader who chooses not to read the proofs in Chapter 3 can omit most parts of Chapter 2 with the exception of the first part of Section 2.1 where some notation is introduced which is being used in Chapter 3. In order to read Chapter 4 it is advised that Chapter 3 is read first. Chapter 5, even though being similar to Chapter 2-4 in terms on content, is almost independent of the other chapters. A suggestion is to read the introduction of Chapter 2 before reading Chapter 5.

Chapter 1

Introduction

The field of networked and multi-agent systems has received a growing interest from researchers within robotics and control theory during the last decade [1]. This increased attention to network science is partly due to the recent advancement of communication technologies such as cellular phones, the Internet, GPS, wireless sensor networks etc. The widespread use and ongoing development of such technologies is a testament to the great potential applicability of the work carried out within this research field.

The theme of this thesis is the study of collective behavior in multi-agent systems. A multi-agent system in this context is to be understood as a system or network of agents, where each agent has an associated dynamical equation describing its behavior in relation to itself, a subset of the other agents in the network and the environment. Within the field of multi-agent systems, we address the following subjects which are listed in the order appearance in the thesis.

1. **Convergence tools for consensus**,
   which is the subject of Chapter 2.

2. **Consensus on $SO(3)$ or attitude synchronization**,
   which is the subject of Chapter 3 and Chapter 4.

3. **Optimal output consensus control**,
   which is the subject of Chapter 5.

4. **Multi-robot pursuit-evasion**,
   which is the subject of Chapter 6.

Now we continue with a short introduction and overview of these four subjects, including summaries of the results that we provide.

1.1 Convergence tools for consensus

Consensus is a key problem in multi-agent systems theory and it has also been one of the main objects of attention [2–10]. Apparently, among all the collective behaviors in multi-agent systems, consensus is one of the simplest, while still important, behavior. To a large extent, the early works on consensus addressed only first or second order dynamics. For example, a pioneer work is the famous Vicsek model [11], in which a consensus scheme was proposed based on a simple discrete-time model for the headings of n autonomous agents moving in a plane. Theoretical explanations for the consensus behavior of the Vicsek model were given in [2, 4, 12]. In [3] the average-consensus problem of a first order multi-agent system with a strongly connected and balanced directed graph was solved. In [5, 6, 13, 14], to name a few, consensus for second order multi-agent systems is discussed. Various connectivity conditions are assumed in order to assure the consensus.

Due to the vast amount of publications, it is a challenge to provide a complete overview of the subject, and this introduction merely comprises a selection from the body of knowledge. There are books [1, 15], and surveys [16–19] covering the subject from different perspectives.

The problem of consensus or state agreement can roughly be explained as follows. Given a multi-agent system where each agent has a state in a space which is common for all the agents' states and where the state is updated according to a dynamic equation, design a distributed control law for the system such that the states of the agents converge to the same value. The convergence is usually defined in the asymptotic sense (as the time goes to infinity). The connectivity in a multi-agent system is represented by a graph. Each agent has a corresponding node in the graph and edges in the graph represent communication between agents.

In general, the dynamics for the agents can either be defined in discrete time [20,21] or continuous time [22]. This work considers continuous time dynamics. Furthermore, if the dynamics is linear, much of the work has centered around graph theoretic concepts such as the graph Laplacian matrix and its importance for the convergence of the states to the consensus set [1, 9, 23].

More general linear models have been used in for example [24–28]. In [28] the so called consensusability of linear time-invariant multi-agent systems is studied, where the admissible consensus protocol is based on static output feedback. In [29] a quite general linear model is considered, where the dynamics of each agent can be of any order. Recently, for homogeneous systems of agents with linear dynamics, the question of which properties must hold in order to guarantee consensus has been answered [30].

The type of multi-agent systems we consider in this work has n agents, where each agent i has a corresponding (unique) state $x_i \in \mathbb{R}^n$. Let $x = [x_1^T, \ldots, x_n^T]^T \in \mathbb{R}^{mn}$ comprise the state of the entire system and let $u = [u_1^T, \ldots, u_n^T]^T$ be a control signal or control law, where $u_i \in \mathbb{R}^p$. Except for the state, there is also an ordinary differential equation with corresponding initial conditions x_0 and t_0 that describes the system. This dynamical equation has the following structure

$$\begin{aligned}\dot{x}_1 &= f_1(t, x, u_1),\\ &\vdots\\ \dot{x}_n &= f_n(t, x, u_n),\end{aligned}$$

or written in a compact form as

$$\dot{x} = f(t, x, u). \tag{1.1}$$

In Chapter 2, we consider systems on the form

$$\dot{x} = f(t, x), \tag{1.2}$$

which can be seen as systems on the form (1.1) with the control signal chosen as a function of x and the time t.

If the system is in consensus, this means that the state of the system is contained in the following set

$$\mathcal{A} = \{x = [x_1^T, \ldots, x_n^T]^T \in \mathbb{R}^{mn} : x_i = x_j \text{ for all } i, j\}.$$

If the system (1.2) reaches consensus asymptotically, this means that $x(t)$ approaches the set $\mathcal{A}$ as the time t goes to infinity. More formally, for $\epsilon > 0$ there is T as a function of ϵ, the initial state and the time such that for for all $t \geq t_0 + T$ it holds that the distance between $x(t)$ and $\mathcal{A}$ is less than ϵ. The distance is defined as

$$\text{dist}(x, \mathcal{A}) = \inf_{y \in \mathcal{A}} \|x - y\|.$$

The convergence to the consensus set is illustrated in Figure 1.1, where a system of agents with positions in the plane asymptotically reach consensus in their positions.

The contribution of Chapter 2 is in essence two theorems. Provided certain conditions are fulfilled for the system, the theorems can be used to show consensus for the system. The theorems can be combined in order to show consensus under the convexity assumptions in [7, 31, 32]. However, as we show, there are examples when the convexity assumptions do not hold but where the proposed theorems can be used. These theorems will later be used in Chapter 3.

Among the examples that are treated in Chapter 2, two are based on the material in the journal papers [33] and [34] that are written by the author of this thesis together with his colleagues.

1.2 Consensus on $SO(3)$ or attitude synchronization

The second subject of this thesis is consensus on $SO(3)$ or attitude synchronization. Here each agent in the multi-agent system has a corresponding rotation matrix, defined in a common reference coordinate system (frame) and the objective is to synchronize or reach

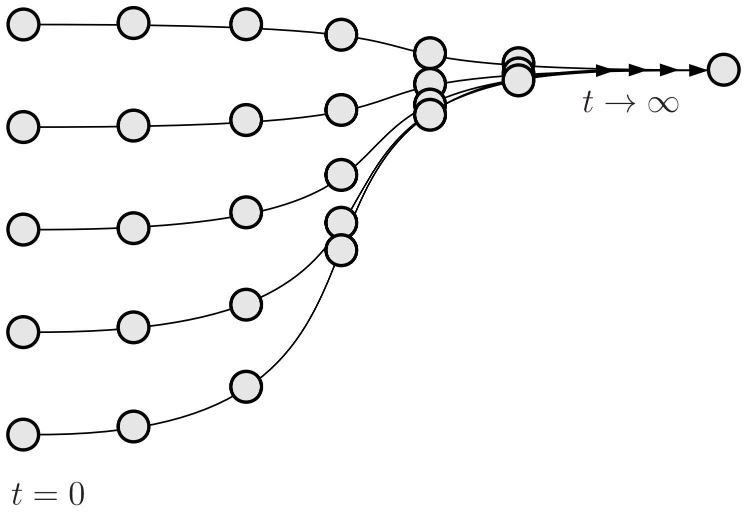

Figure 1.1: A system of five agents with states or positions in the plane reach asymptotic consensus in their states.

consensus in all these rotations. We are considering a system of n agents, each equipped with a matrix in the group of rotation matrices $SO(3)$. This matrix group is defined as follows,

$$SO(3) = \{R \in \mathbb{R}^{3\times 3} : R^T R = I, \det(R) = 1\}.$$

In real world applications, these rotation matrices represent the rotations of rigid bodies, *e.g.*, the rotation of a camera, or the rotation of a satellite in space. The problem is illustrated in Figure 1.2.

We assume that the control action can either be performed on a kinematic level, which results in a system of first order, or on a dynamic level, which results in a system of second order. The kinematics of R_i, the rotation matrix of agent i, is given by

$$\dot{R}_i = R_i \widehat{\omega}_i,$$

where ω_i, the control signal, is the angular velocity of agent i in the body frame of agent i. The matrix $\widehat{\omega}_i$ is the skew-symmetric matrix generated by the vector ω_i, *i.e.*, for $p =$

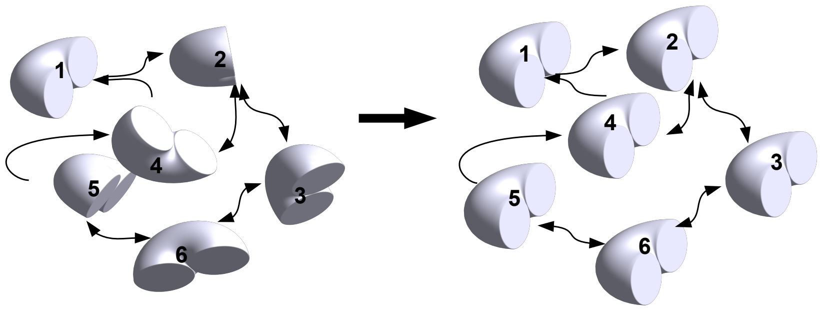

Figure 1.2: A multi-agent system with six agents and corresponding rigid bodies with unsynchronized rotations, left, shall synchronize (or reach consensus in) their rotations, right. In this figure the communication is illustrated by arrows. The direction of the arrows denote which agent receives information.

$[p_1, p_2, p_3]^T \in \mathbb{R}^3$ we have that

$$\widehat{p} = \begin{bmatrix} 0 & -p_3 & p_2 \\ p_3 & 0 & -p_1 \\ -p_2 & p_1 & 0 \end{bmatrix}.$$

When the control action is performed on a dynamic level, we design a control torque $\boldsymbol{\tau}_i$. In this case, the angular velocity is a state variable. The dynamical equation has the following structure.

$$\begin{aligned} \dot{R}_i &= R_i \widehat{\omega}_i, \\ J_i \dot{\omega}_i &= -\widehat{\omega}_i J_i \omega_i + \boldsymbol{\tau}_i, \end{aligned}$$

where J_i is the inertia matrix.

In general, the problem of designing a kinematic control law is a subproblem of the problem of designing a torque control law. A reason for anyway studying the former problem is that control laws in the robotics community often are specified on a kinematic level. The second order dynamic equations are platform dependent and differ between applications.

In Chapter 3, for a broad class of local representations of $SO(3)$ we first provide two conceptually different kinematic control laws that solve the consensus on $SO(3)$ problem for switching interconnection topologies. The first control law consists of a weighted sum of pairwise differences between positions of neighboring agents expressed as coordinates in the local representation. The structure of this control law is well known in the consensus community for agents in the Euclidean space with single integrator dynamics [1]. Here we show that the system reaches asymptotic consensus for any of the local representations of $SO(3)$ if the initial rotations are contained within the region for injectivity for the local representation and the interaction graph is uniformly strongly connected. The second control law is based on the relative rotations between neighboring agents, expressed in local coordinates. Under the stronger assumption that the initial rotations are contained in a strongly convex ball with radius smaller than half of the injectivety radius of the local representation, we show that the system reaches asymptotic consensus uniformly if and only if the interaction graph is uniformly quasi-strongly connected [31, 32].

In a later part of Chapter 3, based on the kinematic control laws, we introduce torque control laws that solve the attitude synchronization problem. In this part we first impose the stronger assumption of static graphs but the assumptions of strong and quasi-strong connectivity for said graphs remain. Furthermore, the allowed initial regions for the rotations when the torque control laws are used, are almost as large as when the corresponding kinematic control laws are used. For one torque control law we then allow for a certain type of switching behavior, where there is a continuous in time transition between functions that are time-invariant and Lipschitz continuous in the state. The material in Chapter 3 expands on the publications [33, 35, 36].

In Chapter 4, we solve the problem of consensus on $SO(3)$, where the exact rotations are not available for the agents. In this case we assume that each agent is equipped with a camera. We show that if the agents, instead of using a control law that is based on the rotation matrices, are using a control law that is based on the conjugate rotation matrices, the system will reach consensus in the rotations under quite general assumptions. The conjugate rotation matrices are certain distorted rotation matrices, where the distortion comes from the unknown camera calibration matrices.

The work in Chapter 4 is inspired by [34], where instead of using the rotation matrices in order to reach consensus in the rotations, the epipole vectors are used in the control laws. These epipole vectors lie in the nullspace of the so called fundamental matrix [37] that provides a geometric relationship between two images taken by a pinhole camera. In order to calculate the rotation matrix using camera measurements, one can first calculate the fundamental matrix and then from this matrix, provided the camera is calibrated, calculate the rotation matrix. If the camera is not calibrated, an often nontrivial calibration routine has to be used before the rotation matrix can be obtained. The idea in [34] was to bypass the calibration step and the calculation of the rotation matrix and use the epipoles obtained from the fundamental matrix directly in the control laws. The idea of bypassing the calibration step and the calculation of the rotation matrix is also the main theme in Chapter 4, however here we use the conjugate rotation matrix instead of the fundamental matrix. If a camera is rotating relative to a static scene, two images are related by a homography [37] and the conjugate rotation matrix can be obtained by solving a set of linear equations.

1.3 Optimal output consensus control

In Chapter 5 we study both the asymptotic output consensus problem and the finite-time output consensus problem for homogeneous systems of agents with linear continuous time-invariant dynamics. In the finite-time problem considered, the outputs of the agents shall be equal at some specified finite time, whereas in the asymptotic problem the difference between the outputs of the agents shall asymptotically converge to zero as the time goes to infinity. We derive control laws that solve the problems, while minimizing a cost function of the control signal. Instead of considering a fixed communication topology for the system, we derive the optimal control law without any restrictions on the topology. We show that for all linear output controllable homogeneous systems, the optimal control law uses only relative information but requires the connectivity graph to be complete and in general requires measurements of the state errors. We identify cases where the optimal control law is only based on output errors and in the asymptotic consensus problem we provide a dynamic control law based on the output errors. The control laws are given in closed form.

Instead of using Pontryagin's Minimum Principle (PMP) or dynamic programming in order to solve our problems, we use the Projection Theorem in order to solve the finite time problem. Using this result, we see that as the time goes to infinity, a matrix expression in the control law tends to a matrix satisfying an Algebraic Riccati Equation. By using this observation we can also provide a control law that optimally solves the asymptotic output consensus problem.

1.4 Multi-robot pursuit-evasion

In the last chapter, Chapter 6, the visibility based pursuit-evasion problem is addressed. This problem was first proposed by Suzuki and Yamashita [38] and later studied in *e.g.*, [39–48]. The problem is to find a search strategy for a group of pursuers in a planar environment with polygonal obstacles, such that an evader moving arbitrarily fast, and starting in an unknown location, will be captured no matter what path it decides to take. Captured in this context means that the evader is seen by a pursuer at some time. Here we consider the version of the problem where there are multiple pursuers trying to catch the evader. The group of pursuers comprises a multi-agent system and the problem is to design an algorithm so that this group is guaranteed to catch the evader. An illustration of the problem is provided in Figure 1.3. Note that the velocities of the pursuers are not necessarily constant and only the paths of the pursuers are illustrated in Figure 1.3.

The obvious applications of the pursuit-evasion problem is where security guards or robots are to clear an office, a warehouse, or a shop after closing time. However, search strategies of this type can also be used in search and rescue missions, or when looking for an item that might be moved by a non-adversarial agent in a larger area, such as a warehouse.

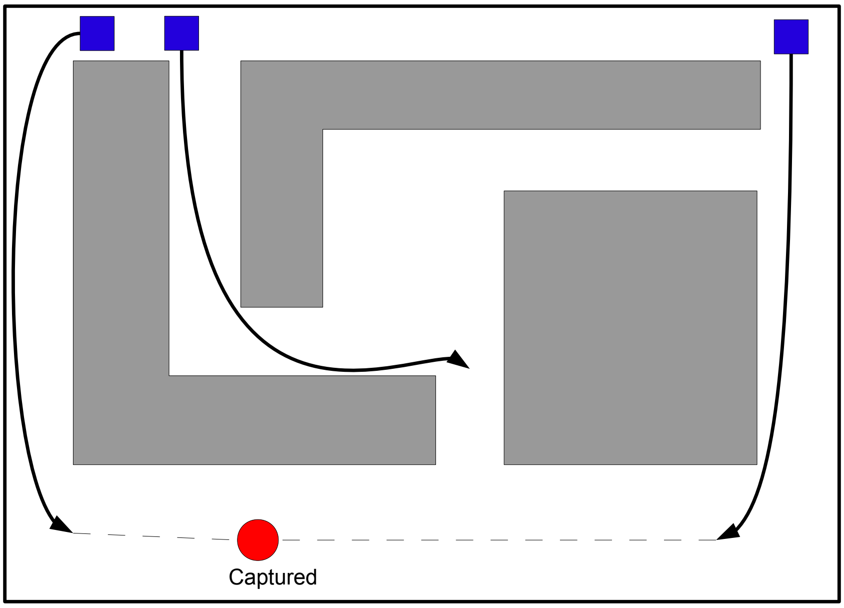

Figure 1.3: Three pursuers move from their initial positions, denoted by blue squares, in such a way that the evader, the red disc, cannot escape no matter what move strategy it decides to take. The evader is assumed to move along a continuous path and has no upper bound on its velocity.

In order to solve the problem, we discretize it in time and space and apply a Mixed Integer Linear Programming (MILP) framework, where we are able to address problems requiring so-called recontamination and also impose additional constraints, such as connectivity between the pursuers. The proposed MILP formulation is less conservative than solutions based on graph discretizations of the environment, but still somewhat more conservative than the original underlying problem. It is well known that MILPs, as well as multi-pursuer pursuit-evasion problems, are NP-hard. Therefore we apply an iterative Receding Horizon Control (RHC) scheme where a number of smaller MILPs are solved over shorter planning horizons.

The content of Chapter 6 is, up to subtleties, consistent with the material in [49].

1.5 Bibliography

[1] M. Mesbahi and M. Egerstedt. *Graph theoretic methods in multiagent networks*. Princeton University Press, 2010.

[2] J. Lin A. Jadbabaie and A. S. Morse. Coordination of groups of mobile autonomous agents using nearest neighbor rules. *IEEE Transactions on Automatic Control*, 48(6):988–1001, 2003.

[3] R. Olfati-Saber and R. Murray. Consensus problems in networks of agents with switching topology and time-delays. *IEEE Transactions on Automatic Control*, 49(9):1520–1533, 2004.

[4] W. Ren and R. W. Beard. Consensus seeking in multi-agent systems using dynamically changing interaction topologies. *IEEE Transactions on Automatic Control*, 50(5):655–661, 2005.

[5] R. Olfati-Saber. Flocking for multi-agent dynamic systems: algorithms and theory. *IEEE Transactions on Automatic Control*, 51(3):401–420, 2005.

[6] Y. Hong, L. Gao, D. Cheng and J. Hu. Lyapunov-based approach to multiagent systems with switching jointly connected interconnection. *IEEE Transactions on Automatic Control*, 52(5):943–948, 2007.

[7] L. Moreau. Stability of multiagent systems with time-dependent communication links. *IEEE Transactions on Automatic Control*, 50(2):169–182, 2005.

[8] R. Olfati-Saber, J.A. Fax and R.M. Murray. Consensus and cooperation in networked multi-agent systems. *Proceedings of the IEEE*, 95(1):215–233, 2007.

[9] R. Olfati-Saber and R. M. Murray. Consensus problems in networks of agents with switching topology and time-delays. *IEEE Transactions on Automatic Control*, 49(9):1520–1533, 2004.

[10] W. Ren and R. W. Beard. Consensus seeking in multiagent systems under dynamically changing interaction topologies. *IEEE Transactions on Automatic Control*, 50(5):655–661, 2005.

[11] T. Vicsek, A. Czirók, E. Ben-Jacob, I. Cohen and O. Shochet. Novel type of phase transition in a system of self-driven particles. *Phys. Rev. Letters.*, 75(6):1226–1229, 1995.

[12] Z. Liu and L. Guo. Connectivity and synchronization of vicsek's model. *Science in China*, 37(8):979–988, 2007.

[13] G. Xie and L. Wang. Consensus control for a class of networks of dynamic agents: switching topology. pages 1382–1387. 2006 American Control Conference, 2007.

[14] J. Wang, D. Cheng and X. Hu. An extension of LaSalle's invariance principle and its application to multi-agent consensus. 53(7):1765–1770, 2008.

[15] W. Ren and R.W. Beard. *Distributed consensus in multi-vehicle cooperative control: theory and applications*. Springer, 2008.

[16] F. Garin and L. Schenato. A survey on distributed estimation and control applications using linear consensus algorithms. In *Networked Control Systems*, pages 75–107. Springer, 2010.

[17] W. Ren, R. W. Beard and E.M. Atkins. A survey of consensus problems in multi-agent coordination. In *American Control Conference, 2005. Proceedings of the 2005*, pages 1859–1864. IEEE, 2005.

[18] J. Fax, R. Olfati-Saber and R. Murray. Consensus and cooperation in networked multi-agent systems. Proceeding of IEEE, 2007.

[19] R. Beard, W. Ren and E. Atkins. Information consensus in multivehicle cooperative control. pages 71–82, 2007.

[20] E. Montijano, J. I. Montijano and C. Sagues. Fast distributed consensus with chebyshev polynomials. In *American Control Conference (ACC), 2011*, pages 5450–5455. IEEE, 2011.

[21] L. Xiao, S. Boyd and S-J. Kim. Distributed average consensus with least-mean-square deviation. *Journal of Parallel and Distributed Computing*, 67(1):33–46, 2007.

[22] L. Moreau. Stability of continuous-time distributed consensus algorithms. In *IEEE Conference on Decision and Control*, volume 4, pages 3998–4003. IEEE, 2004.

[23] R. Olfati-Saber and R.M. Murray. Consensus protocols for networks of dynamic agents. In *Proceedings of the American Control Conference*, 2003.

[24] A. Fax and R. Murray. Information flow and cooperative control of vehicle formations. *IEEE Transactions on Automatic Control*, 49(9):1453–1464, 2005.

[25] Y. Chen, W. Ren and K. Moore. High-Order and Model Reference Consensus Algorithms in Cooperative Control of Multi-Vehicle Systems. *Journal of Dynamic Systems, Measurement, and Control*, 129(5):678–688, 2007.

[26] L. Wang and F. Xiao. Consensus problems for high-dimensional multi-agent systems. *Control Theory Applications*, 10(3):830–837, 2007.

[27] D. Cheng, J. Wang and X. Hu. Consensus of muti-agent linear dynamic systems. *Asian J. Contr.*, 10(2):144–155, 2008.

[28] J. Zhang and C. Ma. Necessary and sufficient conditions for consensusability of linear multi-agent systems. *IEEE Transactions on Automatic Control*, 55(5):1263–1268, 2010.

[29] Z. Liu, J. Wang and X. Hu. *Consensus of High Order Linear Multi-agent Systems Using Output Error Feedback*. IEEE Conference on Descision and Control, 2009.

[30] C-Q. Ma and J-F. Zhang. Necessary and sufficient conditions for consensusability of linear multi-agent systems. *IEEE Transactions on Automatic Control*, 55(5):1263–1268, 2010.

[31] B. Francis, Z. Lin and M. Maggiore. State agreement for continuous-time coupled nonlinear systems. *SIAM Journal on Control and Optimization*, 46(1):288–307, 2007.

[32] G. Shi and Y. Hong. Global target aggregation and state agreement of nonlinear multi-agent systems with switching topologies. *Automatica*, 45(5):1165–1175, 2009.

[33] J. Thunberg, W. Song, E. Montijano, Y. Hong and X. Hu. Distributed attitude synchronization control of multi-agent systems with switching topologies. *Automatica*, 50(3):832–840, 2014.

[34] E. Montijano, J. Thunberg, X. Hu and C. Sagues. Epipolar visual servoing for multi-robot distributed consensus. *IEEE Transactions on Robotics*, 29(5):1212–1225, 2013.

[35] J. Thunberg, W. Song, Y. Hong and X. Hu. Distributed attitude synchronization using backstepping and sliding mode control. *Control Theory and Technology*, 12(1):48–55, 2014.

[36] W. Song, J. Thunberg, X. Hu and Y. Hong. Distributed high-gain attitude synchronization using rotation vectors. *Journal of Systems Science and Complexity*. To appear.

[37] Y. Ma, S. Soatto, J. Kosecka and S. Sastry. *An invitation to 3-D vision*. Springer, 2004.

[38] I. Suzuki and M. Yamashita. Searching for a mobile intruder in a polygonal region. *SIAM Journal on Computing*, 21:863, 1992.

[39] L.J. Guibas, J.C. Latombe, S.M. LaValle, D. Lin and R. Motwani. A visibility-based pursuit-evasion problem. *International Journal of Computational Geometry and Applications*, 1999.

[40] B.P. Gerkey, S. Thrun and G. Gordon. Visibility-based pursuit-evasion with limited field of view. *The International Journal of Robotics Research*, 25(4):299, 2006.

[41] V. Isler, S. Kannan and S. Khanna. Randomized pursuit-evasion in a polygonal environment. *IEEE Transactions on Robotics*, 21(5):875–884, 2005.

[42] G. Hollinger, S. Singh and A. Kehagias. Efficient, Guaranteed Search with Mult-Agent Teams. *2009 Robotics: Science and Systems Conference, RSS*, 2009.

[43] S.M. LaValle and J.E. Hinrichsen. Visibility-based pursuit-evasion: The case of curved environments. *IEEE Transactions on Robotics and Automation*, 17(2):196–202, 2002.

[44] B. Tovar and S. LaValle. Visibility-based pursuit-evasion with bounded speed. *Algorithmic Foundation of Robotics VII*, pages 475–489, 2008.

[45] B.H. Simov, G. Slutzki and S.M. LaValle. Clearing a polygon with two 1-searchers. *International Journal of Computational Geometry and Applications*, 19(1):59–92, 2009.

[46] J. Yu and S.M. LaValle. Tracking hidden agents through shadow information spaces. In *Robotics and Automation, 2008. ICRA 2008. IEEE International Conference on*, pages 2331–2338. IEEE, 2008.

[47] G. Hollinger, S. Singh and A. Kehagias. Improving the efficiency of clearing with multi-agent teams. *International Journal of Robotics Research*, 29(8):1088–1105, 2010.

[48] A. Kolling and S. Carpin. The GRAPH-CLEAR problem: definition, theoretical properties and its connections to multirobot aided surveillance. In *Proceedings of the IEEE/RSJ International Conference on Intelligent Robots and Systems*, pages 1003–1008, 2007.

[49] J. Thunberg and P. Ögren. A mixed integer linear programming approach to pursuit evasion problems with optional connectivity constraints. *Autonomous Robots*, 31(4):333–343, 2011.

Chapter 2

Convergence tools for consensus

In this chapter we develop tools in order to show state-consensus in multi-agent systems where the states in the system are updated by an ordinary differential equation.

Here, similar to [1–3], we consider a broad class of multi-agent systems and provide some criteria in order to guarantee consensus. In those works, consensus is assured by imposing a convexity assumption. Roughly, provided that the existence and uniqueness of the solution is guaranteed, if the right-hand side of each agent's dynamics, is inward-pointing [4] relative to the convex hull of the position of the agent and those of its neighbors (states), asymptotic consensus can be shown.

Instead of relying on a convexity assumption we use two types of functions. The functions of the first type are functions of the states of the agents and the functions of the second type are functions of pairs of states. If certain conditions are fulfilled for the system, two theorems guarantee consensus or state agreement by using these functions. The two theorems differ in the sense that the first theorem is formulated for functions of the first type and the second theorem is formulated for functions of the second type. The theorems can be combined in order to show consensus under the convexity assumptions in [1–3]. However, as we show, there are examples when the convexity assumptions do not hold but where the proposed theorems can be used.

The functions can be interpreted as Lyapunov functions in order to show consensus for multi-agent systems. If a function of the first type is used, a strong form of attractiveness of the consensus set is shown in the first theorem. If a function of the second type is used, uniform asymptotic stability of the consensus set is shown in the second theorem. The second theorem provides a stronger type of convergence under weaker conditions on the topology, but the first theorem can in general be applied in a wider context.

We provide examples that show the usefulness of the theorems. One such example regards nonlinear scaling in a well known consensus control law for agents with single integrator dynamics. This control law consists of a weighted sum of the pairwise differences between the states of neighboring agents. In the modified nonlinear scaled version, either the states have been scaled or the differences between the states have been scaled. If the differences have been scaled, the control law falls into the frameworks of [1–3]. However, if the states are scaled, this situation is not captured by the convexity assumption, but the first theorem we present is still applicable.

Connectivity is key to achieving collective behavior in a multi-agent system and the topologies for practical multi-agent networks may change over time. In the study of variable topologies, a well-known connectivity assumption, called (uniform) joint connection without requiring connectedness of the graph at every moment, was employed to guarantee multi-agent consensus for first-order or second-order linear or nonlinear systems [1, 5–7]. Under these mild switching conditions we allow the right-hand side of the system dynamics to switch between a finite set of functions that are piecewise continuous in the time and Lipschitz continuous in the state, uniformly with respect to time, on some region containing the origin. Similar to earlier works we assume a positive lower bound on the dwell time between two consecutive time instances where the right-hand side switches between two functions in the set of functions. Also, we require in general an upper bound on the dwell time (in the case of time-invariant right-hand sides we do not require such an upper bound).

The time dependence in the right-hand side of the system dynamics is restricted in the sense that it only depends on the time since the last switch between two functions. This type of time dependence can be used in a wide range of applications, for example one can show that for a system switching between a finite set of time-invariant functions, one can define continuous in time transitions between the functions instead of discontinuous switches, so that the right-hand side of the system dynamics is continuous and the same type of convergence properties hold as for the switching system.

In this chapter, in order not to obfuscate the main results with the technical details in the proofs, the proofs to the propositions are relegated to the last section.

2.1 Preliminaries

Hereinafter, throughout the thesis, the real numbers are denoted by $\mathbb{R}$ and the set of integers are denoted by $\mathbb{Z}$. By writing $\mathbb{R}^+$ we exclude all the negative real numbers, and by writing $\mathbb{R}^{++}$ we exclude all the non positive real numbers, the analogous notation holds for $\mathbb{Z}$. We make no distinction between the symbols $+\infty$ and ∞ which symbolize the right extension of the real numbers. The left extension of the real numbers is accordingly denoted by $-\infty$.

An element or a vector x that belongs to $\mathbb{R}^m$ is by default a column vector. Though all norms being equivalent in $\mathbb{R}^m$, if nothing else is mentioned, $\|\cdot\|$ is the Euclidean norm, where the size of the dimension m should either be explained when the norm is used or be apparent by the context. By $B_{r,m}(x_0)$ we denote the open ball in $\mathbb{R}^m$ centered around $x_0 \in \mathbb{R}^m$ with radius $r > 0$ and $\bar{B}_{r,m}(x_0)$ is the closure of said open ball. Sometimes we write $B_{r,m}$ or $\bar{B}_{r,m}$ which is short hand notation for $B_{r,m}(0)$ and $\bar{B}_{r,m}(0)$ respectively. Given $x_1, \ldots, x_n$ where $x_i \in \mathbb{R}^m$ we write the concatenated or stacked vector x in $\mathbb{R}^{mn}$

either as $x = [x_1^T, \dots x_n^T]^T$ or $x = (x_1, \dots, x_n)^T$, where $x_1, \dots x_n$ should be treated as row vectors in the latter notation. Throughout the thesis, the notation $(\cdot)'$ will never used to denote the transpose, $(\cdot)^T$, of a vector, nor will it be used to denote the differentiation operator. Sometimes however, it will be used as part of the name of a variable, a set or a parameter.

2.1.1 Dynamics

Let us introduce the following finite set of functions

$$\mathcal{F} = \{\tilde{f}_1(t,x), \dots, \tilde{f}_{|\mathcal{F}|}(t,x)\},$$

where

$$\tilde{f}_k : \mathbb{R} \times \mathbb{R}^{mn} \to \mathbb{R}^{mn}, \text{ for all } k = \{1, \dots, |\mathcal{F}|\},$$

is continuous in t and Lipschitz in x, uniformly with respect to t, on some open connected set containing the compact region $\mathcal{D} \in \mathbb{R}^{mn}$. We assume that $\mathcal{D}$ contains the origin as an interior point. The symbol $|\mathcal{F}|$ is the number of functions in $\mathcal{F}$. Each function $\tilde{f}_k \in \mathcal{F}$ can be written as $\tilde{f}_k = (\tilde{f}_{k,1}, \dots, \tilde{f}_{k,n})^T$, where

$$\tilde{f}_{k,l} : \mathbb{R} \times \mathbb{R}^{mn} \to \mathbb{R}^m \quad \text{for all } \ l.$$

By following [5], we define switching signal functions which will be used in the definition of the system dynamics. We will assume that a switching signal function σ satisfies either Assumption 2.1 (1,2) or Assumption 2.1 (1,2,3) below (what we mean by *e.g.*, (1,2) is that the conditions 1 and 2 are satisfied).

Assumption 2.1.

1. *The function $\sigma(t) : \mathbb{R} \to \{1, \dots, |\mathcal{F}|\}$ is piecewise right-continuous.*

2. *There is a monotonically increasing sequence $\{\tau_k\}$, such that $\tau_k \to \infty$ as $k \to \infty$ and $\tau_k \to -\infty$ as $k \to -\infty$, where each $\tau_k \in \mathbb{R}$ is such that for any $k \in \mathbb{Z}$ the function σ is constant on $[\tau_k, \tau_{k+1})$ for all k, and there is a $\tau_D > 0$ such that*
$$\inf_k(\tau_{k+1} - \tau_k) \geq \tau_D \text{ and}$$

3. *there is an upper bound $\tau_U > 0$, such that for any*
$$\sup_k(\tau_{k+1} - \tau_k) \leq \tau_U.$$

We define the set of all functions σ that fulfills Assumption 2.1 (1,2) as $\mathcal{S}_{|\mathcal{F}|,D}$ and fulfills Assumption 2.1 (1,2,3) as $\mathcal{S}_{|\mathcal{F}|,D,U}$. The constants τ_D and τ_U might be different for different σ, so condition 2 and 3 in Assumption 2.1 can also be formulated as

$$\inf_k(\tau_{k+1} - \tau_k) > 0 \quad \text{and} \quad \sup_k(\tau_{k+1} - \tau_k) < \infty$$

respectively. For each σ, the sequence $\{\tau_k\}$ is referred to as the switching times of σ, since it is only at those times $\sigma(t)$ changes value. If we compare the upper and lower bounds for two switching signal functions σ_1 and σ_2, we denote the upper and lower bound for σ_1 as $\tau_U^{\sigma_1}$ and $\tau_D^{\sigma_1}$ respectively and the upper and lower bound for σ_2 as $\tau_U^{\sigma_2}$ and $\tau_D^{\sigma_2}$ respectively.

For a given $\sigma \in \mathcal{S}_{|\mathcal{F}|,D}$ with switching times $\{\tau_k\}$ we define (for finite times)

$$\gamma_\sigma(t) = \max\{\tau_k : \tau_k \leq t, k \in \mathbb{Z}\},$$

where $\gamma_\sigma(t)$ is the largest switching time less than or equal to t.

Let us now consider a system of n agents. The state of agent i at time t is defined as $x_i(t) \in \mathbb{R}^m$. The dynamics for the system of agents that we consider is given by

$$\begin{aligned} \dot{x}_1 &= f_1(t,x) = \tilde{f}_{\sigma(t),1}(t - \gamma_\sigma(t), x), \\ &\vdots \\ \dot{x}_n &= f_n(t,x) = \tilde{f}_{\sigma(t),n}(t - \gamma_\sigma(t), x), \end{aligned}$$

where $\sigma \in \mathcal{S}_{|\mathcal{F}|,D}$ and

$$(\tilde{f}_{\sigma(t),1}, \ldots, \tilde{f}_{\sigma(t),n})^T = \tilde{f}_{\sigma(t)} \in \mathcal{F}.$$

Note that $f_i(t,x) \in \mathbb{R}^m$ for $i \in \{1, \ldots, n\}$, whereas $\tilde{f}_i(t,x) \in \mathbb{R}^{mn}$ for $i \in \{1, \ldots, |\mathcal{F}|\}$. The main results in this work regard the restricted case when $\sigma \in \mathcal{S}_{|\mathcal{F}|,D,U}$, however there are cases when we assume the general case when $\sigma \in \mathcal{S}_{|\mathcal{F}|,D}$. The system dynamics can be written as

$$\dot{x} = f(t,x) = \tilde{f}_{\sigma(t)}(t - \gamma_\sigma(t), x), \tag{2.1}$$

where, $f(t,x) = (f_1(t,x), \ldots, f_n(t,x))^T$. For a given σ, the function $f(t,x)$ is piecewise continuous in t. It is Lipschitz in x on $\mathcal{D}$, uniformly with respect to t. The initial state and the initial time for (2.1) is $x_0 \in \mathcal{D}$ and t_0 respectively. Sometimes we write $x(t_0)$ instead of x_0.

The switching signal functions are used in order to indicate which system we are referring to. For a given $\mathcal{F}$, the switching behavior of the system is captured by σ. In order to emphasize this, instead of writing x we can write

$$x^\sigma = (x_1^\sigma, \ldots, x_n^\sigma)^T.$$

In general we omit the parametrization by σ and write x instead of x^σ, but the latter notation is useful when we study solutions of (2.1) for different choices of σ. The solution for the system (2.1) is sometimes also written as $x(t, t_0, x_0)$ or $x^\sigma(t, t_0, x_0)$, where the explicit dependence on the initial time t_0 and the initial state x_0 is emphasized.

Lemma 2.2. *If all the functions in $\mathcal{F}$ are time-invariant, the dynamics* (2.1) *is given by*

$$\dot{x} = \tilde{f}_{\sigma(t)}(x),$$

and if $\sigma \in \mathcal{S}_{|\mathcal{F}|,D}$ but $\sigma \notin \mathcal{S}_{|\mathcal{F}|,D,U}$, it holds that there is a corresponding $\sigma' \in \mathcal{S}_{|\mathcal{F}|,D,U}$ for which the dynamics is the same. i.e.,

$$\dot{x} = \tilde{f}_{\sigma'(t)}(x) = \tilde{f}_{\sigma(t)}(x)$$

for all $t \geq 0$.

Lemma 2.3. *For $\sigma \in \mathcal{S}_{|\mathcal{F}|,D,U}$ with lower bound τ_D^σ and upper bound τ_U^σ on the dwell time between two consecutive switches, there is a finite set of functions (continuous in t and Lipschitz in x on $\mathcal{D}$, uniformly with respect to t)*

$$\mathcal{F}' = \{\tilde{f}'_1, \ldots, \tilde{f}'_{|\mathcal{F}'|}\} \supset \mathcal{F}$$

and $\sigma' \in \mathcal{S}_{|\mathcal{F}'|,D,U}$ with a lower bound $\tau_D^{\sigma'} = \tau_D^\sigma$ and an upper bound $\tau_U^{\sigma'} = 2\tau_D^\sigma$ on the dwell time between two consecutive switches, such that

$$\tilde{f}'_{\sigma'(t)}(t - \gamma_{\sigma'}(t), x) = \tilde{f}_{\sigma(t)}(t - \gamma_\sigma(t), x).$$

The proofs of these lemmas as well as all other proofs that are not given directly are contained in Section 2.4. Due to Lemma 2.3, we will often consider the case when $\tau_U = 2\tau_D$ since we can replace $\mathcal{F}$ with $\mathcal{F}'$ and σ with σ'. Note that τ_D^σ and τ_U^σ do not need to be the greatest lower bound and the least upper bound respectively for the dwell time between two consecutive switches of σ.

2.1.2 Connectivity

In a multi-agent system the dynamical behavior in general depends on the connectivity between the agents. The connectivity is described by a graph.

Definition 2.4. A directed graph (or digraph) $\mathcal{G} = (\mathcal{V}, \mathcal{E})$ consists of a set of nodes, $\mathcal{V} = \{1, ..., n\}$ and a set of edges $\mathcal{E} \subset \mathcal{V} \times \mathcal{V}$.

In our setting, each node in the graph corresponds to a unique agent. Thus $\mathcal{V}$ is henceforth defined as $\mathcal{V} = \{1, ..., n\}$. We also define neighbor sets or neighborhoods. Let $\mathcal{N}_i \in \mathcal{V}$ comprise the neighbor set (sometimes referred to simply as neighbors) of agent i, where $j \in \mathcal{N}_i$ if and only if $(j, i) \in \mathcal{E}$. We assume throughout the thesis that $i \in \mathcal{N}_i$ *i.e.*, we restrict the collection of graphs to those for which $(i, i) \in \mathcal{E}$ for all $i \in \mathcal{V}$.

A directed path of $\mathcal{G}$ is an ordered sequence of distinct nodes in $\mathcal{V}$ such that any consecutive pair of nodes in the sequence corresponds to an edge in the graph. An agent i is connected to an agent j if there is a directed path starting in j and ending in i.

Definition 2.5. A digraph is strongly connected if each node i is connected to all other nodes.

Definition 2.6. A digraph is quasi-strongly connected if there exists a rooted spanning tree or a center, *i.e.*, at least one node such that all the other nodes are connected to it.

We are now ready to address time-varying graphs. From Definition 2.4 we see that there are 2^{n^2} possible directed graphs with n nodes. For $k \in \{1, \ldots, |\mathcal{F}|\}$ we associate a corresponding graph $\mathcal{G}_k = (\mathcal{V}, \mathcal{E}_k)$. Note that the graphs $\mathcal{G}_k$ and $\mathcal{G}_l$ might be the same for $k \neq l$ (*i.e.*, the set of edges is equal for the two graphs $\mathcal{G}_k$ and $\mathcal{G}_l$).

For $\sigma \in \mathcal{S}_{|\mathcal{F}|,D}$ we define the time-varying graph corresponding to σ as $\mathcal{G}_{\sigma(t)}$ and the time-varying neighborhoods as $\mathcal{N}_i(t)$ for all i. If we want to emphasize explicitly which switching signal function is used, we write $\mathcal{N}_i^{\sigma}(t)$ or $\mathcal{N}_i^{\sigma(t)}$.

Definition 2.7. For $\sigma \in \mathcal{S}_{|\mathcal{F}|,D}$, the union graph of $\mathcal{G}_{\sigma(t)}$ during the time interval $[t_1, t_2)$ is defined as

$$\mathcal{G}([t_1, t_2)) = \textstyle\bigcup_{t \in [t_1, t_2)} \mathcal{G}_{\sigma(t)} = (\mathcal{V}, \bigcup_{t \in [t_1, t_2)} \mathcal{E}_{\sigma(t)}),$$

where $t_1 < t_2 \leq +\infty$.

Definition 2.8. The graph $\mathcal{G}_{\sigma(t)}$ is uniformly (quasi-) strongly connected if $\sigma \in \mathcal{S}_{|\mathcal{F}|,D}$ and there exists a constant $T^{\sigma} > 0$ such that the union graph $\mathcal{G}([t, t + T^{\sigma}))$ is (quasi-) strongly connected for all t.

2.1.3 Some special functions, sets and operators

Definition 2.9. For $V : \mathbb{R}^m \to \mathbb{R}$ we define $f_{V,m} : \mathbb{R}^{mn} \to \mathbb{R}$ as

$$f_{V,m}(x) = \max_{j \in \mathcal{V}} V(x_j).$$

Definition 2.10. For $W : \mathbb{R}^m \times \mathbb{R}^m \to \mathbb{R}$ we define $f_{W,m,m} : \mathbb{R}^{mn} \to \mathbb{R}$ as

$$f_{W,m,m}(x) = \max_{(i,j) \in \mathcal{W} \times \mathcal{V}} V(x_i, x_j).$$

Definition 2.11. Suppose for $\sigma \in \mathcal{S}_{|\mathcal{F}|,D}$ that x^{σ} is a solution to (2.1) and $x^{\sigma}(t)$ is contained in $\mathcal{D}$ on an interval $[t_0, t_0 + \tilde{t})$ where $\tilde{t} > 0$. Suppose also that $V : \mathbb{R}^m \to \mathbb{R}$ and $W : \mathbb{R}^m \times \mathbb{R}^m \to \mathbb{R}$ are continuously differentiable. On $[t_0, t_0 + \tilde{t})$, let

$$\begin{aligned}
\mathcal{I}_V(t_1, t_2) &= \{i : V(x_i(t_2)) = f_{V,m}(x(t_1))\}, \\
\mathcal{J}_W(t_1, t_2) &= \{(i,j) : W(x_i(t_2), x_j(t_2)) = f_{W,m,m}(x(t_1))\}, \\
\mathcal{I}_V^*(t) &= \mathcal{I}_V(t,t) \cap \left\{ i : \frac{d}{dt} V(x_i(t)) < 0, i \in \mathcal{V} \right\}, \\
\mathcal{J}_W^*(t) &= \mathcal{J}_W(t,t) \cap \left\{ (i,j) : \frac{d}{dt} W(x_i(t), x_j(t)) < 0, (i,j) \in \mathcal{V} \times \mathcal{V} \right\}.
\end{aligned}$$

These sets, except for being functions of the times t_1, t_2 or t, also depend on the initial conditions x_0, t_0 and the switching signal function. In order to simplify the notation, we do not parameterize these sets by σ, t_0 and x_0.

The upper Dini derivative of a function $V(t, x(t))$ with respect to t is defined as

$$D^+ V(t, x(t)) = \limsup_{\epsilon \downarrow 0} \frac{V(t + \epsilon, x(t + \epsilon)) - V(t, x(t))}{\epsilon}.$$

Given this definition we now proceed with a useful lemma, [1,2].

Lemma 2.12.

- *If* $V : \mathbb{R}^m \to \mathbb{R}$ *is continuously differentiable, then*

$$D^+ f_{V,m}(x(t)) = \max_{i \in \mathcal{I}_V(t,t)} \frac{d}{dt} V(x_i(t)).$$

- *If* $V : \mathbb{R}^m \times \mathbb{R}^m \to \mathbb{R}$ *is continuously differentiable, then*

$$D^+ f_{V,m,m}(x(t)) = \max_{(i,j) \in \mathcal{J}_V(t,t)} \frac{d}{dt} V(x_i(t), x_j(t)).$$

2.1.4 Stability

Let us introduce two equivalent definitions of uniform stability for the origin of (2.1). The first one is similar to the classic version [8], whereas the second one is a multi-agent systems version. In the definitions of stability here, we consider the stability for a set or a family of systems, where the systems in the set differ in the choice of switching signal function σ. Thus, the stability holds for all choices of switching signal functions in $\mathcal{S}_{|\mathcal{F}|,D}$, where the right-hand side of (2.1) switches between functions in $\mathcal{F}$.

We assume that all the balls in the following definition are contained in $\mathcal{D}$. The existence of such regions is assured by the assumption that 0 is in the interior of $\mathcal{D}$.

Definition 2.13.

1. The point $0 \in \mathbb{R}^{mn}$ is uniformly stable for (2.1) if for $\varepsilon > 0$, there is $\delta(\epsilon) > 0$ such that

$$x^\sigma(t_0) \in \bar{B}_{\delta,mn} \Rightarrow x^\sigma(t) \in \bar{B}_{\epsilon,mn}, \quad \text{for all } t \geq t_0, \sigma \in \mathcal{S}_{|\mathcal{F}|,D}.$$

2. The point $0 \in \mathbb{R}^m$ is uniformly stable for (2.1) if for $\varepsilon > 0$, there is $\delta(\epsilon) > 0$ such that

$$x_i^\sigma(t_0) \in \bar{B}_{\delta,m} \Rightarrow x_i^\sigma(t) \in \bar{B}_{\epsilon,m}, \quad \text{for all } i, t \geq t_0, \sigma \in \mathcal{S}_{|\mathcal{F}|,D}.$$

In the multi-agent systems setting it feels often more intuitive to define the region of stability in the space where the agents reside, using 2, since then each agent only needs to check that its state is inside the region of stability.

For a set $\mathcal{A} \subset \mathbb{R}^{mn}$, let

$$\text{dist}(x, \mathcal{A}) = \inf_{y \in \mathcal{A}} \|x - y\|.$$

We say that $x(t)$ approaches $\mathcal{A}$ or $x(t) \to \mathcal{A}$ as $t \to \infty$, on a subset of $\mathcal{D}$ if for all $\epsilon > 0$ and x_0 in the subset, there exists $T(\epsilon, x_0, t_0)$ such that $\text{dist}(x(t), \mathcal{A}) < \epsilon$ for all

$t \geq T(\epsilon, x_0, t_0) + t_0$. Let us proceed with the definition of invariance of a set for the system (2.1). We start with the standard definition of invariance, and proceed with the multi-agent systems definition which is similar to the one in *e.g.*, [2].

Definition 2.14.

1. A set $\mathcal{A} \in \mathbb{R}^{mn}$ is (positively) invariant for the system (2.1) if for all t_0, it holds that

$$x_0 \in \mathcal{A} \Longrightarrow x^\sigma(t, t_0, x_0) \in \mathcal{A}$$

   for all $t > t_0$ and $\sigma \in \mathcal{S}_{|\mathcal{F}|,D}$.

2. A set $\mathcal{A} \in \mathbb{R}^{m}$ is (positively) invariant for the system (2.1) if for all i, t_0, it holds that

$$x_i^\sigma(t_0) \in \mathcal{A} \Longrightarrow x_i^\sigma(t, t_0, x_0) \in \mathcal{A}$$

   for all i, $t > t_0$ and $\sigma \in \mathcal{S}_{|\mathcal{F}|,D}$.

When we use either one of these definitions, the choice should be apparent by the context. We define

$$\mathcal{D}^*(\tilde{t}) = \{x_0 \in \mathbb{R}^{mn} : x^\sigma(t, t_0, x_0) \in \mathcal{D} \quad \text{for all } t_0, t \in [t_0, t_0 + \tilde{t}) \text{ and } \sigma \in \mathcal{S}_{|\mathcal{F}|,D}\}$$

and formulate the following lemma.

Lemma 2.15. *For any $\tilde{t} \in [0, \infty]$, the set $\mathcal{D}^*(\tilde{t})$ is compact and the set $\mathcal{D}^*(\infty)$ is also invariant.*

In the definitions of stability of the origin and the definitions of invariance, we assumed that $\sigma \in \mathcal{S}_{|\mathcal{F}|,D}$ is arbitrary, *i.e.*, the statements must hold for any $\sigma \in \mathcal{S}_{|\mathcal{F}|,D}$. However, in the definitions of stability of a set which we now are to formulate, we only consider the case when σ is fixed. Thus, in the following definitions we write x instead of x^σ. We restrict the state to be contained in the invariant compact set $\mathcal{D}^*(\infty)$. Hence, the stability of the set is only defined in the relative sense, relative to $\mathcal{D}^*(\infty)$. In these definitions we assume that $\mathcal{D}^*(\infty)$ is nonempty, and we will later show how to assure this.

Definition 2.16. For (2.1) where $\sigma \in \mathcal{S}_{|\mathcal{F}|,D}$, the set $\mathcal{A}$ is

1. stable relative to $\mathcal{D}^*(\infty)$ if for all t_0 and for all $\epsilon > 0$, there is $\delta(t_0, \epsilon) > 0$ such that for $x_0 \in \mathcal{D}^*(\infty)$ it holds that

$$\text{dist}(x_0, \mathcal{A}) \leq \delta \Longrightarrow \text{dist}(x(t), \mathcal{A}) \leq \epsilon \quad \text{for all } t \geq t_0.$$

2. uniformly stable relative to $\mathcal{D}^*(\infty)$ if it fulfills 1 and δ as a function of t_0 is constant.

3. attractive relative to $\mathcal{D}^*(\infty)$ if there is $c(t_0)$ such that $x(t) \to \mathcal{A}$ as $t \to \infty$ for all $x_0 \in \mathcal{D}^*(\infty)$ such that $\text{dist}(x_0, \mathcal{A}) \leq c$.

4. uniformly attractive relative to $\mathcal{D}^*(\infty)$ if it fulfills 3 and c as a function of t_0 is constant. Furthermore, if $\text{dist}(x_0, \mathcal{A}) \leq c$, for $\eta > 0$ there is $T(\eta)$ such that
$$t \geq t_0 + T(\eta) \Longrightarrow \text{dist}(x(t), \mathcal{A}) < \eta.$$
5. asymptotically stable relative to $\mathcal{D}^*(\infty)$ if it fulfills 1 and 3.
6. uniformly asymptotically stable relative to $\mathcal{D}^*(\infty)$ if it fulfills 2 and 4.
7. globally uniformly asymptotically stable relative to $\mathcal{D}^*(\infty)$, if it fulfills 6 and
$$c = \sup_{y \in \mathcal{D}^*(\infty)} \text{dist}(y, \mathcal{A}).$$
8. globally quasi-uniformly attractive relative to $\mathcal{D}^*(\infty)$ if $x(t) \to \mathcal{A}$ as $t \to \infty$ for all $x_0 \in \mathcal{D}^*(\infty)$ and all t_0. Furthermore, for all $\eta > 0$ there is $T(\eta)$ such that
$$\min_{t \in [t_0, t_0 + T(\eta)]} \text{dist}(x(t), \mathcal{A}) < \eta$$
for all $x_0 \in \mathcal{D}^*(\infty)$ and t_0.

Let us in the following choose the set $\mathcal{A}$ as the consensus set, *i.e.*,
$$\mathcal{A} = \{x = (x_1, \ldots, x_n)^T \in \mathbb{R}^{mn} : x_i = x_j \text{ for all } i, j\}.$$

We now formulate an assumption that creates a relationship between the functions in $\mathcal{F}$ and the neighborhoods of the agents.

Assumption 2.17. *For any given t and $\sigma \in \mathcal{S}_{|\mathcal{F}|,D}$, it holds that $\tilde{f}_{\sigma(t),i}(s, x)$ is, except for being a function of s, only a function of $\{x_j\}_{j \in \mathcal{N}_i^{\sigma(t)}}$ for all s, $i \in \mathcal{V}$, and $x \in \mathcal{D}$.*
Or equivalently. $\tilde{f}_{k,i}(s, x)$ is, except for being a function of s, only a function of $\{x_j\}_{j \in \mathcal{N}_i^k}$ for all s, $i \in \mathcal{V}$, $x \in \mathcal{D}$ and $k \in \{1, \ldots, |\mathcal{F}|\}$.

We continue with two central assumptions.

Assumption 2.18. *Let $V : \mathbb{R}^m \to \mathbb{R}$ be a continuously differentiable function on $\mathcal{D}$. The function V fulfills the following.*

1. *V is positive definite.*
2. *For any initial time t_0, initial state $x_0 \in \mathcal{D}$ and $\sigma \in \mathcal{S}_{|\mathcal{F}|,D}$, if there is $\epsilon > 0$ such that the solution to* (2.1) *exists and is contained in $\mathcal{D}$ during $[t_0, t_0 + \epsilon)$, then for $t \in [t_0, t_0 + \epsilon)$ it holds that*
$$D^+ f_{V,m}(x^\sigma(t)) \leq 0 \quad \textit{and}$$
3. *for each agent $i \in \mathcal{I}_V(t,t)$ it holds that $i \in \mathcal{I}_V^*(t)$ if there is $j \in \mathcal{N}_i^\sigma(t)$ such that $x_i^\sigma(t) \neq x_j^\sigma(t)$. Furthermore, if $i \in \mathcal{I}_V(t,t)$ and $i \notin \mathcal{I}_V^*(t)$ it holds that $\tilde{f}_{\sigma(t),i}(s, x) = 0$ for all s.*

Assumption 2.19. *Let $V : \mathbb{R}^m \times \mathbb{R}^m \to \mathbb{R}^+$, be a continuously differentiable on $\mathcal{D}$. The function V fulfills the following.*

1. *$V(x, y) = 0$ if and only if $x = y$,*

2. *For any initial time t_0, initial point $x_0 \in \mathcal{D}$ and $\sigma \in \mathcal{S}_{|\mathcal{F}|,D}$, if there is an $\epsilon > 0$ such that the solution to (2.1) exists and is contained in $\mathcal{D}$ during $[t_0, t_0 + \epsilon)$, then for $t \in [t_0, t_0 + \epsilon)$*
$$D^+ f_{V,m,m}(x^\sigma(t)) \leq 0 \quad \textit{and}$$

3. *for each pair of agents $(i, j) \in \mathcal{J}_V(t, t)$ it holds that $(i, j) \in \mathcal{J}_V^*(t)$ if there is $k \in \mathcal{N}_i^\sigma(t)$ such that $x_i^\sigma(t) \neq x_k^\sigma(t)$, or there is $l \in \mathcal{N}_j^\sigma(t)$ such that $x_j^\sigma(t) \neq x_l^\sigma(t)$. Furthermore, if $(i, j) \in \mathcal{J}_V(t, t)$ and $(i, j) \notin \mathcal{J}_V^*(t)$ it holds that $\tilde{f}_{\sigma(t),i}(s, x) = 0$ and $\tilde{f}_{\sigma(t),j}(s, x) = 0$ for all s, and*

4. *for each pair of agents $(i, j) \in \mathcal{J}_V(t, t)$ it holds that $(i, j) \in \mathcal{J}_V^*(t)$ only if there is $k \in \mathcal{N}_i^\sigma(t)$ such that $x_i^\sigma(t) \neq x_k^\sigma(t)$, or there is $l \in \mathcal{N}_j^\sigma(t)$ such that $x_j^\sigma(t) \neq x_l^\sigma(t)$.*

The easiest way to verify that 2-3 are fulfilled in Assumption 2.18 and 2-4 are fulfilled in Assumption 2.19, is to use Lemma 2.12. For example the condition 2 in Assumption 2.18 can be verified as follows. If $x \in \mathcal{D}$ and

$$i = \arg\max_{k \in \mathcal{V}}(V(x_k)),$$

where $x = (x_1, \ldots, x_n)^T$, then if $\nabla V(x_i)\tilde{f}_j(t, x) \leq 0$ for all $j \in \{1, \ldots, |\mathcal{F}_i|\}$, 2 is fulfilled. Condition 2 in Assumption 2.19 is verified in the analogous way.

2.2 Main results

Theorem 2.20. *Suppose Assumption 2.18 (1,2) holds, then 0 is uniformly stable for (2.1). Furthermore, suppose that $\widehat{\beta}_1$ and $\widehat{\beta}_2$ are class $\mathcal{K}$ functions such that*

$$\widehat{\beta}_1(\|y\|) \leq V(y) \leq \widehat{\beta}_2(\|y\|),$$

then for ϵ such that $(\bar{B}_{\epsilon,m})^n \subset \mathcal{D}$, it holds that

$$x_0 \in \bar{B}_{\delta,m} \Longrightarrow x_i^\sigma(t, t_0, x_0) \in \bar{B}_{\epsilon,m}, \quad \textit{for all } i, t \geq t_0, \sigma \in \mathcal{S}_{|\mathcal{F}|,D},$$

where $\delta = \widehat{\beta}_2^{-1}(\widehat{\beta}_1(\epsilon))$.

Theorem 2.21. *Suppose assumptions 2.17 and 2.18 (2,3) hold and $\sigma \in \mathcal{S}_{|\mathcal{F}|,D,U}$ is such that $\mathcal{G}_{\sigma(t)}$ is uniformly strongly connected, then the consensus set $\mathcal{A}$ is globally quasi-uniformly attractive relative to $\mathcal{D}^*(\infty)$.*

Theorem 2.22. *Suppose assumptions 2.17 and 2.19 hold, and $\sigma \in \mathcal{S}_{|\mathcal{F}|,D,U}$. It follows that the consensus set $\mathcal{A}$ is globally uniformly asymptotically stable relative to $\mathcal{D}^*(\infty)$ if and only if $\mathcal{G}_{\sigma(t)}$ is uniformly quasi-strongly connected.*

Remark 2.1. What we mean when we say that Assumption 2.18 (2,3) hold, is that everything in Assumption 2.18 holds except possibly (1). This notation will be used throughout the chapter.

Remark 2.2. If Assumption 2.17 holds and Assumption 2.19 (1,2,3) holds, Theorem 2.22 holds provided that the phrase "if and only if $\mathcal{G}_{\sigma(t)}$ is uniformly quasi-strongly connected" is replaced with "if $\mathcal{G}_{\sigma(t)}$ is uniformly quasi-strongly connected".

Remark 2.3. Provided Assumption 2.18 (1,2) hold, we can show that $\mathcal{D}^*(\infty)$ is nonempty, and an easy way of guaranteeing that $x_0 \in \mathcal{D}^*(\infty)$ is to use Theorem 2.20 and let $x_0 \in (\bar{B}_{\delta,m})^n \subset \mathcal{D}^*(\infty)$. When we know that $\mathcal{D}^*(\infty)$ is nonempty and $x_0 \in \mathcal{D}^*(\infty)$, we do not require V to be positive definite in Theorem 2.21, *i.e.*, it is sufficient that only conditions 2 and 3 hold for V in Assumption 2.18. This means that we can use one positive definite function V_1 in Theorem 2.20 in order to construct a set that is contained in $\mathcal{D}^*(\infty)$, and another not necessarily positive definite function V_2, in order to show that $\mathcal{A}$ is attractive in Theorem 2.21.

We proceed with two corollaries. These corollaries follow as a consequence of the fact that if the functions in $\mathcal{F}$ are time-invariant and $\sigma \in \mathcal{S}_{|\mathcal{F}|,D}$, then there is σ' in $\mathcal{S}_{|\mathcal{F}|,D,U}$ such that $f_{\sigma(t)}(x) = f_{\sigma'(t)}(x)$ for all $t \geq 0$, see Lemma 2.2.

Corollary 2.23. *If the functions in $\mathcal{F}$ are time-invariant, Assumption 2.17 and 2.18 (2,3) hold and $\sigma \in \mathcal{S}_{|\mathcal{F}|,D}$ is such that $\mathcal{G}_{\sigma(t)}$ is uniformly strongly connected, then the consensus set $\mathcal{A}$ is globally quasi-uniformly attractive relative to $\mathcal{D}^*(\infty)$.*

Corollary 2.24. *If the functions in $\mathcal{F}$ are time-invariant, Assumption 2.17 and 2.19 hold, and $\sigma \in \mathcal{S}_{|\mathcal{F}|,D}$ it follows that the consensus set $\mathcal{A}$ is globally uniformly asymptotically stable relative to $\mathcal{D}^*(\infty)$ if and only if $\mathcal{G}_{\sigma(t)}$ is uniformly quasi-strongly connected*

2.3 Examples and interpretations

In this section we provide some examples of systems on the form (2.1) for which the theorems are applicable.

2.3.1 Non-convexity

Suppose Assumption 2.17 is fulfilled and there is a function V such that Assumption 2.18 is fulfilled for this V. In general the set $\{y \in \mathbb{R}^m : V(y) \leq \alpha\}$ does not need to be convex, it depends on the function V. This is illustrated in Figure 2.1, in which the two solid curves comprise the boundary of the set $\{y \in \mathbb{R}^m : V(y) \leq \alpha\}$ for some $\alpha > 0$. If all the agents are contained in this set at some time t and there is an agent i on the boundary which has a neighbor j such that $x_i \neq x_j$, then x_i must move away from the boundary into the interior of the set $\{y \in \mathbb{R}^m : V(y) \leq \alpha\}$. This is illustrated in Figure 2.1, where the arrows indicate that the agent move into the interior of the set $\{y \in \mathbb{R}^m : V(y) \leq \alpha\}$.

The dashed curve defines the boundary of the set $\mathcal{D}^*(\infty)$. Since the agents are contained in $\mathcal{D}^*(\infty)$ and V fulfills Assumption 2.18, provided $\mathcal{G}_{\sigma(t)}$ is uniformly strongly connected, the system will reach consensus.

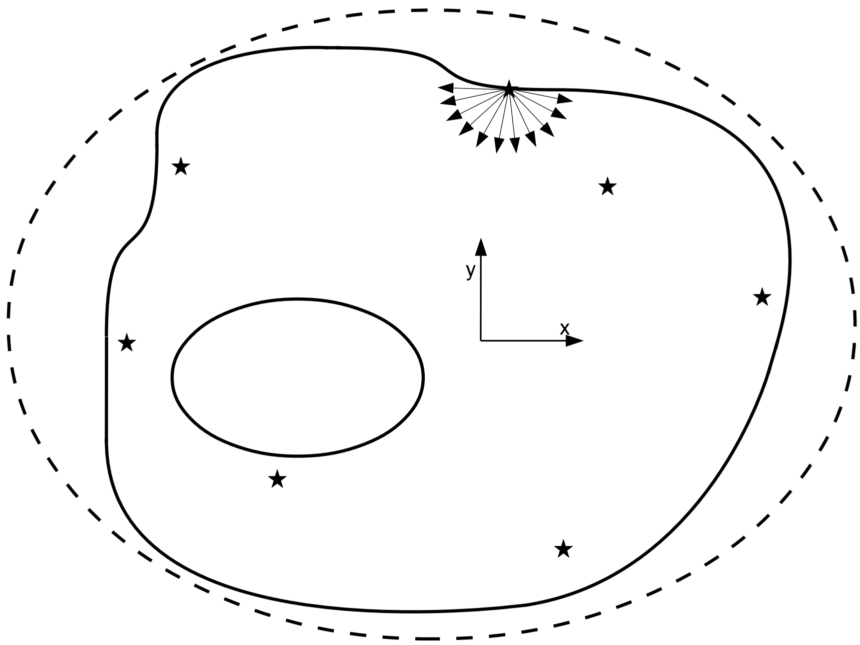

Figure 2.1: Here we consider the case when $m = 2$ and $n = 7$. The positions of the agents at a time t are denoted by stars. The solid curves is the set $\{y \in \mathbb{R}^m : V(y) = \alpha\}$. The dashed curve is the boundary of $\mathcal{D}^*(\infty)$.

Another example where the theorems can be used is when the agents are contained in a geodesic convex and closed subset of a sphere. In this case we can choose $f_{W,m,m}(x_i, x_j)$ as the geodesic distance squared between x_i and x_j. If $f_i(t, x)$ corresponds to a tangent vector that is inward-pointing [4] relative to the convex hull on the sphere (not to mix up with a convex hull in a Euclidean space) of the positions of the neighbors of agent i at time t (provided it is nonempty otherwise $f_i(t, x) = 0$), then one can show that Assumption 2.19 is fulfilled. This is illustrated in Figure 2.2.

2.3.2 Convexity

We continue with a less general case where the decreasing functions are chosen as the Euclidean norm squared of the states and the relative states respectively. Under certain

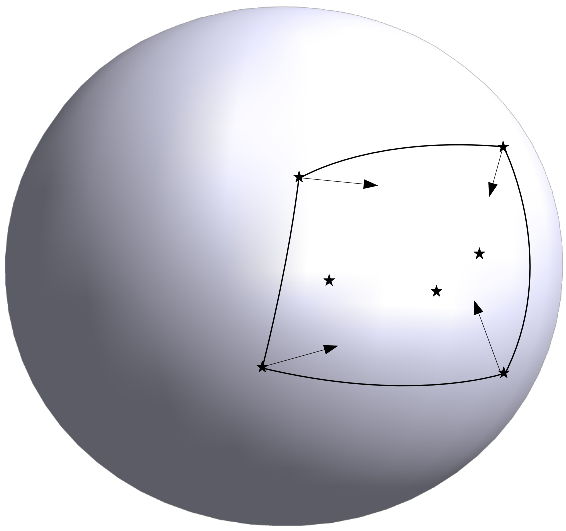

Figure 2.2: Suppose the agents are located in a geodesic convex subset of the sphere $\mathbb{S}^2$. The agents on the sphere are moving into the relative interior of the (geodesic) convex hull of their neighbors. The four connected solid arcs are meant to illustrate the boundary of convex hull of the agents.

conditions, these choices of functions can be used to show a well known convexity result that, provided the right-hand side of each agent's dynamics as an element of the tangent space $T_{x_i}\mathbb{R}^m$ is inward-pointing [4] relative to the convex hull of its neighbors, the system reaches consensus asymptotically [1, 2]. We define the tangent cone to a convex set $S \in \mathbb{R}^m$ at the point y as

$$\mathcal{T}(y, S) = \left\{ z \in \mathbb{R}^m : \liminf_{\lambda \to 0} \frac{\text{dist}(y + \lambda z, S)}{\lambda} = 0 \right\}.$$

This definition can be found in [2], and ξ is inward-pointing relative to S, where $0 \neq \xi \in T_y\mathbb{R}^m$ ($T_y\mathbb{R}^m$ is the tangent space of $\mathbb{R}^m$ at the point y), if ξ belongs to the relative interior of $\mathcal{T}(y, S)$. We use the term *relative interior*, since the dimension of S might be smaller than m. Let us denote the convex hull for $\{x_i\}_{i=1}^n$ by conv$(\{x_i\}_{i=1}^n)$. Similarly, we can denote the convex hull for the positions of the neighbors of agent i as conv$(\{x_j\}_{j \in \mathcal{N}_i})$.

Suppose Assumption 2.17 is fulfilled. We consider the case when

$$V(x_i) = x_i^T x_i \quad \text{and} \quad W(x_i, x_j) = (x_j - x_i)^T (x_j - x_i),$$

where V and W generate the functions $f_{V,m}$ and $f_{W,m,m}$ respectively.

Suppose the functions in $\mathcal{F}$ are Lipschitz in x on $\mathbb{R}^{mn}$, uniformly with respect to t, and continuous in t. Furthermore, suppose V fulfills Assumption 2.18, then in Theorem 2.20 we can choose $\widehat{\beta}_1(\|x_i\|) = \widehat{\beta}_2(\|x_i\|) = \|x_i\|^2$, and obtain the result that any closed ball $\bar{B}_r$ in $\mathbb{R}^m$ is invariant and can be chosen as $\mathcal{D} = \mathcal{D}^*(\infty) = \bar{B}_r$, and the point $x = 0$ is uniformly stable. Thus, by Theorem 2.21 we obtain the result that if $\mathcal{G}_{\sigma(t)}$ is uniformly strongly connected, then $\mathcal{A}$ is globally quasi-uniformly attractive relative to $\mathcal{D}^*(\infty)$. Unless $x_i = x_j$ for all $j \in \mathcal{N}_i$, for any agent i that is furthest away from the origin, $f_i(t, x)$ as an element of the tangent space $T_{x_i}\mathbb{R}^m$ is inward-pointing on the boundary of the closed ball with radius equal to the norm of agent i. This is illustrated in Figure 2.3. An example of this situation is provided in Section 2.3.5 in the application of reaching consensus for a system of rotation matrices.

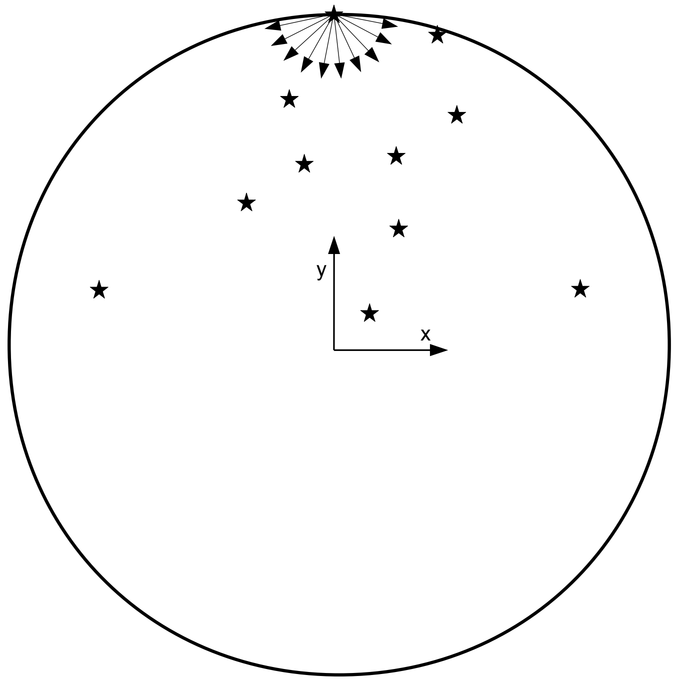

Figure 2.3: In this case $m = 2$. The positions of the agents at a time t are denoted by stars. When at least one of the neighbors of an agent i on the boundary of the ball $\bar{B}_{\max\limits_{k\in\mathcal{V}} \|x_k(t)\|,2}$ is located in the interior of the ball, $f_i(t, x) \in T_{x_i}\mathbb{R}^2$ is inward-pointing (relative to the ball).

Suppose not only that V fulfills Assumption 2.18, but also that W fulfills Assumption 2.19. In this case, any closed ball in $\mathbb{R}^m$ is invariant and can be chosen as $\mathcal{D}^*(\infty)$, but also the largest Euclidean distance between any pair of agents is decreasing. This is illustrated in Figure 2.4. Now Theorem 2.22 holds and $\mathcal{A}$ is globally uniformly asymptomatically stable relative to $\mathcal{D}^*(\infty)$ if and only if $\mathcal{G}_{\sigma(t)}$ is uniformly quasi-strongly connected. For agent i, if $f_i(t, x)$ is inward-pointing relative to the convex hull of its neighbors [1, 2], then these conditions are fulfilled.

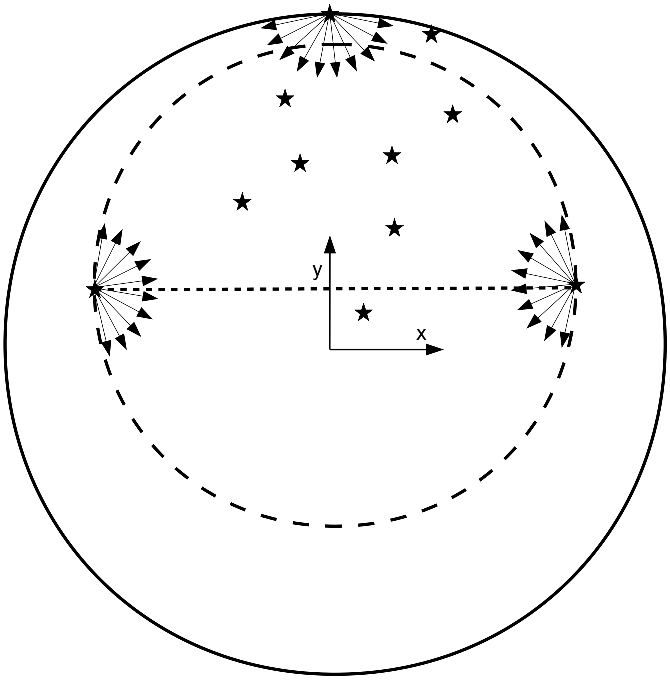

Figure 2.4: In this case $m = 2$. The positions of the agents at some time t are denoted by stars. The solid circle denotes the boundary of the ball with radius $\sqrt{f_{V,m}(x(t))}$ and the dashed circle denotes the boundary of the ball with radius $\sqrt{f_{W,m,m}(x(t))}$. The dashed line denotes the distance between the two agents that are furthest away from each other.

As a special case let

$$f_i(t, x) = \sum_{j \in \mathcal{N}_i(t)} a_{ij}(t - \gamma_\sigma(t))(x_j - x_i),$$

where $\alpha_{ij}(t) > 0$ is continuous, positive and bounded for all t. Let us construct the set of functions $\mathcal{F}$ in the following way. There are 2^{n^2} graphs. For each graph $\mathcal{G}_k$ we define a corresponding function

$$\tilde{f}_k(x) = \left(\sum_{j \in \mathcal{N}_1} \alpha_{ij}(t)(x_j - x_1), \ldots, \sum_{j \in \mathcal{N}_n} \alpha_{ij}(t)(x_j - x_n) \right)^T$$

where $\mathcal{N}_i$ in this case is the neighborhood of agent i in the graph $\mathcal{G}_k$. Now we let

$$\mathcal{F} = \{\tilde{f}_k\}_{k=1}^{2^{n^2}},$$

and $\sigma \in \mathcal{S}_{|\mathcal{F}|,D,U}$. In the following examples and in Chapter 3, if $\mathcal{F}$ is not explicitly defined, we assume that $\mathcal{F}$ is the set of functions that has been constructed in the way analogous to this construction, *i.e.* all the possible right-hand sides.

Now, using the functions

$$V(x_i) = x_i^T x_i \quad \text{and} \quad W(x_i, x_j) = (x_j - x_i)^T (x_j - x_i),$$

with the corresponding functions $f_{V,m}$ and $f_{W,m,m}$ respectively, one can show global uniform asymptotic consensus relative to $\mathcal{D}^*(\infty)$.

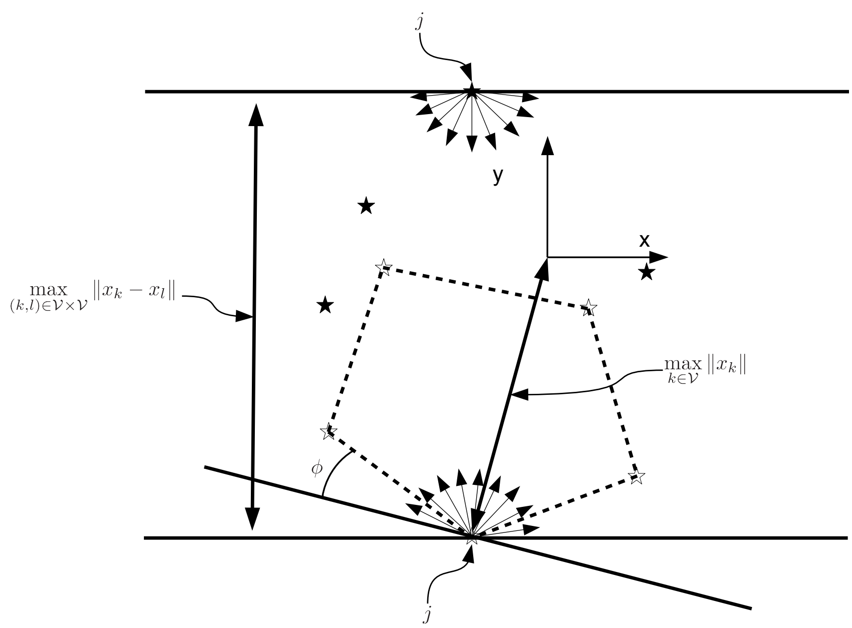

Figure 2.5: Suppose $V(x_i) = x_i^T x_i$ and $W(x_i, x_j) = (x_j - x_i)^T (x_j - x_i)$, then $f_i(t, x)$ does not need to be inward-pointing relative to conv$(\{x_j\}_{j\in\mathcal{N}_i})$ whose boundary comprises the dashed curve.

It is not necessary that $f_i(t, x)$ as an element of the tangent space $T_{x_i}\mathbb{R}^m$ is inward-pointing relative to conv$(\{x_j\}_{j\in\mathcal{N}_i})$. If $i \notin \mathcal{I}_V(t, t)$ and there is no j such that $(i, j) \notin \mathcal{J}_W(t, t)$, then there are no constraints on the direction of $f_i(t, x)$. If $i \in \mathcal{I}_V(t, t)$ or $(i, j) \in$

$\mathcal{J}_W(t,t)$, we can relax the assumption that $f_i(t,x)$ as an element of the tangent space $T_{x_i}\mathbb{R}^m$ is inward-pointing relative to conv$(\{x_j\}_{j\in\mathcal{N}_i})$. This is illustrated in Figure 2.5.

2.3.3 Nonlinear scaling

Here we show how the theorems 2.21 and 2.22 can be used to assure consensus when the states and the relative states for pairs of agents have been scaled with a nonlinear scale function.

In this context, let us define a nonlinear scale function as follows. The function g is strictly increasing on $[0,\eta)$ where $\eta > 0$ and the map

$$h : x_i \mapsto \frac{g(\|x_i\|)}{\|x_i\|}x_i$$

restricted to $B_{\eta,m}$ is a diffeomorphism between $B_{\eta,m}$ and $B_{\eta',m}$, where $\eta' > 0$.

The interesting observation here regards the order of application of h. Suppose that

$$f_i(t,x) = \sum_{j\in\mathcal{N}_i(t)} a_{ij}(t-\gamma_\sigma(t))(x_j - x_i).$$

Within this context, if we define the following map

$$d(x_i,x_j) = x_j - x_i,$$

we can write the function f_i as follows

$$f_i(t,x) = \sum_{j\in\mathcal{N}_i(t)} a_{ij}(t-\gamma_\sigma(t))d(x_i,x_j),$$

and we know that f_i, as an element of the tangent space $T_{x_i}\mathbb{R}^m$, is inward-pointing relative to the convex hull of the neighbors of agent i. Consequently, on $B_{\eta,m}$, we can use Theorem 2.21 together with Theorem 2.22 in order to show consensus when the graph $\mathcal{G}(t)$ is uniformly quasi-strongly connected. Now, for each pair of agents, if we modify f_i into the following form

$$f_i'(t,x) = \sum_{j\in\mathcal{N}_i(t)} a_{ij}(t-\gamma_\sigma(t))h(d(x_i,x_j)),$$

this new function still fulfills the same convexity assumption.

However, if we reverse the order of application of the functions h and d we get the following modified version of f_i

$$f_i''(t,x) = \sum_{j\in\mathcal{N}_i(t)} a_{ij}(t-\gamma_\sigma(t))d(h(x_i),h(x_j)),$$

and in this case it is not necessarily true that $f_i''(t,x)$ as an element of $T_{x_i}\mathbb{R}^m$ is inward-pointing relative to the convex hull of the neighbors of agent i. However, consensus can be guaranteed on $B_{\eta,m}$ by Theorem 2.21 when the graph $\mathcal{G}(t)$ is uniformly strongly connected by using the function $V(x_i) = x_i^T x_i$ in Theorem 2.21.

2.3.4 Avoiding discontinuities

Suppose that $\mathcal{F}$ contains only time-invariant functions, $\sigma \in \mathcal{S}_{|\mathcal{F}|,D,U}$ and Assumption 2.17 holds. We show how it is possible to modify the system defined by $\mathcal{F}$ and σ into a system where the right-hand side is no longer discontinuous in t. Close to each switching time we can modify the system so that there is a continuous in time transition between the two time-invariant functions that are being switched between. For the modified system where there are no longer any discontinuities in t, Assumption 2.17 still holds and if there is a V such that Assumption 2.18 holds for this V for the discontinuous system (or a W such that Assumption 2.19 holds for this W for the discontinuous system), then Assumption 2.18 holds for V (or Assumption 2.19 holds for W) for the modified continuous system.

We start by extending $\mathcal{F}$ with time varying functions to a finite set of functions $\mathcal{F}'$ (Lipschitz in x on $\mathcal{D}$, uniformly with respect to t), where $\mathcal{F}'$ contains functions that serve as continuous in time transitions between functions in $\mathcal{F}$. For $\sigma \in \mathcal{S}_{|\mathcal{F}'|,D,U}$ we create a $\sigma' \in \mathcal{S}_{|\mathcal{F}'|,D,U}$ in the following way. Let $\tau_D^{\sigma'} < \tau_D^{\sigma}$. At each switching time τ_k of σ, we squeeze in an extra interval of length $\tau_D^{\sigma'}$ during which the neighbor set $\mathcal{N}_i^{\sigma'}$ of each agent i is equal to $\mathcal{N}_i^{\sigma}(\tau_{k-1}) \cup \mathcal{N}_i^{\sigma}(\tau_k)$. These added time intervals can be seen as transition periods, during which there is a continuous in time transition between two functions in $\mathcal{F}$.

We extend $\mathcal{F}$ to $\mathcal{F}'$ in the following way. First we define a continuous function

$$\alpha : (-\infty, \infty) \to [0, 1],$$

such that $\alpha(0) = 1$ and $\alpha(\tau_D^{\sigma'}) = 0$. Secondly, for each pair of functions $(\tilde{f}_i, \tilde{f}_j)$ where $\tilde{f}_i$ and $\tilde{f}_j$ belong to $\mathcal{F}$, we define a function

$$\tilde{f}_{(i,j)}(t, x) = \alpha(t)\tilde{f}_i(x) + (1 - \alpha(t))\tilde{f}_j(x).$$

The set of functions $\mathcal{F}'$ is the set of all functions $\tilde{f}_i$ and $\tilde{f}_{(i,j)}$. At each switching time of the original system, between the right-hand side $\tilde{f}_i$ and $\tilde{f}_j$, we now squeeze in the function $\tilde{f}_{(i,j)}$ during a time period of length $\tau_D^{\sigma'}$ in the new system. Note that we can make $\tau_D^{\sigma'}$ much smaller than τ_D^{σ}.

If all functions in $\mathcal{F}$ are time-invariant $\mathcal{C}^1$ functions in x, and we want the new continuous right-hand side to be $\mathcal{C}^1$ in t when x is regarded as a function of t, we impose the additional requirement that $\dot{\alpha}(0) = 0$ and $\dot{\alpha}(\tau_D^{\sigma'}) = 0$. A function fulfilling these requirements is

$$\alpha(t) = \frac{1}{2} + \frac{1}{2}\cos\left(\frac{t\pi}{\tau_D^{\sigma'}}\right).$$

We now proceed with some other application oriented examples.

2.3.5 Consensus on $SO(3)$ using the Axis-Angle Representation

This is a brief introduction to the subject of Chapter 3 where a system of n rotation matrices in $SO(3)$ (controlled on a kinematic level) shall asymptotically reach consensus in the rotation matrices. For a rotation matrix R_i there is a corresponding vector x_i, referred to as the Axis-Angle Representation of R_i. Locally around the identity matrix, in terms of kinematics we have that

$$\dot{R}_i = R_i\widehat{\omega}_i \qquad \text{or} \qquad \dot{x}_i = L_{x_i}\omega_i,$$

where

$$L_{x_i} = I_3 + \frac{\widehat{x}_i}{2} + \frac{1}{\|x_i\|^2}\left(1 - \frac{\text{sinc}(\|x_i\|)}{\text{sinc}^2(\frac{\|x_i\|}{2})}\right)\widehat{x}_i^2,$$

and $\widehat{\omega}_i$, $\widehat{x}_i$ are the skew-symmetric matrices generated by $\omega_i, x_i \in \mathbb{R}^3$ respectively, see Chapter 3, and we require that $x_i(t_0) \in B_{\pi,3}$ for all i. Now we consider the case when

$$\omega_i = \sum_{j \in \mathcal{N}_i(t)} \alpha_{ij}(t - \gamma_\sigma(t))(x_j - x_i),$$

where the continuous function $\alpha_{ij}(t)$ is positive and bounded, and $\sigma \in \mathcal{S}_{|\mathcal{F}|,D,U}$. The symmetric part of the matrix L_{x_i} is positive definite on $B_{\pi,3}$, and the system is at an equilibrium if and only if $x = (x_1, \ldots, x_n)^T \in \mathcal{A}$.

Let $V(x_i) = x_i^T x_i$. By observing that $x_i^T L_{x_i} = x_i^T$, it is easy to show that Assumption 2.18 holds for V. We can apply Theorem 2.20 with $\widehat{\beta}_1(\|x_i\|) = \widehat{\beta}_2(\|x_i\|) = \|x_i\|^2$, and show that any ball $\bar{B}_{r,3}$ is invariant for $r < \pi$ and may serve as $\mathcal{D} = \mathcal{D}^*(\infty)$. Also, by Theorem 2.21, if the graph $\mathcal{G}_{\sigma(t)}$ is uniformly strongly connected, then $\mathcal{A}$ is globally quasi-uniformly attractive.

2.3.6 Consensus on $SO(3)$ for networks of cameras using the epipoles

This example is based on the work in [9, 10], where a more detailed description can be obtained. Undefined terminology that is used in this example can be found in any standard text book on computer vision such as [11]. This example also regards consensus for rotation matrices, but the setting is a bit different and the rotations are restricted to be only around one common axis. We consider a system of n robots positioned in the two-dimensional plane. Each robot is equipped with a camera and is at each time observing a subset of the other robots. Since the rotational axes are fixed and equal, we only need the scalar θ_i in order to represent the rotation of each agent i, where θ_i is the angle of rotation. In the context of this example, instead of letting $\theta_i \in [0, \pi)$, we let $\theta_i \in (-\pi, \pi)$. We assume that all the cameras have the same intrinsic parameters.

The robots are not moving and are only rotating. The position of each robot i in the world coordinate frame is given by $x_i \in \mathbb{R}^2$. The position of agent j in the body frame of agent i is given by

$$x_{ij}(\theta_i) = R(\theta_i)(x_j - x_i),$$

where

$$R(\theta_i) = \begin{bmatrix} \cos(\theta_i) & -\sin(\theta_i) \\ \sin(\theta_i) & \cos(\theta_i) \end{bmatrix}.$$

Let

$$\psi_{ij}(\theta_i) = \text{arctan}\left(\frac{x_{ijx}}{x_{ijy}}\right),$$

where x_{ijx} and x_{ijy} are the two components of x_{ij}.

Now, instead of measuring the rotation directly, using stereo vision one retrieves the *epipoles* as certain nullspace vectors of the so called fundamental matrix. The fundamental matrix defines the (epipolar) geometric relationship between two images [11], and should not be mixed up with the fundamental matrix in the solution of a linear time-invariant dynamical system. We will only consider the x-component (the first component) of these two-dimensional epipole vectors, which are defined as

$$e_{ij} = \alpha \tan(\psi_{ij}), \quad e_{ji} = \alpha \tan(\psi_{ij} - \theta_{ij}),$$

where $\theta_{ij} = \theta_j - \theta_i$ and $\alpha = 1$ if the cameras are calibrated, *i.e.*, the focal length is known (we assume that the position of the principal point is known in the image plane), otherwise $\alpha > 0$ is unknown.

Let us define

$$\omega_{ij} = \arctan\left(\frac{e_{ij}}{\beta}\right) - \arctan\left(\frac{e_{ji}}{\beta}\right)$$

where $\beta > 0$ is a constant to choose.

We define $\theta(t) = (\theta_1(t), \ldots, \theta_n(t))^T$ and the region

$$\mathcal{D} = \{\theta : -\theta_M \leq \theta_i \leq \theta_M \text{ for } i = 1, \ldots, n\},$$

where $0 < \theta_M \ll \pi/2$. The set $\mathcal{D}$ could be seen as being a function of θ_M. Furthermore, we assume $x_{ijx}(0)/x_{ijy}(0) = 1$ for all i, j, in which case the robots or the cameras are standing on a line and are oriented in the same direction that forms an angle of $\pi/4$ to the direction of the line. This means that $\psi_{ij} \in \{-\pi/4, 3\pi/4\}$ for all i, j and this configuration is illustrated in Figure 2.6.

Let us choose the dynamics for the system as

$$\begin{aligned}
\dot{\theta}_1 &= \sum_{j \in \mathcal{N}_1(t)} \alpha_{1j}(t - \gamma_\sigma(t))\omega_{1j}, \\
&\vdots \\
\dot{\theta}_n &= \sum_{j \in \mathcal{N}_n(t)} \alpha_{nj}(t - \gamma_\sigma(t))\omega_{nj}.
\end{aligned}$$

We assume that $\alpha_{ij}(t)$ is continuous, positive and bounded, and $\sigma \in \mathcal{S}_{|\mathcal{F}|,D,U}$. Provided θ_M is sufficiently small, on $\mathcal{D}$ it can be shown that ω_{ij} is Lipschitz for all $(i, j) \in \mathcal{V} \times \mathcal{V}$. It is obvious that Assumption 2.17 holds. We choose θ_M small enough so that $|\omega_{ij}| < \pi/2$ on $\mathcal{D}$. According to [9], it is true that

$$\theta_{ij}(t) \neq 0 \Longrightarrow \theta_{ij}(t)\omega_{ij}(t) > 0. \tag{2.2}$$

Let us now consider the function $V(\theta_i) = \theta_i^2$, where

$$\frac{d}{dt}V(\theta_i) = 2\theta_i \sum_{j \in \mathcal{N}_i(t)} \alpha_{ij}(t)\omega_{ij}.$$

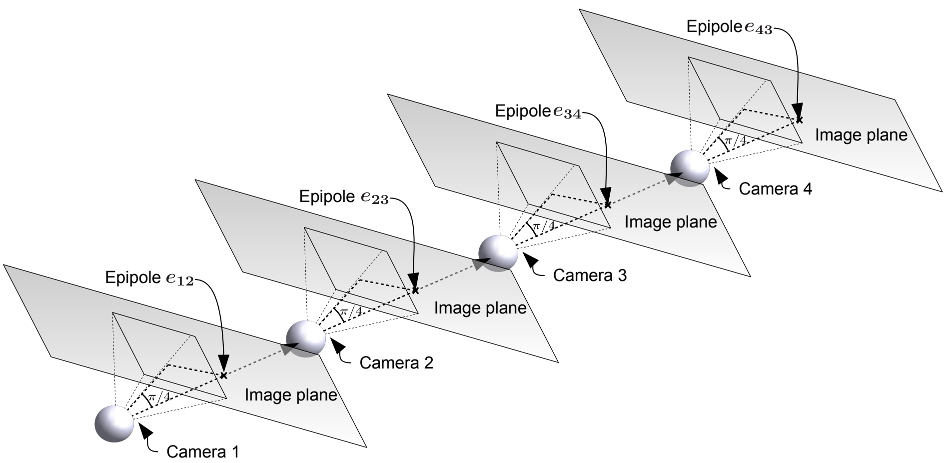

Figure 2.6: When $\theta_i = 0$ for all i we assume that $\psi_{ij} \in \{-\pi/4, 3\pi/4\}$ for all i, j. The epipole e_{ij} is the point in the image plane of robot (camera) i where the vector between the position of robot i and the position of robot j crosses the image plane. This vector is expressed in the body coordinate frame of robot i.

Suppose $i \in \mathcal{I}_V(t,t)$, and $\theta_j(t) = \theta_i(t)$ for all $j \in \mathcal{N}_i(t)$, then it follows that $\dot{V}(\theta_i(t)) = 0$. Now, consider the situation where $i \in \mathcal{I}_V(t,t)$ and there is at least one j such that $\theta_j(t) \neq \theta_i(t)$ when $j \in \mathcal{N}_i(t)$. Since $i \in \mathcal{I}_V(t,t)$, if $\theta_i \neq \theta_j$, using (2.2) we get that

$$\theta_i \omega_{ij} < 0.$$

Hence, Assumption 2.18 also holds.

In Theorem 2.20 we can now choose $\widehat{\beta}_1(|\theta_i|) = \widehat{\beta}_2(|\theta_i|) = |\theta_i|^2$ and reach the conclusion that $\mathcal{D}$ is positively invariant and $\mathcal{D}^*(\infty) = \mathcal{D}$. The point 0 is uniformly stable. Furthermore, according to Theorem 2.21, $\mathcal{A}$ is globally quasi-uniformly attractive relative to $\mathcal{D}^*(\infty)$ if $\mathcal{G}_{\sigma(t)}$ is uniformly strongly connected. But we can actually weaken the assumptions on the graph $\mathcal{G}_{\sigma(t)}$.

Let us consider the function $W(\theta_i, \theta_j) = (\theta_j - \theta_i)^2$, where

$$\begin{aligned}
&\frac{d}{dt}W(\theta_i, \theta_j) \\
&= 2(\theta_j - \theta_i)\left(\sum_{k\in\mathcal{N}_j(t)} \alpha_{jk}(t-\gamma_\sigma(t))\omega_{jk} - \sum_{l\in\mathcal{N}_l(t)} \alpha_{il}(t-\gamma_\sigma(t))\omega_{il}\right).
\end{aligned}$$

If $(i,j) \in \mathcal{J}_V(t,t)$, we can without loss of generality assume that $\theta_j \geq \theta_k$ and that $\theta_i \leq \theta_k$ for all $k \in \mathcal{V}$. This implies that $\text{sign}(\theta_{ij}) = \text{sign}(\theta_{kj}) = \text{sign}(\theta_{il}) = 1$ for all $k, l \in \mathcal{V}$, so from (2.2) we get that $\text{sign}(\theta_{ij})\text{sign}(\omega_{jk}) = -1$ and $\text{sign}(\theta_{ij})\text{sign}(\omega_{il}) = 1$. Thus Assumption 2.19 holds for $f_{W,m,m}$ and Theorem 2.22 can be used. Thus, when $x(t) \in \mathcal{D}^*(\infty)$ it follows that $\mathcal{A}$ is globally uniformly asymptotically stable relative to $\mathcal{D}^*(\infty)$ if and only if $\mathcal{G}_{\sigma(t)}$ is uniformly quasi-strongly connected.

2.3.7 Stabilization

Let us now, as a special case of the consensus problem, consider the stabilization problem, where we use our consensus results in order to provide known conditions for when $\{0\}$ is asymptotically stable for a system

$$\dot{y} = g(t, y), \tag{2.3}$$

where $y \in \mathbb{R}^m$.

We show that this problem is a special case of a consensus problem with two agents in $\mathbb{R}^m$, so that we can use Theorem 2.22 in order to show that $\{0\}$ is globally uniformly asymptotically stable relative to some compact invariant set in $\mathbb{R}^m$.

Proposition 2.25. *Suppose there is an invariant compact set $\mathcal{D}' \subset \mathbb{R}^m$ containing the point 0 and a finite set $\mathcal{F}' = \{\tilde{f}'_1, \ldots, \tilde{f}'_{|\mathcal{F}'|}\}$ of functions that are piecewise continuous in t and Lipschitz in y on $\mathcal{D}'$, uniformly with respect to t. For each function $\tilde{f}'_k$ it holds that $\tilde{f}'_k(t,0) = 0$ for all k and all t. Furthermore, $\sigma \in \mathcal{S}_{|\mathcal{F}'|,D,U}$ and the right-hand side of* (2.3) *is*

$$g(t,y) = \tilde{f}'_{\sigma(t)}(t - \gamma_\sigma(t), y).$$

If there is a positive definite function $V(y)$, which is continuously differentiable on an open set containing $\mathcal{D}'$ such that

$$\nabla V(y)\tilde{f}'_i(t,y) < 0$$

for all $i \in \{1, \ldots, |\mathcal{F}'|\}$, all t and nonzero y in $\mathcal{D}'$, then $\{0\}$ is globally uniformly asymptotically stable relative to $\mathcal{D}'$.

Proof: The set $\mathcal{D}'$ is assumed to be invariant for any choices of switching signal functions in $\mathcal{S}_{|\mathcal{F}'|,D}$. Let us define a system of two agents, agent 1 and agent 2. Based on the set $\mathcal{F}'$ we create a new set $\mathcal{F}''$ of functions with range $\mathbb{R}^{2m}$ in the following way

$$\mathcal{F}'' = \{(\tilde{f}'_1(t, y_2 - y_1), 0)^T, \ldots, (\tilde{f}'_{|\mathcal{F}'|}(t, y_2 - y_1), 0)^T\}.$$

Now, for all $t \geq 0$ and for all $\sigma \in \mathcal{S}_{|\mathcal{F}''|,D}$ we define

$$\mathcal{N}_1^\sigma(t) = \{1,2\} \quad \text{and} \quad \mathcal{N}_2^\sigma(t) = \{2\}.$$

The system dynamics for this extended system is given as

$$\begin{aligned} \dot{y}_1 &= \tilde{f}_1'(t - \gamma_\sigma(t), y_2 - y_1), \\ \dot{y}_2 &= 0. \end{aligned}$$

This system fulfills Assumption 2.17 and we define a function W as

$$W(y_1, y_2) = V(y_2 - y_1).$$

The function W fulfills Assumption 2.19. Now, if the initial positions of $y_1(t)$ and $y_2(t)$ are $y_1^0 \in \mathcal{D}'$ and $y_2^0 = 0 \in \mathcal{D}'$ respectively, we see that the dynamics for the extended system is equivalent to the original system (2.1). For the extended system, the set $\mathcal{D}' \times \{0\} \subset ((\mathcal{D}')^2)^*(\infty)$. Since $\mathcal{G}_{\sigma(t)}$ is uniformly quasi-strongly connected, $\mathcal{A}$ is globally uniformly asymptotically stable relative to $((\mathcal{D}')^2)^*(\infty)$. Since $y_2(t) = 0$ for all t, we see that the state will converge to the point $(0,0)^T \in \mathbb{R}^{2m}$ in the extended system. ■

2.4 Proofs

In this section we provide the proofs. Theorem 2.20 is proven directly, whereas for the two other theorems, in order to make the proofs more comprehensible, we first introduce some lemmas, used as building blocks for the final proof.

Proof of Lemma 2.2: We can construct the σ' as follows. Let us first choose $\tau_D^{\sigma'} = \tau_D^\sigma$ and $\tau_U^{\sigma'} \geq 2\tau_D^\sigma$. For any k such that $\tau_{k+1} - \tau_k > \tau_U^{\sigma'}$, we split $[\tau_k, \tau_{k+1})$ into a partition of smaller half-open intervals each with equal length smaller than $\tau_U^{\sigma'}$ but larger than $\tau_D^{\sigma'}$. On these half-open intervals $\sigma'(t) = \sigma(t)$. For all k such that $\tau_{k+1} - \tau_k \leq \tau_U^{\sigma'}$ we let $\sigma'(t) = \sigma(t)$ for $t \in [\tau_k, \tau_{k+1})$. ■

Proof of Lemma 2.3: Let $\tau_U = \tau_U^\sigma$ and $\tau_D = \tau_D^\sigma$. The function σ' is constructed in a way similar to the procedure in the proof of Lemma 2.2, but here the number of half-open intervals that $[\tau_k, \tau_{k+1})$ is split into is bounded from above by $\lfloor \tau_U/\tau_D \rfloor$.

We define the partition of intervals as follows

$$\begin{aligned} [\tau_k, \tau_{k+1}) = &\left(\bigcup_{i=1}^{\lfloor (\tau_{k+1} - \tau_k)/\tau_D \rfloor - 1} [\tau_k + (i-1)\tau_D, \tau_k + i\tau_D) \right) \\ &\cup [\tau_k + (\lfloor (\tau_{k+1} - \tau_k)/\tau_D \rfloor - 1)\tau_D, \tau_{k+1}). \end{aligned}$$

We define $\mathcal{F}'$ as follows

$$\begin{aligned}\mathcal{F}' = \{&\tilde{f}'_1 = \tilde{f}_1(t,x),\\ &\tilde{f}'_2 = \tilde{f}_1(t+\tau_D,x),\dots,\\ &\tilde{f}'_{\lfloor \tau_U/\tau_D \rfloor} = \tilde{f}_1(t+(\lfloor \tau_U/\tau_D \rfloor - 1)\tau_D, x),\dots,\\ &\tilde{f}'_{\lfloor \tau_U/\tau_D \rfloor (N-1)+1} = \tilde{f}_N(t+\tau_D,x),\dots,\\ &\tilde{f}'_{\lfloor \tau_U/\tau_D \rfloor N} = \tilde{f}_N(t+(\lfloor \tau_U/\tau_D \rfloor - 1)\tau_D, x)\},\end{aligned}$$

where $N = |\mathcal{F}|$. The set $\mathcal{F}'$ is constructed by creating $\lfloor \tau_U/\tau_D \rfloor - 1$ number of new time-shifted functions from each function $\tilde{f}_i \in \mathcal{F}$.

Now σ' is constructed by choosing a function in $\mathcal{F}'$ on each half-open interval in each partition so that

$$\tilde{f}_{\sigma(t)}(t,x) = \tilde{f}'_{\sigma'(t)}(t,x)$$

for all t and $x \in \mathcal{D}$. ■

Proof of Lemma 2.12: We only prove the first statement for $f_{V,m}$, the procedure in order to prove the second statement for $f_{V,m,m}$ is similar and hence omitted.

Since V is Lipschitz in x on $\mathcal{D}$ it follows that $f_{V,m}$ is Lipschitz in x on $\mathcal{D}$. Since $f_{V,m}$ is Lipschitz in x, it follows that

$$D^+(f_{V,m}(x(t))) = D^+_{f_{V,m}}(f_{V,m}(x^*)),$$

where

$$D^+_{f_{V,m}}(f_{V,m}(x^*)) = \limsup_{\epsilon \downarrow 0} \frac{f_{f_{V,m}}(t+\epsilon, x_0 + \epsilon f_{V,m}(t,x^*))}{\epsilon}$$

and $x^* = x(t)$. This result can be obtained from Chapter 1 in [12]. In [13] it is formulated as a Theorem (Theorem 4.1 in Appendix I).

The next step is to prove that

$$D^+_{f_{V,m}}(f_{V,m}(t,x^*)) = \max_{i \in \mathcal{I}_V(t,t)} \frac{d}{dt} V(x_i(t)).$$

This result can for example be obtained from Theorem 2.1. in [14]. ■

Proof of Lemma 2.15: Since $\mathcal{D}$ is compact, we only need to verify that $\mathcal{D}^*(\tilde{t})$ is closed in order to show that $\mathcal{D}^*(\tilde{t})$ is compact. Suppose there is $x_0 \notin \mathcal{D}^*(\tilde{t})$, such that there is a sequence $\{x_0^i\}_{i=1}^\infty$ that converges to x_0, where each element in the sequence is in $\mathcal{D}^*(\tilde{t})$. We would like to obtain a contradiction by showing that the solution $x^\sigma(t,t_0,x_0)$ does exist in $\mathcal{D}$ on the interval $[t_0, t_0+\tilde{t})$ for any t_0, and $\sigma \in \mathcal{S}_{|\mathcal{F}|,D}$.

By using the fact that $\mathcal{D}$ is compact and that the right-right side of (2.1) is uniformly Lipschitz in x on $\mathcal{D}$ and piecewise continuous in t, we can use the Continuous Dependency Theorem of initial conditions in order to guarantee that $\{x^\sigma(t,t_0,x_0^i)\}_{i=1}^\infty$ is a Cauchy sequence for arbitrary $t \in [t_0, t_0+\tilde{t})$. Now we know, since $\mathcal{D}$ is compact, that

$$x^*(t) = \lim_{i\to\infty} x^\sigma(t,t_0,x_0^i)$$

exists and $x^*(t) \in \mathcal{D}$. We want to prove that $x^*(t)$ is the solution for (2.1) on $[t_0, t_0 + \tilde{t})$ for the given σ, t_0 and x_0.

$$\begin{aligned} x^*(t) &= \lim_{i\to\infty} x^\sigma(t, t_0, x_0^i) \\ &= \lim_{i\to\infty} \int_{t_0}^t f(s, x^\sigma(s, t_0, x_0^i))ds \\ &= \int_{t_0}^t \lim_{i\to\infty} f(s, x^\sigma(s, t_0, x_0^i))ds \\ &= \int_{t_0}^t f(s, x^*(s)). \end{aligned}$$

Hence, $x^*(t)$ is contained $\mathcal{D}$ for all t, but since σ and t_0 were arbitrary, it follows that $x_0 \in \mathcal{D}^*(\tilde{t})$ which is a contradiction.

Now we prove the statement that $\mathcal{D}^*(\infty)$ is invariant. Suppose $x_0 \in \mathcal{D}^*(\infty)$ is arbitrary and let

$$y = x^{\sigma_1}(t_1, t_0, x_0)$$

for $\sigma_1 \in \mathcal{S}_{|\mathcal{F}|,D}$ and $t_1 \geq t_0$. Consider $x^{\sigma_2}(t, t_1', y)$ for some arbitrary $\sigma_2 \in \mathcal{S}_{|\mathcal{F}|,D}$ and t_1'. We need to show that $x^{\sigma_2}(t, t_1', y)$ is contained in $\mathcal{D}$ for all $t \geq t_1'$.

We define

$$\sigma(t) = \begin{cases} \sigma_1(t - (t_1' - t_1)) & \text{if } t < t_1', \\ \sigma_2(t) & \text{if } t \geq t_1'. \end{cases}$$

which is contained in $\mathcal{S}_{|\mathcal{F}|,D}$. Thus

$$x^{\sigma_2}(t, t_1', y) = x^\sigma(t, t_0 + (t_1' - t_1), x_0)$$

which is contained in $\mathcal{D}$ for all $t \geq t_0$ since $x_0 \in \mathcal{D}^*(\infty)$. Thus $y \in \mathcal{D}^*(\infty)$.

■

Proof of Theorem 2.20: Since the origin is an interior point of $\mathcal{D}$, there is a ball $B_{\epsilon,m}$ such that $(B_{\epsilon,m})^n \subset \mathcal{D}$ and $\epsilon > 0$. Suppose $x_0 \in (B_{\epsilon,m})^n$, then there is a closed ball

$$\bar{B}_{\epsilon',mn}(x_0) \subset (B_{\epsilon,m})^n$$

with $\epsilon' > 0$. Now according to Theorem 3.1. in [8], there is a $\delta' > 0$ such that the system has a unique solution $x(t, t_0, x_0)$ on $[t_0, t_0 + \delta']$. We choose $[t_0, t_0 + T')$ as the maximal half-open interval of existence of the unique solution. We know there are class $\mathcal{K}$ functions β_1 and β_2 such that

$$\beta_1(\|y\|) \leq V(y) \leq \beta_2(\|y\|)$$

for $y \in \mathbb{R}^m$.

Now, using property (2) of Assumption 2.18 we get from the Comparison Lemma (Lemma 3.4 in [8]), that

$$f_{V,m}(x(t)) \leq f_{V,m}(x_0)$$

for $t \in [t_0, t_0 + T')$. Now let $\delta = \beta_2^{-1}(\beta_1(\epsilon))$. We suppose that x_0 was chosen such that

$$x_i(t_0) \in \bar{B}_{\delta,m} \subset \bar{B}_{\epsilon,m} \text{ for all } i.$$

It follows that for $t \in [t_0, t_0 + T')$,

$$\begin{aligned}
&\max_{i\in\{1,\dots,n\}} \|x_i(t)\| = \beta_1^{-1}(\beta_1(\max_{i\in\{1,\dots,n\}} \|x_i(t)\|)) \\
&= \beta_1^{-1}(\max_{i\in\{1,\dots,n\}} \beta_1(\|x_i(t)\|)) \le \beta_1^{-1}(f_{V,m}(x(t))) \\
&\le \beta_1^{-1}(f_{V,m}(x(t_0))) \le \beta_1^{-1}(\max_{i\in\{1,\dots,n\}} \beta_2(\|x_i(t_0)\|)) \\
&\le \beta_1^{-1}(\beta_2(\max_{i\in\{1,\dots,n\}}(\|x_i(t_0)\|))) \le \beta_1^{-1}(\beta_2(\delta)) = \epsilon.
\end{aligned}$$

Now it follows by using Theorem 3.3 in [8], that the solution will stay in $(\bar{B}_{\epsilon,m})^n$ for arbitrary times larger than t_0, *i.e.*, $T' = \infty$. ■

In the following lemma we use the positive limit set $L^+(x_0, t_0)$ of the solution $x(t, t_0, x_0)$ when $x_0 \in \mathcal{D}^*(\infty)$ (we assume that $\sigma \in \mathcal{S}_{|\mathcal{F}|,D}$ is fixed here). This limit set exists and is compact, and $x(t)$ approaches it as the time goes to infinity, however it is not guaranteed to be invariant which is the case for an autonomous system. Now, in the case that $x_0 \in \mathcal{D}^*(\infty)$, the set $L^+(x_0, t_0)$ is contained in $\mathcal{D}^*(\infty)$, so any alternative solution of (2.1) that starts in $L^+(x_0, t_0)$ will remain in $\mathcal{D}^*(\infty)$.

Lemma 2.26. *Suppose that $x_0 \in \mathcal{A}^c \cap \mathcal{D}^*(\infty)$ and that Assumption 2.18 (2) holds. Suppose that there is a non-negative function $\beta(y, \tilde{t})$ that is increasing in $\tilde{t}$ for $y \in \mathcal{A}^c \cap \mathcal{D}^*(\infty)$. Furthermore, suppose that for $y \in \mathcal{A}^c \cap \mathcal{D}^*(\infty)$, there is $\tilde{t}'(y) > 0$ such that for $\tilde{t} \ge \tilde{t}'(y)$ it holds that $\beta(y, \tilde{t}) > 0$.*

If

$$f_{V,m}(x(t_0 + \tilde{t}, t_0, x_0)) - f_{V,m}(x_0) \le -\beta(x_0, \tilde{t}),$$

then $x(t) \to \mathcal{A}$ as $t \to \infty$ for all t_0.

Furthermore, if β is lower semi-continuous in y, and $\tilde{t}'$ is independent of y, then $\mathcal{A}$ is globally quasi-uniformly attractive relative to $\mathcal{D}^*(\infty)$.

Proof: Let us consider an arbitrary $x_0 \in \mathcal{A}^c \cap \mathcal{D}^*(\infty)$ and t_0 for which the solution $x(t, t_0, x_0)$ generates the limit set $L^+(x_0, t_0) \subset \mathcal{D}^*(\infty)$. From the fact that $f_{V,m}(x(t))$ is continuous in t, the fact that $f_{V,m}(x(t))$ is decreasing and the fact that $x(t)$ is contained in the compact set $\mathcal{D}^*(\infty)$, it follows that $f_{V,m}(x(t, t_0, x_0))$ converges to a lower bound $\alpha(x_0, t_0) \ge 0$ as $t \to \infty$. Suppose $L^+(x_0, t_0) \not\subset \mathcal{A}$. We want to prove the lemma by showing that this assumption leads to a contradiction. Let $t_1 \ge t_0$ be arbitrary and y_1 be an arbitrary point in $L^+(x_0, t_0) \cap \mathcal{A}^c$. Since $y_1 \in \mathcal{D}^*(\infty)$, we know that $x(t, t_1, y_1)$ exists and is contained in $\mathcal{D}^*(\infty)$ for any time $t > t_1$.

Since each function in $\mathcal{F}$ is uniformly Lipschitz continuous in x with respect to t on the compact set $\mathcal{D}^*(\infty)$ and the number of functions in $\mathcal{F}$ is finite, we can use the Continuous

Dependency Theorem of initial conditions (*e.g.*, Theorem 3.4 in [8]). For $\epsilon > 0$ and $\tilde{t} \geq 0$ there is $\delta(\epsilon, \tilde{t}) > 0$ such that

$$\|y_1 - y_1'\| \leq \delta \Longrightarrow \|f_{V,m}(x(t_2, t_1, y_1)) - f_{V,m}(x(t_2, t_1, y_1'))\| \leq \epsilon,$$

where $t_2 = t_1 + \tilde{t}$. Let us now choose $\tilde{t} \geq \tilde{t}'(y_1)$ and $\epsilon = \beta(y_1, \tilde{t})/2$, from which it follows that ϵ is guaranteed to be positive. Since $y_1 \in L^+(x_0, t_0)$, there is $t' > t_0$ such that $\|y_1 - x(t', t_0, x_0)\| \leq \delta$. We choose $t_1 = t'$ and $y_1' = x(t', t_0, x_0)$. But then since $f_{V,m}(x(t_2, t_1, y_1)) \leq \alpha - \beta(y_1, \tilde{t})$ it follows that $f_{V,m}(x(t_2, t_0, x_0)) \leq \alpha - \beta(y_1, \tilde{t})/2 = \alpha - \epsilon$. Since $\epsilon > 0$, this contradicts the fact that α is a lower bound for $f_{V,m}$.

Now we shall prove the second part of the statement. We prove this by a contradiction argument. Suppose there is $\eta > 0$ such that there is no $T(\eta) \in \mathbb{R}^+$ such that

$$\min_{t \in [t_0, t_0 + T(\eta)]} \text{dist}(x(t, t_0, x_0), \mathcal{A}) < \eta$$

for all $x_0 \in \mathcal{D}^*(\infty)$ and all t_0. Let

$$\beta_{\min} = \min_{z \in \mathcal{D}^*(\infty) \cap \{y : \text{dist}(y, \mathcal{A}) \geq \eta\}} \beta(z, \tilde{t}') > 0.$$

Now, for each positive integer N there is $t_0(N) \geq 0$ and $x_0(N) \in \mathcal{D}^*(\infty)$ such that

$$\min_{t \in [t_0(N), t_0(N) + N\tilde{t}']} \text{dist}(x(t, t_0(N), x_0(N)), \mathcal{A}) \geq \eta,$$

otherwise we can choose $T(\eta) = N\tilde{t}$, but we assumed that there is no such $T(\eta)$. We have that

$$f_{V,m}(x(t, t_0(N) + N\tilde{t}', x_0(N))) - f_{V,m}(x(t, t_0(N), x_0(N))) \leq -N\beta_{\min}.$$

Now,

$$f_{V,m}(x(t, t_0(N) + N\tilde{t}', x_0(N))) - f_{V,m}(x(t, t_0(N), x_0(N))) \to -\infty \quad \text{as } N \to \infty,$$

which is a contradiction since $f_{V,m}$ is bounded on $\mathcal{D}^*(\infty)$. ■

Remark 2.4. Note that the special structure of $\mathcal{A}$ being the consensus set is not used in this proof. Also the special structure of $f_{V,m}$ is not used in the proof.

Lemma 2.27. *Suppose Assumption 2.17 and 2.18 (2,3) hold, $\sigma \in \mathcal{S}_{|\mathcal{F}|,D,U}$, $x^\sigma(t_0) \in \mathcal{D}^*(\infty) \cap \mathcal{A}^c$ and $\mathcal{G}_{\sigma(t)}$ is uniformly strongly connected. If t_0 is a switching time of σ, it follows that $f_{V,m}(x^\sigma(t)) < f_{V,m}(x^\sigma(t_0))$ for any any $t \geq n(T^\sigma + 2\tau_D)$, where T^σ is given in Definition 2.8.*

Proof: We assume without loss of generality, that the longest time between two consecutive switches of $\sigma(t)$ is bounded from above by $2\tau_D$. This assumption is justified by Lemma 2.3. Let us consider the solution at an arbitrary switching time τ_k, and prove that $f_{V,m}(x(n(T^\sigma + 2\tau_D) + \tau_k)) < f_{V,m}(x(\tau_k))$.

Part 1: We show that if $i \notin \mathcal{I}_V(\tau_k, s)$, then $i \notin \mathcal{I}_V(\tau_k, t)$ for $t > s \geq \tau_k$. Suppose that $i \notin \mathcal{I}_V(\tau_k, s)$ and that there is a $t' > s$ such that $i \in \mathcal{I}_V(\tau_k, t')$. Then since $V(x_i(t))$ is continuous, there is a $t_1 > s$ such that $i \in \mathcal{I}_V(\tau_k, t_1)$ and $i \notin \mathcal{I}_V(\tau_k, t)$ for $t \in [s, t_1)$. Since $\sigma \in \mathcal{S}_{|\mathcal{F}|,D}$ we know that there is $\epsilon > 0$ such that $\sigma(t)$ is constant and $f_i(t, x(t))$ is continuous during $[t_1 - \epsilon, t_1)$, where $t_1 - \epsilon > s$.

We define the following constant

$$\dot{V}_i^* = \lim_{t \uparrow t_1} \dot{V}(x_i(t)).$$

Now we claim that $\dot{V}_i^* \leq 0$, which we justify as follows. If t_1 is not equal to a switching time, it is immediate that this claim is true since $i \in \mathcal{I}_V(\tau_k, t_1)$, see Assumption 2.18 (2) and Lemma 2.12. On the other hand, if t_1 is equal to a switching time, the claim is also true and can be shown as follows. If σ is the switching signal function for our solution, we can create another switching signal function $\sigma' \in \mathcal{S}_{|\mathcal{F}|,D}$ which satisfies

$$\sigma'(t) = \sigma(t) \quad 0 \leq t < t_1 \quad \text{and} \quad \sigma'(t_1) = \sigma(t_1 - \epsilon).$$

So,

$$\dot{V}_i^* = \lim_{t \uparrow t_1} \dot{V}(x_i(t)) = \dot{V}(x_i^{\sigma'}(t)) \leq 0,$$

where the last inequality follows from Assumption 2.18 (2) and Lemma 2.12.

We now know that $\dot{V}_i^* \leq 0$. Thus there are two options for $\dot{V}^*$; either it is (1) strictly negative or (2) zero. In case (1), since $\sigma(t)$ is piecewise right-continuous there is a positive $\epsilon' < \epsilon$ such that $\dot{V}(x_i(t))$ is continuous and strictly negative on $[t_1 - \epsilon', t_1)$. We also know, since $V(x_i(t_1)) = f_{V,m}(x(\tau_k))$, that $V(x_i(t)) \leq V(x_i(t_1))$ for all $t \geq \tau_k$. Using these two facts, we get that

$$V(x_i(t_1)) = V(x_i(t_1 - \epsilon')) + \int_{t_1 - \epsilon'}^{t_1} \dot{V}(x_i(t))dt < V(x_i(t_1))$$

which is a contradiction.

Now we consider case (2). By using Assumption 2.18 (3) we can show that

$$x(t_1) = \lim_{t \uparrow t_1} x(t)$$

satisfies $x_i(t_1) = x_j(t_1)$ and $\lim_{t \uparrow t_1} \dot{V}(x_j(t)) = 0$ for all $j \in \mathcal{N}_i(t_1 - \epsilon)$ (note that $\sigma(t)$ is constant on $[t_1 - \epsilon, t_1)$, so $\mathcal{N}_i(t) = \mathcal{N}_i(t_1 - \epsilon)$ on this half-open interval), otherwise $V(x_j(t_1)) = f_{V,m}(x(\tau_k))$ and

$$\lim_{t \uparrow t_1} \dot{V}(x_j(t)) < 0,$$

which we just showed is a contradiction. For any j such that $j \in \mathcal{N}_i(t_1 - \epsilon)$ it holds that $x_k(t_1) = x_j(t_1)$ and $\lim_{t \uparrow t_1} \dot{V}(x_k(t)) = 0$, for all $k \in \mathcal{N}_j(t_1 - \epsilon)$. By using the same argument for the neighbors of the neighbors of agents in $\mathcal{N}_i(t_1 - \epsilon)$ and so on, we get that $x_i(t_1) = x_j(t_1)$ for all j that belongs to the connected component of node i in $\mathcal{G}_{\sigma(t_1-\epsilon)}$. Let us denote the state in this connected component by $x_{c_i}(t)$, where $c_i \subset \mathcal{V}$ are all neighbors in this connected component. It holds that

$$\lim_{t\uparrow t_1} \dot{V}(x_j(t)) = 0,$$

for all $j \in c_i$. During $[t_1 - \epsilon, t_1)$ the dynamics for x_{c_i} is

$$\dot{x}_{c_i} = f^{c_i}(t, x_{c_i}).$$

The function f^{c_i} is the part of f corresponding to the connected component c_i. By using Assumption 2.18 (3) we get that

$$\lim_{t\uparrow t_1} f^{c_i}(t, x_{c_i}(t)) = 0,$$

which is a contradiction, since x_{c_i} cannot reach such an equilibrium point in finite time without violating the uniqueness of the solution property (the functions in $\mathcal{F}$ are continuous in t and Lipschitz in x).

Part 2: Using part 1 we show that $\mathcal{I}_V(\tau_k, t)$ is empty for $t \geq n(T^\sigma + 2\tau_D) + \tau_k$. Suppose that $\mathcal{I}(\tau_k, \tau_k) \subset \mathcal{I}(\tau_k, \tau_{k'})$, where $\tau_{k'}$ is the first switching time after $\tau_k + T^\sigma$. We know from part 1 that $\mathcal{I}(\tau_k, \tau_k)^c \subset \mathcal{I}(\tau_k, \tau_{k'})^c$ (where complements are taken with respect to the set $\mathcal{V}$) which implies that $\mathcal{I}(\tau_k, \tau_{k'}) \subset \mathcal{I}(\tau_k, \tau_k)$, so our assumption has the consequence that $\mathcal{I}(\tau_k, \tau_k) = \mathcal{I}(\tau_k, \tau_{k'})$. Now, since $\mathcal{G}_{\sigma(t)}$ is uniformly strongly connected, there is a switching time $\tau_{k''}$ such that $\tau_k \leq \tau_{k''} \leq \tau_k + T^\sigma$ for which there are i, j that satisfy $i \in \mathcal{I}(\tau_k, \tau_k)$, $j \in \mathcal{I}(\tau_k, \tau_k)^c$ and $j \in \mathcal{N}_i(\tau_{k''})$. But then $j \in \mathcal{N}_i(s)$ for $s \in [\tau_{k''}, \tau_{k''} + \tau_D)$. Thus, $i \in \mathcal{I}_V^*(s)$ for $s \in [\tau_{k''}, \tau_{k''} + \tau_D)$, which means that $\dot{V}(x_i(s)) < 0$ on $[\tau_{k''}, \tau_{k''} + \tau_D)$. But since $i \in \mathcal{I}_V(\tau_k, s)$ for $s \in [\tau_{k''}, \tau_{k''} + \tau_D)$, the function $V(x_i(s))$ is constant on $[\tau_{k''}, \tau_{k''} + \tau_D)$, which is a contradiction. Our hypothesis that $\mathcal{I}(\tau_k, \tau_k) \subset \mathcal{I}(\tau_k, \tau_{k'})$ leads to a contradiction. Thus, $\mathcal{I}(\tau_k, \tau_{k'})$ is a strict subset of $\mathcal{I}(\tau_k, \tau_k)$.

Now, there are two cases for $\mathcal{I}_V(\tau_k, \tau_{k'})$. It is either (1) empty, or (2) nonempty. In case (1) we are done. In case (2) we have that $\mathcal{I}_V(\tau_k, \tau_{k'}) = \mathcal{I}_V(\tau_{k'}, \tau_{k'})$. We know that $\tau_{k'} \leq \tau_k + T^\sigma + 2\tau_D$ by the assumption that $\tau_U = 2\tau_D$. Now we can apply the same procedure for the set $\mathcal{I}_V(\tau_{k'}, \tau_{k'})$. By repeating the procedure n times, we know that $\mathcal{I}_V(\tau_k, t) = \emptyset$ for $t \geq n(T^\sigma + 2\tau_D) + \tau_k$. ■

Proof of Theorem 2.21: We prove this theorem by showing that there is a function β with the properties given in Lemma 2.27. For each $\sigma \in \mathcal{S}_{|\mathcal{F}|,D,U}$, there is a corresponding β.

Initially we assume that t_0 is a switching time. This assumption will be relaxed towards the end of the proof, so that we consider arbitrary times. We assume once again without loss of generality that $\tau_U = 2\tau_D$, and from Lemma 2.27 it follows that for a switching time t_0, it holds that $f_{V,m}(x(t_0 + \tilde{t})) < f_{V,m}(x(t_0))$ where $\tilde{t} \geq n(T^\sigma + 2\tau_D)$. In the following, let us choose $\tilde{t} \geq \tilde{t}' = n(2T^\sigma + 2\tau_D)$. Obviously, since $f_{V,m}(x(t))$ is decreasing,

$f_{V,m}(x(t_0+\tilde{t})) < f_{V,m}(x(t_0))$ for $\tilde{t} \geq \tilde{t}'$, and this particular choice of $\tilde{t}'$ will have its explanation towards the end of the proof.

During the time interval $[t_0, t_0+\tilde{t}]$ there is an upper bound M_u and a lower bound M_d on the number of switches of $\sigma(t)$. Now we create something which we call scenarios. A scenario s is defined as follows,

$$s = (f_0', f_1', \dots f_k').$$

The function $f_i' \in \mathcal{F}$ for $i \in \{1, \dots, k\}$, where $k \in \{M_d, M_d+1, \dots, M_u\}$. What this illustrates is that during the time period between t_0 and the first switching time τ_1 after t_0, the function f_0' is the right-hand side of (2.1), during the second time period between τ_1 and τ_2, f_1' is the right-hand side of (2.1) and so on. By a slight abuse of notation, τ_1 is the first switching time after t_0 and τ_i is the first switching time after τ_{i-1} for $i \in \{2, \dots, k\}$. The number of possible scenarios is finite and do not dependent on where the actual switches occur in time.

Now, for a specific scenario s with k switching times, and where the switching times are the elements in the vector $\tau = (\tau_1, \dots, \tau_k)^T$, we write the solution to (2.1) as

$$\begin{aligned} x^{(s,\tau)}(t_0+\tilde{t}) &= x^{(s,\tau)}(t_0) + \int_{t_0}^{\tau_1} f_0'(t-t_0, x^{(s,\tau)}(t))dt + \dots \\ &+ \int_{\tau_{k-1}}^{\tau_k} f_{k-1}'(t-\tau_{k-1}, x^{(s,\tau)}(t))dt + \int_{\tau_k}^{t_0+\tilde{t}} f_k'(t-\tau_k, x^{(s,\tau)}(t)). \end{aligned}$$

Thus, instead of parameterizing x by the switching signals, we here on the interval $[t_0, t_0+\tilde{t}]$ parameterize x by the scenarios and the switching times vector τ.

The function $x^{(s,\tau)}(t_0+\tilde{t})$ is continuous in τ on the set

$$\begin{aligned} \mathcal{C}_s = \{\tau : \; & t_0 \leq \tau_i \leq t_0+\tilde{t} \text{ for } i = 1, \dots, k, \\ & \tau_1 \geq t_0 + \tau_D, \\ & \tau_1 \leq t_0 + 2\tau_D, \\ & \tau_{i+1} \geq \tau_i + \tau_D \text{ for } i = 1, \dots, k-1, \\ & \tau_{i+1} \leq \tau_i + 2\tau_D \text{ for } i = 1, \dots, k-1 \\ & t_0 + \tilde{t} \leq \tau_k + 2\tau_D\}. \end{aligned}$$

This is a consequence of the Continuous Dependency Theorem of initial conditions and is shown by the following argument. For a specific τ, suppose τ_i is changed to τ_i', where $|\tau_i' - \tau_i|$ is small and $i \in \{1, \dots, k\}$. Then we define $\tau' = (\tau_1, \dots, \tau_{i-1}, \tau_i', \tau_{i+1}, \dots, \tau_k)^T$.

$$\begin{aligned} x^{(s,\tau')}(t_0+\tilde{t}) &= x^{(s,\tau')}(t_0) + \int_{t_0}^{\tau_1} f_0'(t-t_0, x^{(s,\tau')}(t))dt + \\ \dots &+ \int_{\tau_{i-1}}^{\tau_i'} f_{i-1}'(t-\tau_{i-1}, x^{(s,\tau')}(t))dt + \int_{\tau_i'}^{\tau_{i+1}} f_i'(t-\tau_i', x^{(s,\tau')}(t))dt + \\ \dots &+ \int_{\tau_k}^{t_0+\tilde{t}} f_k'(t-\tau_k, x^{(s,\tau')}(t)), \end{aligned}$$

so $x^{(s,\tau')}$ is an alternative solution where τ_i is replaced by τ_i'. We know that all such alternative solutions exist and $x^{(s,\tau')}(t) \in \mathcal{D}^*(\infty)$ for $t \in [t_0, t_0 + \tilde{t}]$.

Now,

$$\begin{aligned} x^{(s,\tau)}(t_0+\tilde{t}) = x^{(s,\tau)}(\tau_i) + \int_{\tau_i}^{\tau_{i+1}} f_i'(t-\tau_i, x^{(s,\tau)}(t))dt + \\ \ldots + \int_{\tau_k}^{t_0+\tilde{t}} f_k'(t-\tau_k, x^{(s,\tau)}(t)), \\ x^{(s,\tau')}(t_0+\tilde{t}) = x^{(s,\tau')}(\tau_i') + \int_{\tau_i'}^{\tau_{i+1}} f_i'(t-\tau_i', x^{(s,\tau')}(t))dt + \\ \ldots + \int_{\tau_k}^{t_0+\tilde{t}} f_k'(t-\tau_k, x^{(s,\tau')}(t)). \end{aligned}$$

As $|\tau_i - \tau_i'| \to 0$ it holds that

$$\|x^{(s,\tau)}(\tau_{i+1}, \tau_i, x^{(s,\tau)}(\tau_i)) - x^{(s,\tau')}(\tau_{i+1}, \tau_i', x^{(s,\tau')}(\tau_i'))\| \to 0,$$

which implies that

$$\begin{aligned} &\|x^{(s,\tau)}(t_0+\tilde{t}, \tau_{i+1}, x^{(s,\tau)}(\tau_{i+1}, \tau_i, x^{(s,\tau)}(\tau_i))) \\ &- x^{(s,\tau')}(t_0+\tilde{t}, \tau_{i+1}, x^{(s,\tau')}(\tau_{i+1}, \tau_i', x^{(s,\tau')}(\tau_i')))\| \to 0. \end{aligned}$$

The function $f_{V,m}(x^{(s,\tau)}(t_0+\tilde{t}, t_0, x_0))$ is also continuous in τ on $\mathcal{C}_s$.

Only a subset of all scenarios are feasible. We say that a scenario is feasible if there is $\tau' \in \mathcal{C}_s$ and a switching signal function σ' such that $T^{\sigma'} = T^{\sigma}$ and where $x^{\sigma'}(t) = x^{(s,\tau')}(t)$ for $t \in [t_0, t_0+\tilde{t}']$. According to Lemma 2.27, this means that $f_{V,m}(x(t_0)) - f_{V,m}(x^{(s,\tau)}(t_0+\tilde{t}', t_0, x_0)) > 0$ for the $\tau' \in \mathcal{C}_s$. Now, suppose the scenario s is feasible, the question is if it is true that

$$f_{V,m}(x(t_0)) - f_{V,m}(x^{(s,\tau)}(t_0+\tilde{t}', t_0, x_0)) > 0$$

for all $\tau \in \mathcal{C}_s$. By the subsequent argument we show that this is true.

Suppose s is feasible, then there is $\tau \in \mathcal{C}_s$ such that there is a switching signal function σ' (not necessarily σ) which has switching times equal to the elements in τ during $[t_0, t_0+\tilde{t}']$ and $x^{\sigma'}(t) = x^{(s,\tau)}(t)$ for $t \in [t_0, t_0+\tilde{t}']$. The graph $\mathcal{G}_{\sigma'(t)}$ is uniformly strongly connected and $T^{\sigma} = T^{\sigma'}$. Now, if the elements in τ are changed by means of a continuous transformation to an arbitrary $\tau'' \in \mathcal{C}_s$, then there is a $\sigma'' \in \mathcal{S}_{|\mathcal{F}|,D,U}$ for which $\mathcal{G}_{\sigma''(t)}$ is uniformly strongly connected. The switching times of σ'' are given by the elements in τ'' during $[t_0, t_0+\tilde{t}']$, and an upper bound on the length of an half-open interval in time such that the union graph $\mathcal{G}_{\sigma''(t)}$ is strongly connected during that interval is $T^{\sigma''} = 2T^{\sigma}$. This is true since we know that the lower bound between two switching times is τ_D and the upper bound is $2\tau_D$. Thus, by changing τ to τ'', the length of any interval between two consecutive switching times can at most be changed to be twice as long. Now, according to Lemma 2.27, since $\mathcal{G}_{\sigma''(t)}$ is uniformly strongly connected (with an upper bound of $2T^{\sigma}$ on the length of the interval such that the union graph is strongly connected) we know that since $\tilde{t}' = n(2T^{\sigma'} + 2\tau_D) = n(T^{\sigma''} + 2\tau_D)$,

$$f_{V,m}(x(t_0)) - f_{V,m}(x^{(s,\tau'')}(t_0 + \tilde{t}', t_0, x_0)) > 0.$$

Because τ'' is arbitrary in $\mathcal{C}_s$, if s is feasible it holds that

$$f_{V,m}(x(t_0)) - f_{V,m}(x^{(s,\tau)}(t_0 + \tilde{t}', t_0, x_0)) > 0$$

for all $\tau \in \mathcal{C}_s$.

By choosing $\tilde{t} \geq \tilde{t}'$, we now know that for feasible s it holds that

$$f_{V,m}(x^{(s,\tau)}(t_0 + \tilde{t}, t_0, x_0)) - f_{V,m}(x_0) < 0$$

for all τ in $\mathcal{C}_s$. By Weierstrass Extreme Value Theorem there exists $\tau^* \in \mathcal{C}_s$ such that

$$\begin{aligned}\delta_s(x_0, \tilde{t}) &= \min_{\tau \in \mathcal{C}_s} f_{V,m}(x_0) - f_{V,m}(x^{(s,\tau)}(t_0 + \tilde{t}, t_0, x_0)) \\ &= f_{V,m}(x(t_0)) - f_{V,m}(x^{(s,\tau^*)}(t_0 + \tilde{t}, t_0, x_0)) > 0.\end{aligned}$$

Note that this δ_s is not a function of t_0, since all possible switching signal functions are accounted for during $[t_0, t_0 + \tilde{t}]$ for the specific scenario. Thus, t_0 could be any switching time of σ.

Now,

$$\begin{aligned}\inf_{t_0 \in \{\tau_k\}} f_{V,m}(x_0) - f_{V,m}(x^{\sigma}(t_0 + \tilde{t}, t_0, x_0)) \geq \\ \min_{s} \min_{\tau \in \mathcal{C}_s} f_{V,m}(x_0) - f_{V,m}(x^{(s,\tau)}(t_0 + \tilde{t}, t_0, x_0)) = \\ \min_{s} \delta_s(x_0, \tilde{t}) > 0,\end{aligned}$$

where $\{\tau_k\}$ is the set of all switching times of σ. The set of scenarios that we minimize over are only feasible scenarios. Now we define

$$\beta(x_0, \tilde{t}) = \min_{s} \delta_s(x_0, \tilde{t} - 2\tau_D),$$

where δ_s is defined as zero for negative second arguments. The subtraction by $2\tau_D$ is due to the fact that t_0 was assumed to be a switching time, hence we subtract this term in order to be sure that $-\beta(x_0, \tilde{t})$ does not overestimate the decrease of $f_{V,m}(x(t))$.

Now we need to prove that $\beta(x_0, \tilde{t})$ is lower semi-continuous in x_0. We show that $\delta_s(x_0, \tilde{t})$ is continuous in x_0 for all s. From this fact it follows that $\beta(x_0, \tilde{t})$ is continuous in x_0. The function

$$g_s(\tau, \tilde{t}, x_0) = f_{V,m}(x_0) - f_{V,m}(x^{(s,\tau)}(t_0 + \tilde{t}, t_0, x_0))$$

is continuous in τ and x_0. It follows directly that δ_s is continuous in x_0, since

$$\delta_s(x_0, \tilde{t}) = \min_{\tau \in \mathcal{C}_s} g_s(\tau, \tilde{t}, x_0) \tag{2.4}$$

and $\mathcal{C}_s$ is compact. ■

Now we turn to the proof of Theorem 2.22, but first we formulate some lemmas necessary in order to prove this theorem. Before we proceed, let us define

$$\bar{B}_{r,mn}(\mathcal{A}) = \{x \in \mathbb{R}^{mn} : \text{dist}(x, \mathcal{A}) \leq r\}.$$

Lemma 2.28. *Suppose V fulfills Assumption 2.19 (1), then for $x \in \bar{B}_{r,mn}(\mathcal{A}) \cap \mathcal{D}$ there are class $\mathcal{K}$ functions β_1 and β_2 on $[0, r]$ such that*

$$\beta_1(\text{dist}(x, \mathcal{A})) \leq f_{V,m,m}(x) \leq \beta_2(\text{dist}(x, \mathcal{A})).$$

Proof: We follow the procedure in the proof of Lemma 4.3 in [8] and define

$$\psi(s) = \inf_{\{s \leq \text{dist}(x,\mathcal{A}) \leq r\} \cap \mathcal{D}} f_{V,m,m}(x) \quad \text{for } 0 \leq s \leq r$$

from which we have that $\psi(\text{dist}(x, \mathcal{A})) \leq f_{V,m,m}(x)$ on $B_{r,mn}(\mathcal{A}) \cap \mathcal{D}$. We also define

$$\phi(s) = \sup_{\{\text{dist}(x,\mathcal{A}) \leq s\} \cap \mathcal{D}} f_{V,m,m}(x) \quad \text{for } 0 \leq s \leq r$$

from which we have that $f_{V,m,m}(x) \leq \phi(\text{dist}(x, \mathcal{A}))$ on $B_{r,mn}(\mathcal{A}) \cap \mathcal{D}$. The functions ψ and ϕ are continuous, positive definite and increasing, however not necessarily strictly increasing. The positive definiteness of ψ is guaranteed by the fact that $\inf$ is taken over compact sets, and since $f_{V,m,m}(x)$ is positive and continuous on the sets the result follows by using Weierstrass Extreme Value Theorem.

Now there exist class $\mathcal{K}$ functions β_1 and β_2 such that $\beta_1(s) \leq k\psi(s)$ for some $k \in (0, 1)$, and $\beta_2(s) \geq k\phi(s)$ for some $k > 1$ where $s \in [0, r]$. It follows that

$$\beta_1(\text{dist}(x, \mathcal{A})) \leq f_{V,m,m}(x) \leq \beta_2(\text{dist}(x, \mathcal{A}))$$

on $\bar{B}_{r,mn}(\mathcal{A}) \cap \mathcal{D}$. ■

Lemma 2.29. *Suppose $x(t) \in \mathcal{D}$ for all $t \geq t_0$ and Assumption 2.19 (1,2) holds, then the set $\mathcal{A}$ is uniformly stable for* (2.1).

Proof: Compared to the proof of Theorem 2.20 we do not have to address the issue of existence of the solution, since by assumption it exists in $\mathcal{D}$. Using Assumption 2.19 (2) we get from the Comparison Lemma (*e.g.*, Lemma 3.4 in [8]), that

$$f_{V,m,m}(x(t)) \leq f_{V,m,m}(x_0).$$

From Lemma 2.28 we know that there exist class $\mathcal{K}$ functions β_1 and β_2 defined on $[0, r]$ such that

$$\beta_1(\text{dist}(x, \mathcal{A})) \leq f_{V,m,m}(x) \leq \beta_2(\text{dist}(x, \mathcal{A})).$$

Now let $\epsilon \in (0, r)$ and $\delta = \beta_2^{-1}(\beta_1(\epsilon))$. Then if $x(t_0) \in B_{\delta,mn}(\mathcal{A})$, it follows that

$$\begin{aligned} \text{dist}(x, \mathcal{A}) &\leq \beta_1^{-1}(f_{V,m,m}(x(t))) \leq \beta_1^{-1}(f_{V,m,m}(x_0)) \\ &\leq \beta_1^{-1}(\beta_2(\text{dist}(x(t_0), \mathcal{A})) \leq \beta_1^{-1}(\beta_2(\delta)) = \epsilon. \end{aligned}$$

■

If $x_0 \in \mathcal{D}^*(\infty)$, the set $\mathcal{A}$ is uniformly stable for any $\sigma \in \mathcal{S}_{|\mathcal{F}|,D}$.

Lemma 2.30. *Suppose $x_0 \in \mathcal{A}^c \cap \mathcal{D}^*(\infty)$ and t_0 are arbitrary and Assumption 2.19 (1,2) holds. Suppose there is a non-negative function*

$$\beta(y, \tilde{t}) : \mathbb{R}^+ \times \mathbb{R}^+ \to \mathbb{R}^+$$

that is increasing in $\tilde{t}$ and lower semi-continuous in y. Furthermore, suppose there is $\tilde{t}' > 0$, such that for $\tilde{t} \geq \tilde{t}'$, it holds that $\beta(y, \tilde{t}) > 0$ for all $y \in \mathbb{R}^{++}$.

If

$$f_{V,m,m}(x(t, t_0, x_0)) - f_{V,m,m}(x_0) \leq -\beta(\text{dist}(x_0, \mathcal{A}), t - t_0),$$

$\mathcal{A}$ is globally uniformly asymptotically stable relative to $\mathcal{D}^*(\infty)$.

Proof: We already know from Lemma 3.3 that $\mathcal{A}$ is uniformly stable relative to $\mathcal{D}^*(\infty)$. What is left to prove is that $\mathcal{A}$ is globally uniformly attractive relative to $\mathcal{D}^*(\infty)$. In order to show this, the procedure is analogous to the procedure in Lemma 2.27, where we use the positive limit set $L^+(x_0, t_0)$ for the solution $x(t, t_0, x_0)$.

Let us consider arbitrary t_0 and $x_0 \in \mathcal{D}^*(\infty) \cap \mathcal{A}^c$. By using the fact that $f_{V,m,m}(x(t))$ is continuous and $\mathcal{D}^*(\infty)$ is compact and invariant, it follows that $f_{V,m,m}(x(t))$ converges to a lower bound $\alpha(x_0, t_0) \geq 0$ as $t \to \infty$. Suppose that $L^+(x_0, t_0) \not\subset \mathcal{A}$. We want to prove that $\mathcal{A}$ is attractive by showing that this assumption leads to a contradiction. Let $t_1 = t_0 + \tilde{t}'$ and let y_1 be an arbitrary point in $L^+(x_0, t_0) \cap \mathcal{A}^c \subset \mathcal{D}^*(\infty)$. By using the Continuous Dependency Theorem of initial conditions (*e.g.* Theorem 3.4 in [8]), for any $\epsilon > 0$ there is $\delta(\epsilon, \tilde{t}') > 0$ such that

$$\|y_1 - y_1'\| \leq \delta \Longrightarrow \|f_{V,m,m}(x(t_2, t_1, y_1)) - f_{V,m,m}(x(t_2, t_1, y_1'))\| \leq \epsilon,$$

where $t_2 = t_1 + \tilde{t}'$. Let us choose $\epsilon = \beta(\text{dist}(y_1, \mathcal{A}), \tilde{t}')/2$. Since $y_1 \in L^+(x_0, t_0)$, there is a t' such that $\|y_1 - x(t', t_0, x_0)\| \leq \delta$, thus we choose $t_1 = t'$ and $y_1' = x(t', t_0, x_0)$. But then

$$f_{V,m,m}(x(t_2, t_0, x_0)) \leq \alpha - \beta(\text{dist}(y_1, \mathcal{A}), \tilde{t}')/2 < \alpha,$$

which contradicts the fact that α is a lower bound for V. Hence, $x(t, t_0, x_0) \to \mathcal{A}$ as $t \to \infty$ for all t_0 and $x_0 \in \mathcal{D}^*(\infty)$.

What is left to prove is that for all $\eta > 0$ and $x_0 \in \mathcal{D}^*(\infty)$, there is $T(\eta)$ such that

$$t \geq t_0 + T(\eta) \Longrightarrow \text{dist}(x(t, t_0, x_0), \mathcal{A}) < \eta.$$

We use a contradiction argument. Suppose there is an $\eta > 0$ such that there is no such $T(\eta)$. We know, since $\mathcal{A}$ is uniformly stable relative to $\mathcal{D}^*(\infty)$, that there is a $\delta'(\eta) > 0$ such that for $x_0 \in \mathcal{D}^*(\infty)$ it holds that

$$\text{dist}(x_0, \mathcal{A}) \leq \delta' \Longrightarrow \text{dist}(x(t), \mathcal{A}) \leq \eta$$

for all $t \geq t_0$. Let

$$d_{\max} = \max_{y \in \mathcal{D}^*(\infty)} \text{dist}(y, \mathcal{A})$$

and

$$\beta' = \min_{d \in [\delta'(\eta), d_{\max}]} \beta(d, \tilde{t}') > 0.$$

For any (positive integer) N there are $t_0(N)$ and $x_0(N)$ in $\mathcal{D}^*(\infty)$ such that

$$\text{dist}(x(t, t_0(N), x_0(N)), \mathcal{A}) > \delta'$$

when $t_0 \leq t \leq t_0 + N\tilde{t}'$, otherwise $T(\eta)$ would exist which we assume it does not. From this it follows that

$$f_{V,m,m}(x(t_0(N) + N\tilde{t}', t_0(N), x_0(N))) - f_{V,m,m}(x_0(N)) \leq -N\beta'.$$

Since β' is a constant, it follows that

$$\lim_{N \to \infty} (f_{V,m,m}(x(t_0(N) + N\tilde{t}', t_0(N), x_0(N))) - f_{V,m,m}(x_0(N))) - \infty.$$

This is a contradiction since $f_{V,m,m}$ is bounded on $\mathcal{D}^*(\infty)$. ■

Lemma 2.31. *Suppose Assumption 2.17 and 2.19 (1,2,3) hold, $x_0 \in \mathcal{D}^*(\infty) \cap \mathcal{A}^c$ and $\sigma \in \mathcal{S}_{|\mathcal{F}|,D,U}$. Furthermore, suppose $\mathcal{G}_{\sigma(t)}$ is uniformly quasi-strongly connected, then*

$$f_{V,m,m}(x^\sigma(t)) < f_{V,m,m}(x_0)$$

if t_0 is a switching time and $t \geq n(T^\sigma + 2\tau_D) + t_0$, where T^σ is given in Definition 2.8.

Proof: The proof of this lemma is to a large extent similar to the proof of Lemma 2.27 and hence omitted. In part 1, instead of one connected component c_i, there are two connected components, where the states in the connected components reach an equilibrium in finite time which cannot be reached since the right-hand side of the dynamics is Lipschitz in x. Thus, one obtains the desired contradiction. In part 2, the main difference is that now

$$\mathcal{J}_V(\tau_k, \tau_k + T^\sigma + 2\tau_D)$$

is a strict subset of $\mathcal{J}_V(\tau_k, \tau_k)$ and the graph is uniformly quasi-strongly connected instead of uniformly strongly connected. The reason for not letting the graph be uniformly quasi-strongly connected in Lemma 2.27, is that if it is uniformly quasi-strongly connected, we might have the situation that the union graph during $[\tau_k, \tau_k + T^\sigma)$ is a rooted spanning tree, with the root corresponding to an agent in $\mathcal{I}_V(\tau_k, \tau_k)$ and in that case $\mathcal{I}_V(\tau_k, \tau_k) = \mathcal{I}_V(\tau_k, \tau_k + T^\sigma + 2\tau_D)$ might hold.

■

Proof of Theorem 2.22: **Only if**: Assume $\mathcal{G}_{\sigma(t)}$ is not uniformly quasi-strongly connected. Then for any $T' > 0$ there is $t_0(T')$ such that the union graph $\mathcal{G}([t_0, t_0 + T'))$ is not quasi strongly connected. During $[t_0, t_0 + T')$ the set of nodes $\mathcal{V}$ can be divided into two disjoint sets of nodes $\mathcal{V}_1$ and $\mathcal{V}_1$ (see proof of Theorem 3.8 in [2]) where there are no edges (i, j) or (j, i) in $\mathcal{G}([t_0, t_0 + T'))$ such that $i \in \mathcal{V}_1$ and $j \in \mathcal{V}_2$ or $j \in \mathcal{V}_1$ and $i \in \mathcal{V}_2$ respectively.

We introduce $y_1^*, y_2^* \in \mathcal{D}^*(\infty)$, where $y_1^* \neq y_2^*$ and let $x_i(t_0) = y_1^*$ and $x_j(t_0) = y_2^*$ for all $i \in \mathcal{V}_1$, $j \in \mathcal{V}_2$. Let $\eta = \text{dist}(x_0, \mathcal{A})/2$. Suppose now that $\mathcal{A}$ is globally uniformly asymptotically stable relative to $\mathcal{D}^*(\infty)$, then there is a $T(\eta)$ such that

$$t \geq t_0 + T(\eta) \Longrightarrow \text{dist}(x(t), \mathcal{A}) < \eta.$$

We choose $T' > T(\eta)$. Due to Assumption 2.19 (3) we have that $x_i(t) = y_1^*$ and $x_j(t) = y_2^*$ when $i \in \mathcal{V}_1$ and $j \in \mathcal{V}_2$ for $t \in [t_0(T'), t_0(T') + T')$. Thus, $\text{dist}(x(t), \mathcal{A}) > \eta$ for some $t \geq t_0(T') + T(\eta)$ which is a contradiction.

If: Once again we assume without loss of generality that $\tau_U = 2\tau_D$. We prove this part of the proof by constructing a function β according to Lemma 2.30. The proof is to a large extent similar to the proof of Theorem 2.21 and hence only the important part is addressed. Along the lines of the proof of Theorem 2.21, we define $\delta_s(x_0, \tilde{t})$, where we use Lemma 2.31 which assures that if t_0 is a switching time of σ and $\tilde{t}' = n(2T^\sigma + 2\tau_D)$, it holds that

$$f_{V,m,m}(x(t_0 + \tilde{t}')) < f_{V,m,m}(x(t_0))$$

for $x_0 \in \mathcal{A}^c \cap \mathcal{D}^*(\infty)$.

Now we define

$$\beta(v, \tilde{t}) = \min_s \min_{\mathcal{D}^*(\infty) \cap \{x_0 : \text{dist}(x_0, \mathcal{A}) = v\}} (\delta_s(x_0, \tilde{t} - 2\tau_D)),$$

where the minimization is over feasible scenarios only. Feasible scenarios are defined in the analogous way as in the proof of Theorem 2.21. Since $\mathcal{D}^*(\infty) \cap \{x_0 : \text{dist}(x_0, \mathcal{A}) = v\}$ is compact and $\delta_s(x_0, \tilde{t})$ is positive and continuous on this set for $\tilde{t} \geq \tilde{t}'$, it holds that $\beta(v, \tilde{t})$ is positive for positive v. Also $\beta(v, \tilde{t})$ is actually not only lower semi-continuous, but continuous in v. ■

Note, that in the **only if** part of the proof of Theorem 2.22 we have not shown that $x(t) \not\to \mathcal{A}$ when $t \to \infty$ if $\mathcal{G}_{\sigma(t)}$ is not uniformly quasi-strongly connected. But we can guarantee that if convergence would occur, it cannot be uniform if $\mathcal{G}_{\sigma(t)}$ is not uniformly quasi-strongly connected.

2.5 Bibliography

[1] G. Shi and Y. Hong. Global target aggregation and state agreement of nonlinear multi-agent systems with switching topologies. *Automatica*, 45(5):1165–1175, 2009.

[2] B. Francis, Z. Lin and M. Maggiore. State agreement for continuous-time coupled nonlinear systems. *SIAM Journal on Control and Optimization*, 46(1):288–307, 2007.

[3] L. Moreau. Stability of multiagent systems with time-dependent communication links. *IEEE Transactions on Automatic Control*, 50(2):169–182, 2005.

[4] B. Afsari. Riemannian Lp center of mass: Existence, uniqueness and convexity. In *Proc. Amer. Math. Soc*, volume 139, pages 655–673, 2011.

[5] D. Cheng, J. Wang and X. Hu. An extension of LaSalle's invariance principle and its application to multi-agent consensus. *IEEE Transactions on Automatic Control*, 53(7):1765–1770, 2008.

[6] Y. Hong, L. Gao, D. Cheng and J. Hu. Lyapunov-based approach to multiagent systems with switching jointly connected interconnection. *IEEE Transactions on Automatic Control*, 52(5):943–948, 2007.

[7] A. Jadbabaie, J. Lin and A.S. Morse. Coordination of groups of mobile autonomous agents using nearest neighbor rules. *IEEE Transactions on Automatic Control*, 48(6):988–1001, 2003.

[8] H. K. Khalil. *Nonlinear systems*, Third Edition. Prentice hall, 2002.

[9] E. Montijano, J. Thunberg, X. Hu and C. Sagues. Epipolar visual servoing for multi-robot distributed consensus. *IEEE Transactions on Robotics*, 29(5):1212–1225, 2013.

[10] E. Montijano, J. Thunberg, X. Hu and C. Sagues. Multi-robot distributed visual consensus using epipoles. In *IEEE Conference on Decision and Control and European Control Conference (CDC-ECC)*, pages 2750–2755, 2011.

[11] Y. Ma, S. Soatto, J. Kosecka and S. Sastry. *An invitation to 3-D vision*. Springer, 2004.

[12] T. Yoshizawa. *Stability theory by Liapunov's second method*. Mathematical Society of Japan (Tokyo), 1966.

[13] N. Rouche, P. Habets, M. Laloy and A-M. Ljapunov. *Stability theory by Liapunov's direct method*. Springer-Verlag New York, 1977.

[14] F. H. Clarke. Generalized gradients and applications. *Transactions of the American Mathematical Society*, 205:247–262, 1975.

Chapter 3

Consensus on $SO(3)$ or attitude synchronization for switching topologies

In this chapter we address the problem of consensus on $SO(3)$ or attitude synchronization. In this problem each agent in the multi-agent system has a corresponding rotation matrix and the objective is that all the agents shall reach consensus in their rotation matrices. The problem is interesting since it has applications in the real world, *e.g.*, systems of satellites, UAVs or networks of cameras. It is challenging since the kinematics and dynamics are nonlinear and the system evolves on the compact manifold $SO(3)$, *i.e.*, the group of orthogonal matrices in $\mathbb{R}^{3\times 3}$ with determinant equal to 1.

For a broad class of local representations or parameterizations. including the Axis-Angle Representation and the Rodrigues Parameters, we present two types of kinematic control laws that each looks structurally the same for any choice of local representation.

The first control law consists of a weighted sum of pairwise differences between positions of neighboring agents, expressed as coordinates in a local representation. The structure of the control law is well known in the consensus community for consensus in systems of agents with single integrator dynamics and states in $\mathbb{R}^m$. In the Euclidean space $\mathbb{R}^m$, this type of control law is based on so called relative information, where the difference between the positions of two agents is not dependent on the actual positions of the agents expressed in a reference coordinate frame, *i.e.*, the difference is translation invariant. However, in the local representations of $SO(3)$ that we consider, the Euclidean difference between the positions (expressed as vectors in $\mathbb{R}^3$) of two neighboring agents is not translation invariant. For this type of control law, we show that the system reaches asymptotic consensus for any of the local representations, if the initial rotations at time t_0 are contained within the region of injectivity of the local representation and the interaction graph for the system of agents is uniformly strongly connected.

The second control law is based on relative information, where local representations of the relative rotations between neighboring agents are used. Under stronger assumptions on the regions for the initial rotations, namely that the initial rotations are contained in a geodesic convex ball, smaller than the region of injectivety, we show that the system reaches asymptotic consensus uniformly if and only if the interaction graph is uniformly quasi-strongly connected.

Towards the end of this chapter we also consider the second order dynamics and torque control laws. We use a backstepping and a high-gain approach in order to generalize the kinematic control laws to the case of rigid bodies in space. This generalization is performed first for the case of fixed connection topologies and then for switching topologies. The word switching in this context is actually not switching in the same sense as for the kinematic control laws. Here we assume a continuous in time transition between the functions.

There is a vast literature on attitude synchronization for rigid bodies in space. The following two works are examples of when the agents can measure their rotation to a common reference object, which is the case for the first control law we present in this chapter. In [1] a general framework is proposed for coordinating or synchronizing systems of agents with lower triangular dynamics using backstepping. The attitude synchronization problem is considered as an example, where the unit quaternions are used. In [2], a solution to the synchronization problem is given by using the Modified Rodrigues Parameters. In these works the connectivity graph between the agents is either required to be balanced in [1] or undirected in [2]. Also, little is mentioned on how to guarantee injectivity of the local representations.

In this chapter, we are considering the continuous time formulation of the consensus problem. An interesting result is provided in [3] for the adjacent problem of discrete time consensus in $SO(3)$. Using a so called shape function, the authors provide a discrete time protocol that only uses intrinsic information and works for initial rotations on almost all of $SO(3)$. The authors of that paper divide the existing algorithms on consensus on $SO(3)$ into two categories, where methods in the first category, extrinsic methods, embed $SO(3)$ into an ambient space in which classical consensus algorithms can be deployed. Then the states are obtained by means of projection onto $SO(3)$. In the second category the control law is constructed in the tangent space of $SO(3)$ and uses only intrinsic information.

Our second control law uses only intrinsic information. The first control law is not using intrinsic information, but it is not based on a projection from an ambient space. Instead it is constructed by using a local representation of $SO(3)$ around the identity matrix.

Almost-global attitude synchronization was achieved in [4] based on switching joint connection, where auxiliary variables were introduced. This is to regard as an extrinsic approach, using relative information. The question about which information is available to the agents is something that is discussed in [5], using the Modified Rodrigues Parameters a distributed control law is proposed for the agents, where no angular velocity measurements are necessary. The control laws are defined in a common frame of reference, which makes it a control law of the same type as our first control law. The injectivity preservation is not guaranteed in that work, but the author argue that this problem can be mitigated by using the so called shadow set of the Modified Rodrigues Parameters.

3.1 Preliminaries

We consider a system of n agents, each residing in $SO(3)$, the group of rotation matrices, meaning that each agent i has a rotation matrix $R_i(t)$ in this manifold at time $t \geq t_0$. The matrix group $SO(3)$ is defined as follows,

$$SO(3) = \{R \in \mathbb{R}^{3\times3} : R^T R = I, \det(R) = 1\}.$$

Each agent has also a corresponding rigid body. We denote the world frame as $\mathcal{F}_W$ and the instantaneous body frame of the rigid body of any agent i as $\mathcal{F}_i$. We let $R_i(t) \in SO(3)$ be the rotation of $\mathcal{F}_i$ in the world frame $\mathcal{F}_W$ at time t and let $R_{ij}(t) \in SO(3)$ be the rotation of $\mathcal{F}_j$ in the frame $\mathcal{F}_i$, *i.e.*, $R_{ij}(t) = R_i^T(t)R_j(t)$, where $i, j \in \{1, 2, \ldots, n\}$. Mind the notation here, when we write $\mathcal{F}$ (without a subscript) in this chapter, we are referring to the set of functions defined in Section 2.1.1. We refer to the rotation $R_i(t)$ as *absolute rotation*, whereas the rotation $R_{ij}(t)$ will be referred to as *relative rotation*. The difference between the two kinds of rotations is illustrated in Figure 3.1 and Figure 3.2.

We denote the instantaneous angular velocity of $\mathcal{F}_i$ relative to $\mathcal{F}_W$ expressed in the frame $\mathcal{F}_i$ as ω_i. From now on, until Section 3.5, we assume that ω_i is the control variable for agent i. The kinematics for R_i is given by

$$\dot{R}_i = R_i \widehat{\omega}_i,$$

where $R_i\widehat{\omega}_i$ is an element of the tangent space $T_{R_i}SO(3)$ and $\widehat{p}$ denotes the skew-symmetric matrix generated by $p = [p_1, p_2, p_3]^T \in \mathbb{R}^3$, *i.e.*,

$$\widehat{p} = \begin{bmatrix} 0 & -p_3 & p_2 \\ p_3 & 0 & -p_1 \\ -p_2 & p_1 & 0 \end{bmatrix}. \tag{3.1}$$

We also define $(\cdot)^\vee$ as the inverse of $\widehat{(\cdot)}$, *i.e.*, $\widehat{p}^\vee = p$.

We consider local representations or parameterizations of $SO(3)$. Often we simply refer to them as representations or parameterizations. In this context, what is meant by a local representation is a diffeomorphism (smooth bijection) $f : B_r(I) \to B_{r',3}(0) \subset \mathbb{R}^3$, where $B_r(I)$ is an open geodesic ball around the identity matrix in $SO(3)$ of radius r less than or equal to π, and $B_{r',3}(0)$ is an open ball in $\mathbb{R}^3$ with radius r'. A set in $SO(3)$ is convex if any geodesic shortest path segment between any two elements in the set is contained in the set, the set is strongly convex if there is a unique geodesic shortest path segment contained in the set [6]. If $r = \pi$, $B_r(I)$ comprises almost all of $SO(3)$ in terms of measure, and $B_r(I)$ is convex if and only if $r \leq \pi/2$. The radius r is referred to as the radius of injectivety. The parameterizations that we use have the following special structure

$$f(R) = g(\theta)u, \tag{3.2}$$

where θ is the geodesic distance between I and R on $SO(3)$, also referred to as the Riemannian distance which we write as $d(I, R)$. The variable $u \in \mathbb{S}^2$ is the rotational axis of R, and $g : \mathbb{R} \to \mathbb{R}$ is an odd continuously differentiable function that is strictly increasing

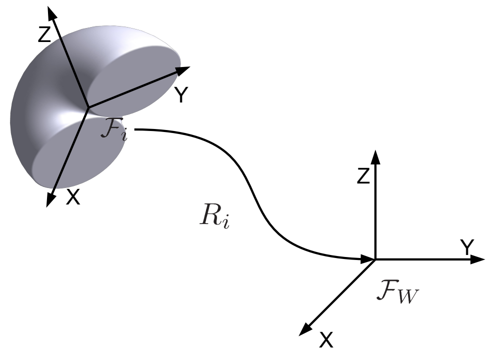

Figure 3.1: A rigid body agent (agent i) here is illustrated as a half torus. The absolute rotation of this rigid body agent is the rotation R_i of its body frame $\mathcal{F}_i$ to the fixed world frame $\mathcal{F}_W$.

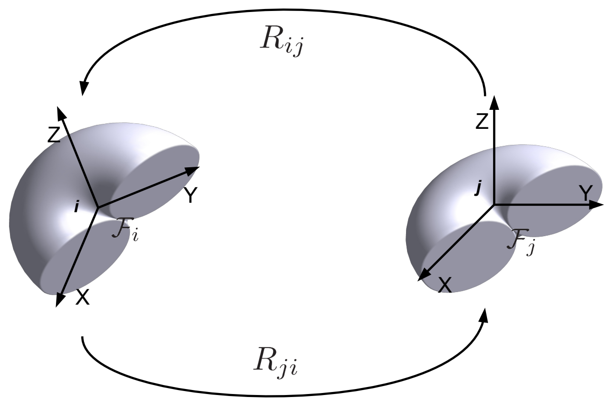

Figure 3.2: Two rigid body agents, agent i and agent j here are illustrated as half tori. The relative rotations R_{ij} and R_{ji} between them is the rotation of $\mathcal{F}_j$ to $\mathcal{F}_i$ and the rotation from $\mathcal{F}_i$ to $\mathcal{F}_j$, respectively.

on $(-r, r)$, where $r \leq \pi$. On $B_\pi(I)$ the vector u and the positive variable θ are obtained as functions of R as follows

$$\theta = \cos^{-1}\left(\frac{\text{trace}(R) - 1}{2}\right), \quad u = \frac{1}{2\sin(\theta)}\begin{bmatrix} r_{32} - r_{23} \\ r_{13} - r_{31} \\ r_{21} - r_{12} \end{bmatrix},$$

where $R = [r_{ij}]$.

Let us denote

$$y_i = f(R_i), \qquad y_{ij} = f(R_{ij}).$$

It holds that

$$y_{ij} = -y_{ji}, \text{ but in general } y_j - y_i \neq y_{ij}.$$

For each representation, *i.e.*, choice of g, $r \leq \pi$ is the largest radius such that f is a diffeomorphism. The radius r is the radius of injectivity and depends on the representation, but we suppress this explicit dependence and throughout Chapter 3 and Chapter 4, r corresponds to the representation at hand, *i.e.*, the one we have chosen. For the representation at hand we also define

$$r' = \sup_{s \uparrow r} g(s).$$

Some common representations are:

- **The Axis-Angle Representation**, in which case $g(\theta) = \theta$, and $r = r' = \pi$. This representation is almost global. The set $SO(3)\backslash B_\pi(I)$ has measure zero in $SO(3)$ and dimension 2 compared to $SO(3)$ which has dimension 3. The Axis-Angle Representation is obtained from the logarithmic map as

$$\begin{aligned} x_i &= (\text{Log}(R_i))^\vee, \\ x_{ij} &= (\text{Log}(R_i^T R_j))^\vee. \end{aligned}$$

  In the other direction a rotation matrix R_i is obtained via the exponential map as

$$R_i(x_i) = \exp(\widehat{x}_i).$$

  The matrix R_{ij} is obtained as

$$R_{ij}(x_i, x_j) = \exp(\widehat{x}_i)^T \exp(\widehat{x}_j).$$

  The function $\exp_{R_i}$ is the exponential map at the point R_i. Using this notation, the function exp is short hand notation for $\exp_I$.

- **The Rodrigues Parameters**, in which case $g(\theta) = \tan(\theta/2)$ and the corresponding $r = \pi$ in this case also but $r' = \infty$. For the Axis-Angle Representation the Jacobian matrix (which we soon address), is also far from singular on $B_\pi(I)$. Thus there are reasons for choosing the Axis-Angle Representation instead of the Rodrigues Parameters. However, the Rodrigues Parameters have the useful property that the mapping f is a geodesic map, *i.e.*, geodesic curve segments on $SO(3)$ correspond to straight lines in the Rodrigues Parameters space. This is a property that is exploited later in this chapter.

- **The Modified Rodrigues Parameters**, in which case $g(\theta) = \tan(\theta/4)$, $r = \pi$ and $r' = 1$. This representation is often preferred, since $\tan(\theta/4) \not\to \infty$ as $\theta \to \pi$ and the Jacobian matrix has a simple structure. This representation is obtained from the rotation matrices by a second order Cayley transform [7].

- **The representation** $(R - R^T)^\vee$, in which case $g(\theta) = \sin(\theta)$, and the corresponding r and r' are $\pi/2$ and 1 respectively. This representation is popular because it is easy to express in terms of the rotation matrices. Unfortunately, since $r = \pi/2$, only $B_{\pi/2}(I)$ is covered.

- **The Unit Quaternions**, or rather parts of it. The unit quaternion q_i expressed as a function of the Axis-Angle Representation $x_i = \theta_i u_i$ of $R_i \in B_\pi(I)$ is given as

$$q(x_i) = (\cos(\theta_i/2), \sin(\theta_i/2)u_i)^T \in \mathbb{S}^3.$$

  This means that we can choose the last three elements of the vector as our representation, *i.e.*, $\sin(\theta_i/2)u_i$, in which case $r = \pi$. The unit quaternion representation is popular since the mapping from $SO(3)$ to the quaternion sphere is a Lie group homomorphism, *i.e.*,

$$q_1 \mapsto R_1 \quad q_2 \mapsto R_2 \quad \Longrightarrow q_1 \cdot q_2 \mapsto R_1 R_2,$$

  where the multiplication of q_1 and q_2 should be interpreted in the sense of quaternion multiplication.

The mapping

$$x_i \mapsto y_i$$

fulfills that $[\widehat{x}_i, \widehat{y}_i] = \widehat{x}_i\widehat{y}_i - \widehat{y}_i\widehat{x}_i = 0$. In fact, only a representation that is a scaled versions of x_i fulfills this criteria, which can be seen from the following lemma.

Lemma 3.1. *For the two vectors p_1 and p_2 in $\mathbb{R}^3$ it holds that $[\widehat{p}_1, \widehat{p}_2] = 0$ if and only if $p_1 = \alpha p_2$ for some $\alpha \in \mathbb{R}$.*

Proof: **If**: $[\widehat{p}_1, \widehat{p}_2] = \alpha\widehat{p}_2^2 - \alpha\widehat{p}_2^2 = 0$. **Only if**: Suppose there is no α such that $p_1 = \alpha p_2$ and $[\widehat{p}_1, \widehat{p}_2] = \widehat{p}_1\widehat{p}_2 - \widehat{p}_2\widehat{p}_1 = 0$. Since there is no α such that $p_1 = \alpha p_2$ it holds that $\widehat{p}_1\widehat{p}_2 p_1 \neq 0$, whereas $\widehat{p}_2\widehat{p}_1 p_1 = 0$, which implies $[\widehat{p}_1, \widehat{p}_2] \neq 0$, which is a contradiction. ■

Let $x_i(t)$ and $x_{ij}(t)$ denote the axis-angle representations of the rotations $R_i(t)$ and $R_{ij}(t)$, respectively. In the following, since we are only addressing representations of (subsets of) $B_\pi(I)$, we choose $x(t) = (x_1(t), x_2(t), \ldots, x_n(t))^T \in (B_\pi(I))^n$ as the state of the system instead of $(R_1(t), \ldots, R_n(t)) \in (B_\pi(I))^n$. Note that $g(\theta_i) = g(\|x_i\|)$ since $\theta_i = \|x_i\|$. The variables y_i and y_{ij} are now functions of x_i and x_i, x_j respectively, *i.e.*,

$$\begin{aligned} y_i(x_i) &= (f \circ \exp)(\widehat{x}_i), \\ y_{ij}(x_i, x_j) &= (f \circ \exp)(\mathrm{Log}(R_i^T(x_i)R_j(x_j))). \end{aligned}$$

Since x_i, x_j are components of the vector x, we can write $y_i(x)$ and $y_{ij}(x)$. When we write $y_i(t)$ and $y_{ij}(t)$, this is short hand notation for $y_i(x)(t)$ and $y_{ij}(x)(t)$ respectively.

The kinematics is given by

$$\dot{x}_i = L_{x_i}\omega_i, \tag{3.3}$$

where the Jacobian (or transition) matrix L_{x_i} is given by

$$L_{x_i} = L_{\theta u_i} = I_3 + \frac{\theta}{2}\widehat{u}_i + \left(1 - \frac{\mathrm{sinc}(\theta_i)}{\mathrm{sinc}^2(\frac{\theta_i}{2})}\right)\widehat{u}_i^2. \tag{3.4}$$

The proof is found in [8]. The function $\mathrm{sinc}(\beta)$ is defined so that $\beta\,\mathrm{sinc}(\beta) = \sin(\beta)$ and $\mathrm{sinc}(0) = 1$. It was shown in [9] that $L_{\theta u}$ is invertible for $\theta \in (-2\pi, 2\pi)$. Note however that $\theta \in [0, \pi)$ here.

To represent the connectivity between the agents, we use a directed graph (or digraph) $\mathcal{G}_{\sigma(t)}$ which is defined in Chapter 2. The function σ is a switching signal function, also defined in Chapter 2.

Instead of using the term *communication graph* for $\mathcal{G}_{\sigma(t)}$, we deliberately use the terms *neighborhood graph*, *connectivity graph* or *interaction graph*. This is due to the reason that direct communication does not necessarily take place between the agents. Instead they can choose to just observe each other via cameras or other sensors, *i.e.*, indirect communication.

We remind the reader that the neighbors of agent i comprises the set $\mathcal{N}_i(t)$. If $j \in \mathcal{N}_i(t)$, agent i obtains rotation information related to agent j. This information is either the absolute rotation R_j or the relative rotation R_{ij}. In Section 3.2 we provide two simple linear control laws which are based on absolute rotations and relative rotations, respectively. If agent i obtains the absolute rotation R_j, this rotation can either be transmitted by means of communication, *i.e.*, agent j sends R_j to agent i, or measured by a camera attached to agent i, *i.e.*, agent i observes agent j together with an object of known rotation in the world frame $\mathcal{F}_W$. In the latter case, agent i can calculate R_j without the need of communication. The relative rotation R_{ij} can often be obtained without communication, if *e.g.*, a camera is used.

3.2 Formulation and control design

Let us now consider the attitude synchronization problem. We shall find a feedback control law ω_i for each agent i using the local representations of either absolute rotations or relative rotations so that the absolute rotations of all agents converge to the set where all the rotations are equal as the time goes to infinity, *i.e.*,

$$R_i - R_j \to 0, \text{ for all } i, j, \text{ as } t \to \infty, \tag{3.5}$$

or equivalently,

$$R_{ij} \to I, \text{ for all } i, j, \quad \text{as } t \to \infty. \tag{3.6}$$

This is illustrated in Figure 3.3. If $y \in (B_{r',3}(0))^n$ it is true that

$$R_i = R_j \iff x_i = x_j \iff x_{ij} = 0 \iff y_i = y_j \iff y_{ij} = 0 \quad \text{for all } i, j. \tag{3.7}$$

As in Chapter 2 we define the set $\mathcal{A}$, as the consensus set for x, and then according to (3.7), the condition (3.5) can equivalently be written as $x(t) \to \mathcal{A}$ as $t \to \infty$. This means that the solution approaches $\mathcal{A}$. A stronger assumption on the convergence to $\mathcal{A}$ is stated in Chapter 2, and is referred to as (global) uniform asymptotic stability of $\mathcal{A}$ relative to a set. In this case the solution $x(t)$ approaches $\mathcal{A}$ uniformly in terms of time and and distance from $\mathcal{A}$ (defined using the euclidean metric).

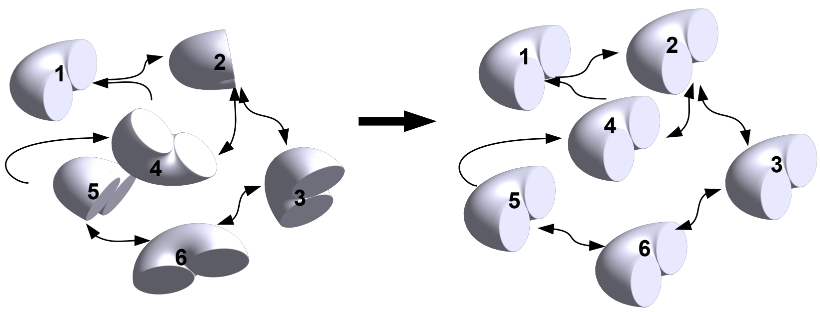

Figure 3.3: The rotations of all the agents in the system shall converge to the set where all the rotations are equal.

The distance (when the Riemannian metric is used) from $(R_1, \ldots, R_n) \in (\bar{B}_q(I))^n$ to the set where all the rotation matrices are equal, is, provided $\|x_{ij}\| < \pi$ for all i, j, bounded from above by

$$n \left(\max_{(j,k) \in \mathcal{V} \times \mathcal{V}} \|x_{jk}\| \right).$$

By using this fact together with (3.7) and the continuity property of the exponential and logarithmic map, one can show that if $\mathcal{A}$ is uniformly asymptotically stable in $(\bar{B}_{q,3})^n$ for $x(t)$ where $q < \pi$, then the set $\{(R_1, \ldots, R_n) \in (\bar{B}_q(I))^n : R_1 = \ldots = R_n\}$ is uniformly asymptotically stable in $(\bar{B}_q(I))^n$.

Now we propose the following control laws based on absolute and relative rotations respectively.

$$\omega_i = \sum_{j \in \mathcal{N}_i(t)} a_{ij}(t - \gamma_\sigma(t))(y_j - y_i), \tag{3.8}$$

$$\omega_i = \sum_{j \in \mathcal{N}_i(t)} a_{ij}(t - \gamma_\sigma(t))y_{ij}, \tag{3.9}$$

where $a_{ij}(t) > 0$ is continuous and bounded, and $\sigma \in \mathcal{S}_{|\mathcal{F}|,D,U}$. For each of the two control laws, the set of functions $\mathcal{F}$ is constructed along the lines of the example on convexity in Section 2.3.2, and for all the control laws we consider in this chapter, the set $\mathcal{F}$ is constructed in the analogous way.

The following two sections are devoted to the study of these control laws. We refer to control law (3.8) as *the first control law*, whereas (3.9) will be referred to as *the second control law*.

3.3 Results for the first control law

The structure of (3.8) is well known from the consensus problem in a system of agents with single integrator dynamics and states in $\mathbb{R}^m$ [10]. The question is if this simple control law also works for rotations expressed in any of the local representations that we consider. The answer is yes.

Theorem 3.2. *If the rotations initially is contained in $\bar{B}_q(I)$ where $q < r$, and the graph $\mathcal{G}_{\sigma(t)}$ is uniformly strongly connected, then if controller* (3.8) *is used, $\bar{B}_{q,3}(0)$ is invariant, $0 \in \mathbb{R}^{mn}$ is uniformly stable and $x(t) \to \mathcal{A}$ as $t \to \infty$.*

Proof of Theorem 3.2: We divide the proof into two different parts, where the invariance of the ball $\bar{B}_{q,3}(0)$ is shown in the first part, and the convergence of x to $\mathcal{A}$ is shown in the second part.

Part 1: The right-hand side of the dynamics for x is switching between a finite number of functions that are continuous in t and Lipschitz in x, uniformly with respect to t. This set of functions is the set $\mathcal{F}$, see Chapter 2. Let

$$V : \mathbb{R}^3 \to \mathbb{R}^+$$

be defined as

$$V(x_i) = x_i^T x_i.$$

The function V is positive definite and $f_{V,3}(x) = \max_{j \in \mathcal{V}} V(x_j)$.

Suppose that $i \in \mathcal{I}_V(t,t)$. We investigate how $\theta_i^2(t)$ changes.

$$\begin{aligned}
\frac{d(\theta_i^2/2)}{dt} &= \frac{d((x_i^T x_i)/2)}{dt} \\
&= x_i^T L_{x_i} \sum_{j \in \mathcal{N}_i(t)} a_{ij}(t-\gamma_\sigma(t))(y_j - y_i) && (3.10) \\
&\leq \sum_{j \in \mathcal{N}_i(t)} a_{ij}(t-\gamma_\sigma(t))(\theta_i g(\theta_j) - \theta_i g(\theta_i)) \leq 0, && (3.11)
\end{aligned}$$

since $x_i^T L_{x_i} = x_i^T$ and g is strictly increasing. This implies that $D^+ f_{V,3}(x(t)) \leq 0$. Now, according to Theorem 2.20 in Chapter 2, $\bar{B}_{q,3}(0)$ is invariant where $\beta_1 = \beta_2 = \|\cdot\|^2$. Since $q \in [0,r)$ is arbitrary, this means that the point $0 \in \mathbb{R}^{mn}$ is uniformly stable.

The key point of this proof of invariance is to use the special structure of the Jacobian matrix L_{x_i}. The second and the third term in (3.4) are orthogonal to x_i, see Figure 3.4.

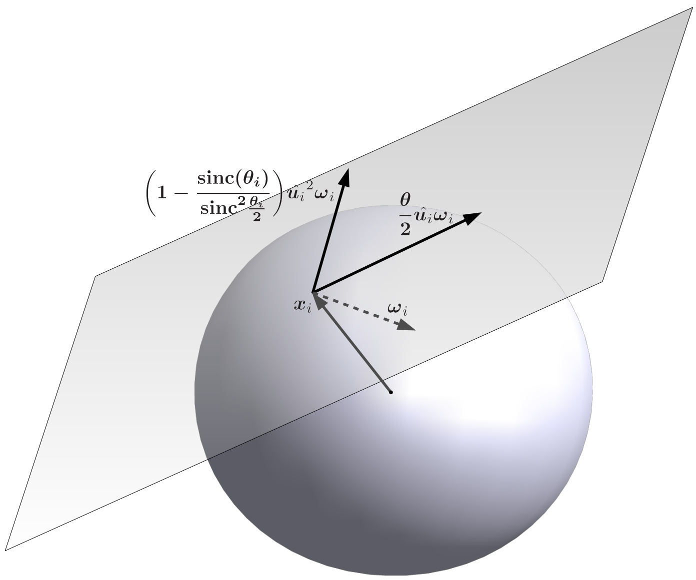

Figure 3.4: The second and the third term of (3.4) are orthogonal to x_i and lie in the tangent plane of the sphere with radius $\|x_i\|_2$ at the point x_i.

Part 2: In this part we show that all properties are satisfied in order to apply Theorem 2.21 in Chapter 2. We know from part 1, that $f_{V,3}(x(t))$ is decreasing and V is positive definite. We will verify that Assumption 2.17 and Assumption 2.18 (3) are fulfilled, then the desired result follows according to Theorem 2.21. Assumption 2.17 is fulfilled. We see that as soon as there is $j \in \mathcal{N}_i(t)$ such that $x_j \neq x_i$, the sum in (3.10) is strictly negative.

If $x_i = x_j$ for all $j \in \mathcal{N}_i(t)$, it holds that $L_{x_i}\omega_i = 0$ for all t. Thus, Assumption 2.18 (3) is fulfilled and $x(t) \to \mathcal{A}$ as $t \to \infty$. ■

Remark 3.1. Instead of using (3.8) one could use feedback linearization and construct the following control law for agent i

$$\omega_i = L_{y_i}^{-1} \sum_{j \in \mathcal{N}_i(t)} a_{ij}(t - \gamma_\sigma(t))(y_j - y_i),$$

where L_{y_i} is the Jacobian matrix for the representation y_i. If this feedback linearization control law is used and the graph $\mathcal{G}_{\sigma(t)}$ is quasi-strongly connected, the consensus set is almost globally asymptotically stable relative to $\bar{B}_{r',3}$. However, for many representations such as the Rodrigues Parameters, the Jacobian matrix L_{y_i} is close to singular as y_i is close to the boundary of $\bar{B}_{r',3}$, which makes this type of control law less robust to measurement errors than (3.8). In Chapter 4 we use distorted measurements of the rotations and in this case it is not possible to construct the matrix $L_{y_i}^{-1}$, but for the type of distorted measurements we consider there, a control law of the type (3.8) still works.

3.4 Results for the second control law

Now we continue with the study of (3.9) where only local representations of the relative rotations are available. Under stronger assumptions on the initial rotations of the agents at time t_0 and weaker assumptions on the graph $\mathcal{G}_{\sigma(t)}$, the following theorem ensures uniform asymptotic convergence to the consensus set.

Theorem 3.3. *If the rotations initially are contained within a closed ball $\bar{B}_q(I)$ of radius $q < r/2$ and the controller* (3.9) *is used, then $x(t) \to \mathcal{A}$ as $t \to \infty$ and $(\bar{B}_{q,3})^n \cap \mathcal{A}$ is globally uniformly asymptotically stable relative to $\bar{B}_{q,3}$ if and only if $\mathcal{G}_{\sigma(t)}$ is uniformly quasi-strongly connected.*

Remark 3.2. In Theorem 3.3, since only information that is independent of $\mathcal{F}_W$ is used in (3.9), the assumption that the rotations initially are contained in $\bar{B}_q(I)$ can be relaxed. As long as there is a $Q \in SO(3)$ such that all the rotations are contained in $B_{r/2}(Q)$ initially, the rotations will reach consensus asymptotically and uniformly with respect to time.

In order to prove Theorem 3.3, we first formulate and prove another theorem, Theorem 3.4, from which the desired result follows by application of Theorem 2.21 and Theorem 2.22. In the proof of Theorem 3.4, $\text{ri}(\mathcal{T}(z_i, \text{conv}(\{z_i, z_j\}))$ is the relative interior of the tangent cone at the point z_i of $\text{conv}(\{z_i, z_j\}$, see Section 2.3.2.

Theorem 3.4. *Suppose that the control law* (3.9) *is used and* $x \in (B_{q,3}(0))^n$*, where* $q < r/2$*. Let* $z_i = \tan(\theta_i/2)u_i$*,* $z = (z_1, \dots, z_n)^T$ *and* $\dot{z}_i = \tilde{f}_i(t, z)$*. The function* $\tilde{f}_i(t, z)$ *is piecewise continuous in* t *(with times of discontinuity only at the switching times of* σ*) and Lipschitz in* z *on* $B_{q,3}(0)$*, uniformly with respect to* t*. The structure of the dynamics is*

$$\dot{z}_1 = \sum_{j \in \mathcal{N}_1(t)} a_{1j}(t - \gamma_\sigma(t))h_{1j}(z_1, z_j)(z_j - z_1),$$

$$\vdots$$

$$\dot{z}_n = \sum_{j \in \mathcal{N}_n(t)} a_{nj}(t - \gamma_\sigma(t))h_{nj}(z_n, z_j)(z_j - z_n),$$

where $h_{ij}(z_i, z_j) \geq 0$ *and* $h_{ij}(z_i, z_j) > 0$ *if and only if* $z_j \neq z_i$*.*

Remark 3.3. The function h_{ij} in Theorem 3.4 depends on the parameterization y.

Proof of Theorem 3.4:

Part 1: Let us introduce the Cayley transform restricted to $B_\pi(I)$. This transform Cay : $B_\pi(I) \to so(3)$ is defined as

$$\text{Cay}(R) = (I - R)(I + R)^{-1}$$

and it is its own inverse, *i.e.*, $\text{Cay}(\text{Cay}(R)) = R$. We state following important known fact about the Cayley transform [11]. The transform Cay, restricted to $B_{\pi/2}(I)$, is a geodesic map, *i.e.*, the geodesic curve segment between two rotations Q_1 and Q_2, corresponds to a line between $(\text{Cay}(Q_1))^\vee$ and $(\text{Cay}(Q_2))^\vee$ in $\mathbb{R}^3$. A convex hull in $B_{\pi/2}(I)$ corresponds to a polytope in $\mathbb{R}^3$ [11]. For the sake of completeness we show this fact, where we use the unit quaternion representation for a rotation matrix and the gnomic projection. The unit quaternion $\bar{q} \in \mathbb{R}^4$, representing a rotation matrix Q is given by

$$\bar{q} = [\cos(\theta/2), \sin(\theta/2)u^T]^T,$$

where once again θ is the rotational angle and u is the rotational axis. A unit quaternion is an element of the sphere $\mathbb{S}^3$ embedded in $\mathbb{R}^4$. We see that the identity matrix corresponds to the quaternion $[1, 0, 0, 0]^T$, since $\theta = 0$. A geodesic line segment between two rotations Q_1 and Q_2 in $B_{\pi/2}(I)$ corresponds to a great circle segment on the quaternion sphere between the corresponding quaternions q_1 and q_2 [11]. Now, if we we use the gnomic projection in order to project the quaternions onto the three dimensional tangent plane touching the point $[-1, 0, 0, 0]^T$ on the sphere, the point in the plane will be

$$\left[-1, -\frac{\sin(\theta/2)}{\cos(\theta/2)}u^T\right]^T = \left[-1, -\tan(\theta/2)u^T\right]^T.$$

The gnomic projection of a point on the sphere is the point in the plane where the continuation of the straight line segment between the sphere point and the sphere center crosses the plane. It is known that the gnomic projection is a geodesic map, so great circles on the sphere correspond to straight lines in the plane. Thus, if we can show that $(\text{Cay}(R))^{\vee} = -\tan\theta/2u$ we are done. A simple calculation shows that this is true, and it follows from Rodrigues formula. We can equivalently show that

$$\tan(\theta/2)\widehat{u}(I+R) = R - I.$$

Using Rodrigues formula we get that

$$\begin{aligned}\tan(\theta/2)\widehat{u}(I+R) =& \tan(\theta/2)(2-(1-\cos(\theta)))\widehat{u} + \tan(\theta/2)\sin(\theta)\widehat{u}^2\\ =& \sin(\theta)\widehat{u} + (1-\cos(\theta))\widehat{u}^2 = R - I.\end{aligned}$$

So the Cayley transform, which up to sign is the map to the Rodrigues Parameter space, is a geodesic map.

Part 2: We use part 1 and observe that since $x_j \in \bar{B}_{q,3}(0)$ for all j, it holds that the strongly geodesic convex hull in $SO(3)$ of the rotations $\{R_j\}_{j=1}^n$, which we denote by $\text{conv}(\{R_j\}_{j=1}^n)$, corresponds to the polytope $\text{conv}(\{z_j\}_{j=1}^n)$ in $\mathbb{R}^3$. Also, $\text{conv}(\{R_j\}_{j\in\mathcal{N}_i})$, corresponds to the polytope $\text{conv}(\{z_j\}_{j\in\mathcal{N}_i})$ contained in $\mathbb{R}^3$.

Now suppose

$$\dot{R}_i = R_i\widehat{y}_{ij} = R_i\frac{g(\|x_i\|)}{\|x_i\|}\widehat{x}_{ij}$$

for some $j \in \mathcal{V}$. The corresponding dynamics for z_i is

$$\dot{z}_i = L_{z_i}y_{ij}$$

which is not equal to zero if $R_i \neq R_j$. The matrix L_{z_i} is the Jacobian matrix [12]. We have that $L_{z_i}y_{ij} \in \text{ri}(\mathcal{T}(z_i, \text{conv}(\{z_i, z_j\}))$ so

$$L_{z_i}y_{ij} = h_{ij}(z_i, z_j)(z_j - z_i)$$

for a function h_{ij} with the structure given in Theorem 3.4. Thus,

$$L_{z_i}\left(\sum_{j\in\mathcal{N}_i(t)} a_{ij}(t-\gamma_\sigma(t))y_{ij}\right) = \sum_{j\in\mathcal{N}_1(t)} a_{ij}(t-\gamma_\sigma(t))h_{ij}(z_i, z_j)(z_j - z_i).$$

■

We are now ready to prove Theorem 3.3 and our main tool will be Theorem 2.22 in Chapter 2.

Proof of Theorem 3.3: Let us define the functions

$$\begin{aligned}V(z_i) =&\ z_i^T z_i \text{ and}\\ W(x) =&(z_j - z_i)^T(z_j - z_i).\end{aligned}$$

The mapping from the Axis-Angle Representation on $\bar{B}_{q,3}(0)$ to the corresponding region in the Rodriugues parameters space is given by

$$f'' = -\text{Cay} \circ \exp \circ \widehat{(\cdot)}.$$

Using Theorem 2.20 in Chapter 2 for the function V, one can show that the closed ball $f''(\bar{B}_{q,3}(0))$ is invariant for $z(t)$, which implies that the ball $\bar{B}_{q,3}(0)$ is also invariant for $x(t)$ and comprises the set $\mathcal{D} = \mathcal{D}^*(\infty)$. Now, using Theorem 2.22 it is easy to show that the set $\{z \in \mathbb{R}^{mn} : z_1 = \cdots z_n\}$ is globally uniformly asymptotically stable relative to $f''(\bar{B}_{q,3}(0))$ for $z(t)$, see the example on convexity in Chapter 2. It follows, by using (3.7) and that f'' is continuous, that $\mathcal{A}$ is globally uniformly asymptotically stable relative to $\mathcal{D}^*(\infty)$. ■

We can actually generalize the results in Theorem 3.2 and Theorem 3.3. Up until now we have assumed that we first fix a representation y_i, y_{ij} and then we use the control laws (3.8) and (3.9) for this representation. Instead, at each switching time τ_k we can allow the representation to switch also, so for example during $[\tau_k, \tau_{k+1})$ we use the Axis-Angle Representation, whereas during $[\tau_{k+1}, \tau_{k+2})$ we use the Modified Rodrigues Parameters. The representations that are used among the agents do not have to be the same either. One agent can for example use the Rodrigues Parameters to represent the rotations to a subset of its neighbors and the Axis-Angle Representation in order to represent the rotations to an other subset of its neighbors. For an agent i, the modified versions of (3.8) and (3.9) might look like

$$\omega_i = \sum_{j \in \mathcal{C}_1} a_{ij}(t - \gamma_\sigma(t))(\tan(\frac{\theta_j}{2})u_j - \tan(\frac{\theta_i}{2})u_i) + \sum_{j \in \mathcal{C}_2} a_{ij}(t - \gamma_\sigma(t))(\theta_i u_j - \theta_i u_i),$$

$$\omega_i = \sum_{j \in \mathcal{C}_1} a_{ij}(t - \gamma_\sigma(t)) \tan(\frac{\theta_{ij}}{2})u_{ij} + \sum_{j \in \mathcal{C}_2} a_{ij}(t - \gamma_\sigma(t))\theta_{ij} u_{ij},$$

respectively, where $\{\mathcal{C}_1, \mathcal{C}_2\}$ is a partition of $\mathcal{N}_i$.

Essentially, a different representation can be used for each pair of agents in the sum. We assume that the number of representations we use is finite, and redefine the radius r to be the smallest radius of injectivety for all representations that are used and q is changed accordingly in Theorem 3.2 and Theorem 3.3.

As a second remark we add that there is an alternative way of proving Theorem 3.3 instead of using Theorem 3.4, which shows the strength of Theorem 2.22. First we need the following lemma.

Lemma 3.5 ([13]). *suppose* $x_i \in B_{\pi/2,3}$ *for all* i*. If* $\theta_i \geq \theta_j$ *then* $x_i^T x_{ij} \leq 0$ *and* $x_i^T x_{ij} < 0$ *if* $x_i \neq x_j$*. Furthermore, if* $\theta_{ij} \geq \theta_{ik}$ *and* $\theta_{ij} \geq \theta_{jk}$ *then* $x_{ij}^T x_{jk} \leq 0$*,* $x_{ji}^T x_{ik} \leq 0$ *and* $x_{ij}^T x_{jk} < 0$*,* $x_{ji}^T x_{ik} < 0$ *if* $x_i \neq x_j \neq x_k$*.*

If we choose

$$V(x_i) = x_i^T x_i \quad \text{and} \quad W(x_i, x_j) = x_{ij}^T x_{ij},$$

we can use Lemma 3.5 in order to show that Assumption 2.18 and Assumption 2.19 hold for the functions V and W respectively. Here we see an example where the function $W(x_j, x_i)$ is not equal to $(x_j - x_i)^T(x_j - x_i)$. Even though Theorem 3.4 is not necessary in order to prove Theorem 3.3 and Lemma 3.5 can be used instead, Theorem 3.4 is interesting on its own and provides some geometric insight. Lemma 3.5 is proven in [13].

3.5 Torque control laws

In this section we construct control laws on a dynamic level for the special case of rigid bodies in space. The dynamics for agent i is given by

$$J_i\dot{\omega}_i = -\widehat{\omega}_i J_i \omega_i + \boldsymbol{\tau}_i, \tag{3.12}$$

where J_i is the inertia matrix and $\boldsymbol{\tau_i}$ is the control torque, which is given as a bold symbol since we do not want to mix it up with a switching time τ_i of the graph $\mathcal{G}_{\sigma(t)}$.

3.5.1 Static topologies

In this first subsection we strengthen the assumptions on $\mathcal{G}_{\sigma(t)}$ by assuming it is constant in time. Thus we denote the time-invariant (also referred to as constant or fixed) graph as $\mathcal{G}$. The reason for choosing time-invariant graphs, is that we are now considering a second order system, and the methods we use here are based on backstepping or high-gain control. In order to show stability, we introduce auxiliary error variables, and in the case of a switching graph, these variables suffer from discontinuities. In the next subsection we get around this problem by replacing the discontinuities with continuous in time transitions.

Based on the two kinematic control laws (3.8) and (3.9), we now propose two torque control laws for each agent i, where the first one is based on absolute rotations and the second one is based on relative rotations. The control laws are

$$\boldsymbol{\tau}_i = J_i(-x_i + \sum_{j\in\mathcal{N}_i} a_{ij}(L_{x_j}\omega_j - L_{x_i}\omega_i - \tilde{\omega}_i)) + \widehat{\omega}_i J_i \omega_i, \tag{3.13}$$

$$\boldsymbol{\tau}_i = J_i(-k_i\tilde{\omega}_i' + \sum_{j\in\mathcal{N}_i} a_{ij} L_{-y_{ij}}\omega_{ij}) + \widehat{\omega}_i J_i \omega_i. \tag{3.14}$$

The parameter k_i is a positive gain. The error variables $\tilde{\omega}_i$ and $\tilde{\omega}_i'$ are defined as follows

$$\tilde{\omega}_i = \omega_i - \sum_{j\in\mathcal{N}_i} a_{ij}(x_j - x_i),$$

$$\tilde{\omega}_i' = \omega_i - \sum_{j\in\mathcal{N}_i} a_{ij} y_{ij},$$

where $a_{ij} > 0$ is constant for all i and j. The matrix $L_{y_{ij}}$ is the Jacobian matrix in the kinematics for y_{ij}, *i.e.*,

$$\dot{y}_{ij} = L_{-y_{ij}}\omega_{ij},$$

and

$$\omega_{ij} = R_{ij}\omega_j - \omega_i$$

is the relative angular velocity between agent i and agent j. We collect all the x_i and $\tilde{\omega}_i$ into $(x, \tilde{\omega}) \in (B_\pi)^n \times (\mathbb{R}^3)^n$ and all the x_i and $\tilde{\omega}'_i$ into $(x, \tilde{\omega}') \in (B_\pi)^n \times (\mathbb{R}^3)^n$. Now, given $i \in \mathcal{V}$, the The closed loop system for $(x_i, \tilde{\omega}_i)^T$ when the torque control law (3.13) is used is

$$\begin{aligned}
\dot{x}_i &= L_{x_i} \sum_{j \in \mathcal{N}_i} a_{ij}(x_j - x_i) + L_{x_i}\tilde{\omega}_i, \\
\dot{\tilde{\omega}}_i &= -x_i - \sum_{j \in \mathcal{N}_i} a_{ij}\tilde{\omega}_i,
\end{aligned}$$

whereas the closed loop system for $(x_i, \tilde{\omega}'_i)^T$ when the torque control law (3.14) is used, is

$$\begin{aligned}
\dot{x}_i &= L_{x_i} \sum_{j \in \mathcal{N}_i} a_{ij} y_{ij} + L_{x_i}\tilde{\omega}'_i, \\
\dot{\tilde{\omega}}'_i &= -k_i \tilde{\omega}'_i.
\end{aligned}$$

We note that in (3.13), each agent i needs to know, not only the absolute rotations of its neighbors, but also the angular velocities of its neighbors. This requirement is fair, in the sense that in order to obtain the absolute rotations of the neighbors, communication is in general necessary, in which case the angular velocities also can be transmitted. In (3.14), we see that each agent i needs to know the relative rotations, relative velocities to its neighbors and the angular velocity of itself. The assumption of knowing the angular velocity of itself is strong, since it is not to regard as relative information. However, in practice the angular velocity of itself is possible to measure without the knowledge of the global frame $\mathcal{F}_W$, hence this velocity is to be regarded as local information.

Proposition 3.6. *Suppose $\mathcal{G}$ is strongly connected. If*

$$\max_{i \in \mathcal{V}} x_i^T(t_0)x_i(t_0) + \tilde{\omega}_i(t_0)^T\tilde{\omega}_i(t_0) \le q < r,$$

i.e., $(x_i(t_0), \tilde{\omega}_i(t_0))^T \in \bar{B}_{q,6}$ for all i and any $q < r$, then if controller (3.13) *is used, $\bar{B}_{q,6}$ is invariant for $(x(t), \tilde{\omega}(t))$ and $x(t) \to \mathcal{A}$ and $\omega_i(t) \to 0$ for all i as $t \to \infty$.*

The following part of this section, up until the proof of Proposition 3.6 is somewhat of a detour from the main subject of the chapter. It essentially explains the difficulties in constructing a quadratic Lyapunov function for the closed loop dynamics of $(x, \tilde{\omega})$ if the graph is not strongly connected. The reason for bringing up this subject is that we are using such a quadratic Lyapunov function in the proof of Proposition 3.6. In the following let $A \in \mathbb{R}^{m \times m}$ be an adjacency matrix [10] for the graph $\mathcal{G}$, meaning that $A = [a_{ij}]$ and $a_{ij} \ge 0$ where $a_{ij} > 0$ if and only if $(i, j) \in \mathcal{E}$. The graph Laplacian matrix for the graph $\mathcal{G}$ with the adjacency matrix A, we write as

$$L(\mathcal{G}, A) = D - A,$$

where

$$D = \text{diag}(d_1, \dots, d_n) = \text{diag}\left(\sum_{j=1}^{n} a_{1j}, \dots, \sum_{j=1}^{n} a_{nj}\right).$$

A graph with adjacency matrix A is balanced if

$$\sum_{j=1}^{n} a_{ij} = \sum_{j=1}^{n} a_{ji}.$$

It is well known that the (symmetric part of the) graph Laplacian matrix is positive semidefinite if the graph is balanced [10]. The **if** part in the lemma is provided in [14].

Lemma 3.7. *For a static quasi-strongly connected graph $\mathcal{G}$, there is a positive vector $\xi = (\xi_1, \dots, \xi_n)^T$ such that $L' = diag(\xi)L(\mathcal{G}, A)$ is the Graph Laplacian matrix of some balanced graph $\mathcal{G}'$, if and only if the graph $\mathcal{G}$ is strongly connected. Furthermore, if $\mathcal{G}$ is not strongly connected but quasi-strongly connected, there is no $\xi = (\xi_1, \dots, \xi_n)^T$ such that*

$$\frac{L' + L'^T}{2}$$

is positive semidefinite, where $L' = diag(\xi)L(\mathcal{G}, A)$.

Proof: **If**: We create a new matrix by $\tilde{L} = D^{-1}L = I - D^{-1}A$. Since the graph $\mathcal{G}$ is strongly connected, the adjacency matrix A is irreducible and the same holds for $D^{-1}A$. The row sum of each row in $D^{-1}A$ is equal to 1. By Perron Frobenius Theorem the largest eigenvalue of $D^{-1}A$ is equal to 1 and the corresponding left eigenvector $v = [v_1, \dots, v_n]^T$ has positive elements. This implies that v is a left eigenvector for $D^{-1}L$ corresponding to the eigenvalue 0. Let us choose $\xi = (\frac{v_1}{d_1}, \dots, \frac{v_n}{d_n})^T$, then it follows that the vector $[1, \dots, 1]^T$ is a left eigenvector of the matrix $L' = \text{diag}(\xi)L(\mathcal{G}, A)$ corresponding to the eigenvalue 0. The matrix L' is a graph Laplacian matrix of a balanced graph.

Only if: We show this by a contradiction argument. Suppose that the graph $\mathcal{G}$ is not strongly connected but quasi-strongly connected. Consider a system of the following form

$$\dot{z} = L(\mathcal{G}, A)z,$$

where $z \in \mathbb{R}^n$. We know that for this linear system $z(t)$ will asymptotically reach consensus since $\mathcal{G}$ is quasi-strongly connected. This is true for all initial conditions z_0 of the system. Now consider the special case where all elements in z_0 that correspond to the root of the spanning tree in the condensed graph is equal to $\alpha > 0$, whereas all other element are equal to 0. The condensed graph is constructed by identifying all the strongly connected components in the graph $\mathcal{G}$ and then replacing each such component with one node, where all the incoming and outgoing edges from each component now are incoming respectively outgoing from the node that replaces the component. Suppose there is a positive vector ξ

such that the symmetric part of $L' = \mathrm{diag}(\xi)L(\mathcal{G}, A)$ is positive semidefinite. In that case

$$V(x) = \sum_{i=1}^{n} \xi_i z_i^2$$

is a Lyapunov function for the system and the right-hand side of $\dot{V}(x(t))$ is non-positive for all $t \geq t_0$. But for our special choice of z_0 it holds that the system must reach consensus in the point $z = (\alpha, \dots, \alpha)^T$, which implies that V must increase during some time period. This is a contradiction. Now we have proven the **only if** statement as well as the last statement in the lemma. ∎

Suppose that the system is controlled on a kinematic level and that

$$\omega_i = \sum_{j \in \mathcal{N}_i} a_{ij}(x_j - x_i).$$

We know from Theorem 3.2 that $x(t) \to \mathcal{A}$ as $t \to \infty$ if $\mathcal{G}$ is strongly connected and $[a_{ij}]$ is an adjacency matrix of $\mathcal{G}$. If there were a positive vector ξ such that $\mathrm{diag}(\xi)L(\mathcal{G}, A)$ is positive semidefinite when $\mathcal{G}$ is quasi-strongly connected but not strongly connected, then we could use $V(x) = \sum_{i=1}^{n} \xi_i x_i^T x_i$ as a candidate Lyapunov for the system and show that $x(t) \to \mathcal{A}$ as $t \to \infty$. According to Lemma 3.7, there is unfortunately no such ξ. A Lyapunov function on this form is desirable, since then we can utilize the special structure of the Jacobian matrix that $x_i^T L_{x_i} = x_i^T$. In the proof of Proposition 3.6, we have the expression $\sum_{i=1}^{n} \xi_i x_i^T x_i$ as a part of the Lyapunov function we use. For this part of the Lyapunov function, we run into the same kind of troubles as for the example above with the kinematic control law, if the graph is not strongly connected.

For the sake of completeness, we provide a proof of the fact that a balanced graph has a positive semidefinite graph Laplacian matrix. We write the incidence matrix [10] of $\mathcal{G}$ as

$$B = B_- + B_+,$$

where each element in B_- is -1 if and only if the corresponding element in B is -1 otherwise the element is 0. The matrix B_+ is defined accordingly where the elements are 1 or 0. Using these matrices we can write the graph Laplacian matrix L for a weighted graph as

$$L(\mathcal{G}, A) = B_- D B^T,$$

where D is a diagonal matrix containing the positive edge weights (positive elements in A) on its diagonal. For a graph that is unweighted, the matrix D is the identity matrix. This alternative way of writing the graph Laplacian matrix L, (compare with the proof of Lemma 3.7), can be used to show that L is positive semidefinite if the graph is balanced. The graph is balanced if

$$B_- D\mathbf{1} + B_+ D\mathbf{1} = 0,$$

where $\mathbf{1}$ is a vector in which each element is equal to 1.

Lemma 3.8. *Suppose the graph $\mathcal{G}$ is quasi-strongly connected and balanced, then*

$$\tilde{L} = \frac{L(\mathcal{G}, A) + L(\mathcal{G}, A)^T}{2}$$

is positive semidefinite. Furthermore, 0 *is the smallest eigenvalue of* $\tilde{L}$ *and all other eigenvalues are strictly larger than* 0*.*

Proof: Let us write the graph Laplacian matrix as follows.

$$L = B_- D^{1/2} D^{1/2} (B_- + B_+)^T = \tilde{B}_- (\tilde{B}_- + \tilde{B}_+)^T,$$

where $\tilde{B}_- = D^{1/2} B_-$, $\tilde{B}_+ = D^{1/2} B_+$ and we define $\tilde{B} = \tilde{B}_- + \tilde{B}_+$. The matrices $\tilde{B}_-^T$ and $\tilde{B}_+^T$ are orthogonal (each column in $\tilde{B}_-^T$ is orthogonal to the other columns in $\tilde{B}_-^T$, likewise for $\tilde{B}_+^T$) and since the graph is balanced it holds that

$$\tilde{B}_- \tilde{B}_-^T = \tilde{B}_+ \tilde{B}_+^T.$$

Now,

$$\begin{aligned}
\tilde{L} &= (\tilde{B}_-(\tilde{B}_- + \tilde{B}_+)^T + (\tilde{B}_- + \tilde{B}_+)\tilde{B}_-^T)/2 \\
&= (\tilde{B}_-(\tilde{B}_-^T + \tilde{B}_+^T) + (\tilde{B}_-\tilde{B}_-^T + \tilde{B}_+\tilde{B}_-^T))/2 \\
&= (\tilde{B}_-(\tilde{B}_-^T + \tilde{B}_+^T) + (\tilde{B}_+\tilde{B}_+^T + \tilde{B}_+\tilde{B}_-^T))/2 \\
&= (\tilde{B}_-(\tilde{B}_-^T + \tilde{B}_+^T) + \tilde{B}_+(\tilde{B}_+^T + \tilde{B}_-^T))/2 \\
&= (\tilde{B}_-\tilde{B}^T + \tilde{B}_+\tilde{B}^T)/2 = \tilde{B}\tilde{B}^T,
\end{aligned}$$

which means that $\tilde{L}$ is positive semidefinite. It follows that

$$\tilde{L}\mathbf{1} = \tilde{B}\tilde{B}^T\mathbf{1} = 0.$$

We also known that $\text{rank}(\tilde{B}\tilde{B}^T) = \text{rank}(\tilde{B}) = n - 1$ (assuming n nodes in the graph $\mathcal{G}$). ■

Remark 3.4. An other way to show that $\tilde{L}$ is positive semidefinite is as follows. There is an orthonormal matrix Q such that

$$Q\tilde{B}_-^T = \tilde{B}_+^T.$$

This means that

$$\tilde{L} = \tilde{B}_- \left(I + \frac{Q + Q^T}{2} \right) \tilde{B}_-^T.$$

Since the absolute values of the eigenvalues of the matrix $(Q + Q^T)/2$ are less or equal to 1, $\tilde{L}$ is positive semidefinite. In the special case when the graph is unweighted, *i.e.*, $D = I$, the matrix Q can be chosen as a permutation matrix.

Proof of Proposition 3.6: In the multi-agent system at hand we have n agents, where each agent i has the state $(x_i, \tilde{\omega}_i)^T$. We first show the invariance of the ball $\bar{B}_{q,6}$.

$$V((x_i, \tilde{\omega}_i)^T) = x_i^T x_i + \tilde{\omega}_i^T \tilde{\omega}_i.$$

We see that

$$\begin{aligned}\frac{d}{dt} V((x_i, \tilde{\omega}_i)^T) &= \sum_{j \in \mathcal{N}_i} a_{ij} (x_i, \tilde{\omega}_i)(x_j - x_i, -\tilde{\omega}_i)^T \\ &= \sum_{j \in \mathcal{N}_i} a_{ij} ((x_i, \tilde{\omega}_i)(x_j, 0)^T - (x_i, \tilde{\omega}_i)(x_i, \tilde{\omega}_i)^T).\end{aligned}$$

Thus,

$$D^+ f_{V,6}((x(t), \tilde{\omega}(t))^T) \leq 0.$$

Now, using Theorem 2.20 in Chapter 2, we can show that $\bar{B}_{q,6}$ is invariant, where $\beta_1 = \beta_2 = \| \cdot \|$, *i.e.*, the Euclidean norm in $\mathbb{R}^6$.

In order to show the convergence, we define the following function

$$\tilde{\gamma}(x, \tilde{\omega}) = \sum_{i=1}^{n} \xi_i (x_i^T x_i + \tilde{\omega}_i^T \tilde{\omega}_i),$$

where $\xi = (\xi_1, \ldots, \xi_n)^T$ is the positive vector chosen as in the proof of Lemma 3.7. We have that

$$\dot{\tilde{\gamma}} = -x^T (L' \otimes I_3) x - \sum_{i=1}^{n} \xi_i \sum_{j \in \mathcal{N}_i} a_{ij} \tilde{\omega}_i^T \tilde{\omega}_i,$$

where, according to Lemma 3.7, L' is positive semidefinite. By LaSalle's theorem, $(x(t), \tilde{\omega}(t))^T$ will converge to the largest invariant set contained in

$$\{(x, \tilde{\omega})^T : \dot{\tilde{\gamma}}((x, \tilde{\omega})^T) \ = 0\}$$

as the time goes to infinity. This largest invariant set is contained in the set $\{(x, \tilde{\omega})^T : x \in \mathcal{A}, \tilde{\omega} = 0\}$. ■

Remark 3.5. In the proof of Proposition 3.6, if we look at the dynamics of $(x, \tilde{\omega})$, we see that the largest invariant set contained in $\{(x, \tilde{\omega})^T : \dot{\tilde{\gamma}}((x, \tilde{\omega})^T) \ = 0\}$ is actually the point 0. Hence, the system will reach consensus in the point $x = 0$.

Proposition 3.9. *Suppose $\mathcal{G}$ is quasi-strongly connected. For any positive r_1 and r_2 such that $r_1 < r_2 < r/2$ and $q > 0$, there is a $k > 0$ such that if $k_i \geq k$ and $(x_i(t_0), \tilde{\omega}_i'(t_0))^T \in \bar{B}_{r_1,3} \times \bar{B}_{q,3}$ for all i, then if controller* (3.14) *is used it holds that $(x_i(t), \tilde{\omega}_i'(t))^T \in \bar{B}_{r_2,3} \times \bar{B}_{q,3}$ for all $i, t \geq t_0$ and*

$$(x(t), \tilde{\omega}'(t))^T \rightarrow (\bar{B}_{r_2,3})^n \cap \mathcal{A} \times \{0\} \quad \textit{as} \quad t \rightarrow \infty.$$

Furthermore, $(\bar{B}_{r_2,3})^n \cap \mathcal{A} \times \{0\}$ is globally asymptotically stable relative to the largest invariant set contained in $(\bar{B}_{r_2,3})^n \times (\bar{B}_{q,3})^n$ for the dynamics of $(x(t), \tilde{\omega}'(t))^T$.

Before we proceed with the proof of Proposition 3.9, we pose a result that can be obtained from [15].

Theorem 3.10 ([15]). *Let $\sum : \dot{\xi} = \tilde{f}(\xi)$ be a dynamical system defined on $\mathcal{X} \subset \mathbb{R}^m$, where $\tilde{f}$ is locally Lipschitz on $\mathcal{X}$. Let Γ_1, Γ_2 and $\mathcal{X}$ be compact and positively invariant for $\sum$ and $\Gamma_1 \subset \Gamma_2 \subset \mathcal{X}$, then Γ_1 is globally asymptotically stable relative to $\mathcal{X}$ if*

1. *Γ_1 is globally asymptotically stable relative to Γ_2,*
2. *Γ_2 is stable,*
3. *Γ_2 is globally attractive relative to $\mathcal{X}$,*

Remark 3.6. In Proposition 3.9 and Theorem 3.10 we use the classical definition of invariance of a set, see [16].

Proof of Proposition 3.9: By treating the closed loop dynamics as a switching system on the form (2.1) (even though the right-hand side is time-invariant) we can borrow the notation $\mathcal{D}^*(\infty)$, where

$$\mathcal{D}^*(\infty) \subset \mathcal{D} = (\bar{B}_{r_2,3})^n \times (\bar{B}_{q,3})^n$$

is the largest set of initial points for the system for which the solution is contained in $\mathcal{D}$ for all times $t > t_0$. We know from Lemma 2.15 that $\mathcal{D}^*(\infty)$ is compact and invariant, *i.e.*, the set $\mathcal{D}^*(\infty)$ is the largest invariant set contained in $\mathcal{D}$.

Now we show that for a proper choice of the constant k, it holds that

$$(\bar{B}_{r_1,3})^n \times (\bar{B}_{q,3})^n \subset \mathcal{D}^*(\infty).$$

We assume without loss of generality that $t_0 = 0$, and note that

$$\|\tilde{\omega}_i'(t)\| = \|\tilde{\omega}_i'(0)\| \exp(-k_i t) \leq q \exp(-k_i t).$$

We choose $\min_{i \in \mathcal{V}} k_i \geq k$ and

$$V(x_i(t)) = x_i(t)^T x_i(t),$$

where k is still left to be determined. By using Lemma 3.5, it is possible to show that there exists an interval $[0, t_1)$ on which it holds that

$$D^+(f_{V,3}(x(t))) \leq q r_2 \exp(-kt).$$

By using the Comparison Principle, it follows that

$$f_{V,3}(x(t)) \leq f_{V,3}(x(0)) + q r_2 \frac{(1 - \exp(-kt))}{k}$$

on $[0, t_1)$. Now if we choose $k \geq q r_2/(r_2 - r_1)$ we see that $f_{V,3}(x(t)) \leq r_2$ for $t \geq 0$, and we can choose $t_1 = \infty$.

In order to show convergence we use Theorem 3.10, where $\mathcal{X} = \mathcal{D}^*(\infty)$, $\Gamma_2 = \mathcal{D}^*(\infty) \cap ((\bar{B}_{r_2/2,3})^n \times \{0\})$ and $\Gamma_1 = \mathcal{D}^*(\infty) \cap (\mathcal{A} \times \{0\})$. Now 1 in Theorem 3.10 can be shown by using Theorem 3.3 and 2 and 3 in Theorem 3.10 follow from the first part of this proof. Note that $(\bar{B}_{r_2,3})^n \cap \mathcal{A} \times 0 \subset \mathcal{D}^*(\infty)$. ■

3.5.2 Dynamic topologies with continuous system dynamics

If we allow the graph $\mathcal{G}$ to be time-varying and $\dot{x}$ be discontinuous in t the main problem of the previous section, as already mentioned in Section 3.5.1, is that the auxiliary error variables $\tilde{\omega}$ and $\tilde{\omega}'$ suffer from discontinuities. In order to avoid this problem we here propose control laws where instead of switching discontinuously between different functions, there are continuous in time transitions between the functions. For the switching signal function σ, with the sequence of switching times is $\{\tau_k\}$, we define the function

$$\gamma_\sigma^\delta(t) = \max\{\tau_k : \tau_k - \delta \leq t, k \in \mathbb{Z}\},$$

where $0 < \delta < \tau_D/4$ is a positive constant.

Now we introduce a modified version of (3.13) given as

$$\boldsymbol{\tau}_i = J_i(-x_i + \dot{\bar{\omega}}_i - \bar{\omega}_i'') + \widehat{\omega}_i J_i \omega_i, \tag{3.15}$$

where L_{x_i} is the Jacobian matrix for the representation x_i, $\tilde{\omega}_i'' = \omega_i - \bar{\omega}_i$ and

$$\bar{\omega}_i = \begin{cases} \sum_{j \in \mathcal{N}_i(t)} a_{ij}(x_j - x_i) - \beta x_i & \text{if } \gamma_\sigma^\delta(t) - t \leq 0, \\ \\ \alpha\left(\gamma_\sigma^\delta(t) - t\right)\left(\sum_{j \in \mathcal{N}_i(t)} a_{ij}(x_j - x_i)\right) & \\ + \left(1 - \alpha\left(\gamma_\sigma^\delta(t) - t\right)\right)\left(\sum_{j \in \mathcal{N}_i(\gamma_\sigma^\delta(t))} a_{ij}(x_j - x_i)\right) - \beta x_i & \text{otherwise,} \end{cases}$$

and

$$\bar{\omega}_i'' = \begin{cases} \sum_{j \in \mathcal{N}_i(t)} a_{ij}\tilde{\omega}_i'' + \beta\tilde{\omega}_i'' & \text{if } \gamma_\sigma^\delta(t) - t \leq 0, \\ \\ \alpha\left(\gamma_\sigma^\delta(t) - t\right)\left(\sum_{j \in \mathcal{N}_i(t)} a_{ij}\tilde{\omega}_i''\right) & \\ + \left(1 - \alpha\left(\gamma_\sigma^\delta(t) - t\right)\right)\left(\sum_{j \in \mathcal{N}_i(\gamma_\sigma^\delta(t))} a_{ij}\tilde{\omega}_i''\right) + \beta\tilde{\omega}_i'' & \text{otherwise.} \end{cases}$$

The function $\alpha(t)$ should be a non-negative $\mathcal{C}^1$-function that is positive on $(0, \delta]$ such that

$$\begin{aligned} \alpha(\delta) = 1, &\quad \alpha(0) = 0, \\ \dot{\alpha}(\delta) = 0, &\quad \dot{\alpha}(0) = 0. \end{aligned}$$

One can for example choose

$$\alpha(t) = \frac{1}{2} + \frac{1}{2}\cos\left(\frac{t\pi}{\delta}\right).$$

The constant $\beta > 0$ should be chosen positive.

Now we formulate a modified version of Proposition 3.6.

Proposition 3.11. *Suppose $\mathcal{G}_{\sigma(t)}$ is uniformly strongly connected. If*

$$\max_{j\in\mathcal{V}} x_j^T(t_0)x_j(t_0) + \tilde{\omega}_j''(t_0)^T\tilde{\omega}_j''(t_0) \leq q < r,$$

i.e., if $(x_i(t_0), \tilde{\omega}_i''(t_0))^T \in \bar{B}_{q,6}$ for all i and any $q < r$, then if controller (3.15) *is used, $\bar{B}_{q,6}$ is invariant for $(x(t), \tilde{\omega}''(t))^T$ and $x(t) \to \mathcal{A}$ and $\tilde{\omega}_i''(t) \to 0$ for all i as $t \to \infty$.*

Proof: The closed loop dynamics for $(x_i, \tilde{\omega}_i'')$ is

$$\begin{cases} \dot{x}_i = L_{x_i}\bar{\omega}_i + L_{x_i}\tilde{\omega}_i'', \\ \dot{\tilde{\omega}}_i'' = -x_i - \bar{\omega}_i'', \end{cases}$$

which fulfills Assumption 2.17. We define

$$V((x_i, \tilde{\omega}_i'')^T) = x_i^T x_i + \tilde{\omega}_i''^T\tilde{\omega}_i''$$

and get that

$$\frac{d}{dt}V((x_i, \tilde{\omega}_i'')^T) = (x_i, \tilde{\omega}_i'')(\bar{\omega}_i, -\bar{\omega}_i'')^T. \tag{3.16}$$

Now we look at the right-hand side of 3.16 for the following two cases.

Case 1: $\gamma_\sigma^\delta(t) - t \leq 0$.
The right-hand side of (3.16) is given by

$$\begin{aligned} &\frac{d}{dt}V((x_i, \tilde{\omega}_i'')^T) = -\beta(x_i, \tilde{\omega}_i'')(x_i, \tilde{\omega}_i'')^T \\ &+ \sum_{j\in\mathcal{N}_i(t)} a_{ij}((x_i, \tilde{\omega}_i'')(x_j, 0)^T - (x_i, \tilde{\omega}_i'')(x_i, \tilde{\omega}_i'')^T). \end{aligned}$$

Case 2: $\gamma_\sigma^\delta(t) - t > 0$.
The right-hand side of (3.16) is given by

$$\begin{aligned} &\frac{d}{dt}V((x_i, \tilde{\omega}_i'')^T) = -\beta(x_i, \tilde{\omega}_i'')(x_i, \tilde{\omega}_i'')^T \\ &+ \alpha\left(\gamma_\sigma^\delta(t) - t\right) \sum_{j\in\mathcal{N}_i(t)} a_{ij}((x_i, \tilde{\omega}_i'')(x_j, 0)^T - (x_i, \tilde{\omega}_i'')(x_i, \tilde{\omega}_i'')^T) \\ &+ \left(1 - \left(\gamma_\sigma^\delta(t) - t\right)\right) \sum_{j\in\mathcal{N}_i(\gamma_\sigma^\delta)} a_{ij}((x_i, \tilde{\omega}_i'')(x_j, 0)^T - \alpha(x_i, \tilde{\omega}_i'')(x_i, \tilde{\omega}_i'')^T). \end{aligned}$$

It follows that Assumption 2.18 is fulfilled for the system and V. One can use Theorem 2.20 and show that $\bar{B}_{q,6}$ is invariant, where $\beta_1 = \beta_2 = \|\cdot\|$, *i.e.*, the Euclidean norm in $\mathbb{R}^6$. The desired convergence result follows by using Theorem 2.21. ∎

Remark 3.7. By including the terms βx_i and $\beta_i \tilde{\omega}_i''$ in the control law, we avoid the problem that Assumption 2.18 (3) fails. If we do not add these terms we cannot guarantee that if $i \in \mathcal{I}_V(t,t)$ and $i \notin \mathcal{I}_V^*(t)$ it holds that the right-hand side of the dynamics for $(x_i, \tilde{\omega}_i'')^T$ is in an equilibrium that is independent of the time, see Assumption 2.18 (3). On the other hand, by adding the terms, it is obvious that the system converges to the point 0. The function $f_{V,6}(x, \tilde{\omega}_i'')$ is now strictly decreasing unless $(x, \tilde{\omega}_i'')^T = 0$.

3.6 Formation control

The objective in the formation problem is the following one. Given some desired constant rotation matrices $R_1^*, \ldots, R_n^*$, construct a control law for the system such that

$$\begin{gathered} R_1(t) \to Q^T R_1^*, \\ \vdots \\ R_n(t) \to Q^T R_n^*, \end{gathered}$$

as $t \to \infty$ for some arbitrary matrix Q, which implies

$$R_i^T(t) R_j(t) \to R_i^{*T} R_j^*$$

as $t \to \infty$.

Now we show that on a kinematic level this problem is equivalent to the consensus problem. Let us define $\tilde{R}_i = R_i R_i^{*T}$ for all i. The kinematics for $\tilde{R}_i$ is given by

$$\dot{\tilde{R}}_i = R_i \widehat{\omega}_i R_i^{*T} = \tilde{R}_i R_i^* \widehat{\omega}_i R_i^{*T} = \tilde{R}_i \widehat{\omega}_i^*,$$

where $\omega_i^* = R_i^* \widehat{\omega}_i R_i^{*T}$. It is easy to see that if the agents reach consensus in the rotations $\tilde{R}_1, \ldots, \tilde{R}_n$, then the system reaches the desired formation. However in order to reach consensus using a kinematic control law ω_i^*, we can use any of the proposed control laws (3.8) and (3.9) where we replace x_i and x_{ij} by

$$\tilde{x}_i = \mathrm{Log}\left(\tilde{R}_i\right), \quad \tilde{x}_{ij} = \mathrm{Log}\left(\tilde{R}_i^T \tilde{R}_j\right) = \mathrm{Log}\left(R_i^{*T} R_{ij} R_j^{*T}\right).$$

Similarly we can replace y_i by $\tilde{y}_i$ and y_{ij} by $\tilde{y}_{ij}$. The actual control law ω_i used by agent i is simply $\omega_i = R_i^{*T} \omega^*$.

On a dynamic level we have that

$$J_i R_i^{*T} \dot{\omega}_i^* = -\left(R_i^{*T} \widehat{\omega}_i^* R_i^*\right) J_i R_i^{*T} \omega_i^* + \boldsymbol{\tau}_i. \tag{3.17}$$

Now we can introduce modified versions of the control laws (3.13) and (3.14)

$$\begin{aligned}\boldsymbol{\tau}_i = J_i R_i^{*T} &\left(-\tilde{x}_i + \sum_{j \in \mathcal{N}_i} a_{ij} \left(L_{\tilde{x}_j} \omega_j^* - L_{\tilde{x}_i} \omega_i^* - \tilde{\omega}_i \right) \right) \\ &+ \left(R_i^{*T} \widehat{\omega}_i^* R_i^* \right) J_i \left(R_i^{*T} \right) \omega_i^*, \end{aligned} \tag{3.18}$$

$$\begin{aligned}\boldsymbol{\tau}_i = J_i R_i^{*T} &\left(-k_i \tilde{\omega}_i' + \sum_{j \in \mathcal{N}_i} a_{ij} L_{-\tilde{y}_{ij}} \omega_{ij} \right) + \\ &\left(R_i^{*T} \widehat{\omega}_i^* R_i^* \right) J_i \left(R_i^{*T} \right) \omega_i^*, \end{aligned} \tag{3.19}$$

where in this context

$$\begin{aligned}\tilde{\omega}_i &= \omega_i^* - \sum_{j \in \mathcal{N}_i} a_{ij} \left(\tilde{x}_j - \tilde{x}_i \right), \\ \tilde{\omega}_i' &= \omega_i^* - \sum_{j \in \mathcal{N}_i} a_{ij} \tilde{y}_{ij}.\end{aligned}$$

Now the same convergence results hold as in Proposition 3.6 and Proposition 3.9 after replacing $y_i(t_0)$ with $\tilde{y}(t_0)$, and where $\tilde{\omega}_i$ and $\tilde{\omega}_i'$ are defined in this new sense.

3.7 Illustrative examples

We will now illustrate the convergence for the two different control laws when $y_i = x_i$ for all i, *i.e.*, we use the Axis-Angle Representation. We consider the case of 5 agents. The simulations were conducted in MATLAB using an Euler method to solve the ordinary differential equations.

In Figure 3.5 and Figure 3.6 the control law (3.8) for absolute rotations is used and in Figure 3.7 and Figure 3.8 the control law (3.9) for relative rotations is used. One can see how the rotations of the agents, expressed in the Axis-Angle Representation, converge from their initial rotations (blue discs in the figure) to the final rotations where they reach consensus.

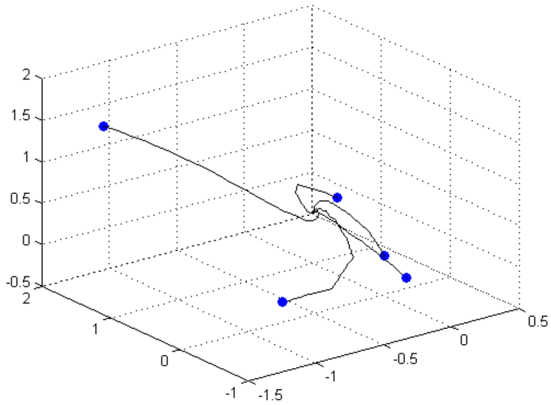

Figure 3.5: There are five agents. The agents use controller (3.8) and their rotations converge to a synchronized rotation as the time goes to infinity. In this example the initial rotations of the agents, marked by blue discs, are contained in the region $B_q(I)$ with $q = 3$. There are two graphs, $\mathcal{E}_1 = \{(1,2),(3,4),(5,1)\}$ with nonzero weights $a_{ij} = 4$ if $(j,i) \in \mathcal{E}_1$, $\mathcal{E}_2 = \{(2,3),(3,5),(4,1)\}$ with nonzero weights $a_{ij} = 6$ if $(j,i) \in \mathcal{E}_2$. We use a periodic switching signal function with period $T = 0.2$. The switching signal function $\sigma(t) = 1$ if $t \in [kT, kT + T/2)$, $\sigma(t) = 2$ if $t \in [kT + T/2, (k+1)T)$, $k = \mathbb{Z}$. The time horizon is 5 sec.

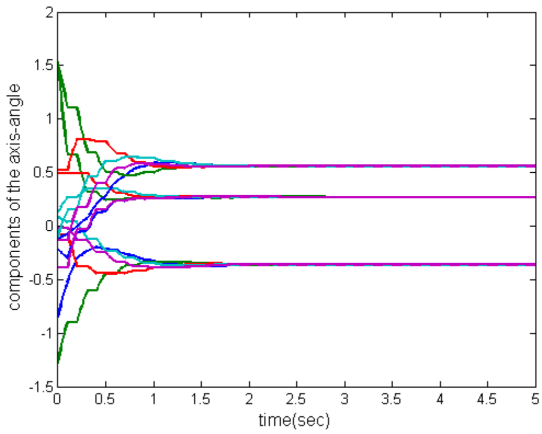

Figure 3.6: The same example as Figure 3.5. The three components of the Axis-Angle Representation x_i of the five agents converge to some common values as the time goes to infinity.

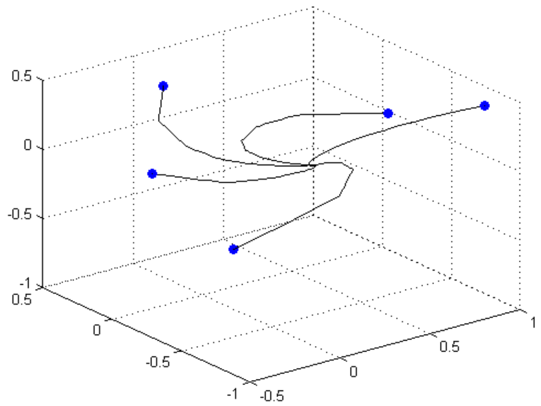

Figure 3.7: The rotations of five agents converge to a synchronized rotation as the time goes to infinity using controller (3.9). In this example the initial rotations of the agents are contained in the region $B_q(I)$ with $q = 1.5$. There are two graphs, $\mathcal{E}_1 = \{(1,2),(3,4)\}$, $\mathcal{E}_2 = \{(2,3),(3,1),(4,5)\}$. The switching signal function is periodic with $\sigma(t) = 1$ if $t \in [kT, kT + T/2)$, $\sigma(t) = 2$ if $t \in [kT + T/2, (k+1)T)$, $k \in \mathbb{Z}$, where the period $T = 0.2$. The time horizon was 5 sec. Blue discs indicate the initial rotations of the agents.

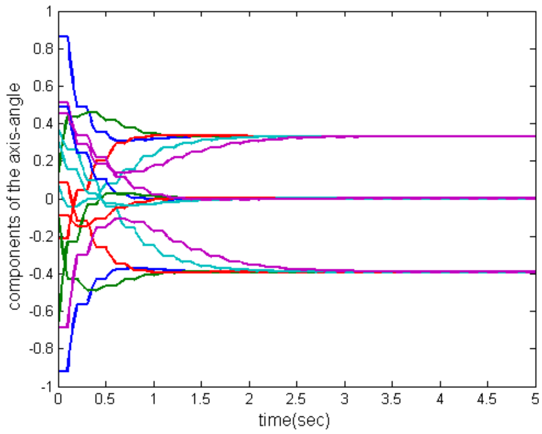

Figure 3.8: The same example as Figure 3.7. The three components of the Axis-Angle Representation x_i of the five agents are synchronized respectively as the time goes to infinity.

3.8 Bibliography

[1] K. D. Listmann, C. A. Woolsey and J. Adamy. Passivity-based coordination of multi-agent systems: a backstepping approach. In *Proceedings of the European Control Conference 2009*, pages 2450–2455, 2009.

[2] D. V. Dimarogonas, P. Tsiotras and K. J. Kyriakopoulos. Laplacian cooperative attitude control of multiple rigid bodies. In *2006 IEEE International Symposium on Intelligent Control*, pages 3064–3069. IEEE, 2006.

[3] R. Tron, B. Afsari and R. Vidal. Intrinsic consensus on SO(3) with almost-global convergence. In *Conference on Decision and Control, CDC*, pages 2052–2058, 2012.

[4] A. Sarlette, R. Sepulchre, and N. E. Leonard. Autonomous rigid body attitude synchronization. *Automatica*, 45(2):572–577, 2009.

[5] W. Ren. Distributed cooperative attitude synchronization and tracking for multiple rigid bodies. *IEEE Transactions on Control Systems Technology*, 18(2):383–392, 2010.

[6] B. Afsari. Riemannian Lp center of mass: Existence, uniqueness and convexity. In *Proc. Amer. Math. Soc*, volume 139, pages 655–673, 2011.

[7] P. Tsiotras, J.L. Junkins, and H. Schaub. Higher-order cayley transforms with applications to attitude representations. *Journal of Guidance, Control, and Dynamics*, 20(3):528–534, 1997.

[8] J.L. Junkins and H. Schaub. Analytical mechanics of space systems. *AIAA Education Series*, 2003.

[9] E. Malis, F. Chaumette and S. Boudet. 2 1/2 D visual servoing. *IEEE Transactions on Robotics and Automation*, 15(2):238–250, 1999.

[10] M. Mesbahi and M. Egerstedt. *Graph theoretic methods in multiagent networks*. Princeton University Press, 2010.

[11] J. Hartley, R. Trumpf and Y. Da. Rotation averaging and weak convexity. *In Proceedings of the 19th International Symposium on Mathematical Theory of Networks and Systems (MTNS)*, pages 2435–2442, 2010.

[12] G.S. Chirikjian and A.B. Kyatkin. *Engineering applications of noncommutative harmonic analysis: with emphasis on rotation and motion groups*. CRC press, 2001.

[13] W. Song, J. Thunberg, X. Hu and Y. Hong. Distributed high-gain attitude synchronization using rotation vectors. *Journal of Systems Science and Complexity*. To appear.

[14] W. Yu, G. Chen, M. Cao and J. Kurths. Second-order consensus for multiagent systems with directed topologies and nonlinear dynamics. *IEEE Transactions on Systems, Man, and Cybernetics, Part B: Cybernetics*, 40(3):881–891, 2010.

[15] M. El-Hawwary and Maggiore M. Reduction theorems for stability of closed sets with application to backstepping control design. *Automatica*, 49:214–222, 2013.

[16] H. K. Khalil. *Nonlinear systems*, Third Edition. Prentice hall, 2002.

Chapter 4

Consensus on $SO(3)$ for networks of uncalibrated cameras using the conjugate rotations

In this chapter, the problem of consensus on $SO(3)$ is studied from a somewhat different angle. In the problem at hand, a system of uncalibrated cameras shall reach consensus in their rotations. To be more precise, we assume that each agent corresponds to an uncalibrated camera, and the estimated rotation matrices are distorted by the intrinsic information in the partially unknown camera calibration matrices.

In [1] the problem of distributed camera calibration is addressed. Given some initial relative rotations between the cameras, the goal is to construct an iterative algorithm that makes the rotation converge to an average rotation, *i.e.*, the Riemannian centre of mass, or the Karcher mean [2], which is a special case of L^p-mean where $p = 2$. In [3], the rotation averaging is addressed from the structure from motion perspective.

In [4, 5], the rotation matrices in a network of cameras are distorted by the unknown focal length of the camera. In those works, the agents use the epipoles obtained from the fundamental matrix, where the fundamental matrix determines the geometric relationship between point features in two images [6–8]. For two agents, agent 1 and agent 2, the epipole of agent 2 at agent 1 is the (possibly distorted) position of agent 2 in the image plane of agent 1. In [4, 5], the agents are assumed to be a group of robots positioned in a plane, equipped with equivalent cameras of unknown focal length. The rotational axis for the rotation of each camera coincide with the normal vector to the plane. Thus, there is only one degree of freedom for the epipolar vectors. Provided the agents are sufficiently close to each other in terms of rotations, the control law guarantees consensus. The size of the region for convergence is provided in terms of geodesic distance in $SO(2)$. If any pair of rotations is closer than $\pi/4$ from each other, convergence is guaranteed.

In order to calculate the rotation matrices by using epipolar geometry, one first calculates the fundamental matrix [9]. Given the fundamental matrix, one then calibrates the camera and calculates the rotation matrix. Since the knowledge of the full calibration and rotation is not necessary to have in order to construct a consensus control law, the main idea in [4, 5] was to skip the calculation of the rotation matrix and the calibration matrix of the camera and use the information from the fundamental matrix directly in the control law.

The idea of bypassing the calculation of the calibration matrix and the rotation matrix in the control design is adopted in this work. However, in this work, instead of using the epipoles in order to construct consensus control laws, we use the so called conjugate rotations. The epipole, in the planar case, as presented in [5], is a local representation of $SO(2)$. The local representations we are considering in this work are local representations of $SO(3)$, and the class of representations we consider is the same as in Chapter 3, which include the Axis-Angle Representation representation, the Rodrigues Parameters and the Modified Rodrigues Parameters. These representations all have a special structure that we utilize. We show that for every local representation in the class, there is a corresponding distorted local representation, given by an invertible linear transformation of the local representation.The transformation is a function of the intrinsic parameters of the camera and is independent of the local representation.

The distorted local representations are not calculated from the fundamental matrix, but instead from the conjugate rotation matrix under the assumption of a zero skew factor. We assume that the conjugate rotation matrices are obtained in either one of the following two ways. (1) The camera is weakly calibrated, *i.e.* up to affine reconstruction [9] or (2) the motion is purely rotational, in which case the conjugate rotation matrices can be calculated from a homography using at least four point correspondences between two images [10].

We deliberately use the phrase *distored local representations* instead of *e.g.*, *local conjugate representations*. The reason being that one needs in general 7 parameters to represent a conjugate rotation [11], but our representation does only have 3 parameters, so the mapping is not injective. The usefulness lies in their simple structure, they can be calculated in a similar way as their undistorted counterparts, and they can be used in stabilization and consensus control laws.

We provide, for the entire class of distorted local representations, three types of control laws that guarantee local consensus under different circumstances.

By using the Rodrigues Parameters, we generalize the local convergence results to almost global results for the three control laws. All the control laws we present are defined on a kinematic level, but they are possible to extend to torque control laws by using a suitable nonlinear control design technique such as backstepping.

In the single agent case, the problem of stabilization falls into the framework of visual servoing, [12, 13]. In this problem, the pose (rotation and position) shall converge to a desired pose, and in the special case of a pure rotation, the rotation matrix shall without loss of generality converge to the identity matrix. We show that the distorted local representations can be used within this framework also.

4.1 Preliminaries

Consider a system of n agents. Each agent i has a camera, with a corresponding camera coordinate frame $\mathcal{F}_i$. As in Chapter 3 we have a world coordinate frame $\mathcal{F}_W$. At time $t \geq 0$, the rotation of the body frame $\mathcal{F}_i$ in the frame $\mathcal{F}_W$ is denoted as $R_i(t) \in SO(3)$. The relative rotation of $\mathcal{F}_j$ in $\mathcal{F}_i$ at time t is denoted as $R_{ij}(t) \in SO(3)$. Sometimes we write $(SO(3), d)$, where d is the Riemannian metric given as

$$d(R_1, R_2) = \frac{1}{\sqrt{2}}\|\log(R_1^T R_2)\|_2.$$

Each agent also has a corresponding position or translation denoted by $t_i(t)$ which is the position of the origin of $\mathcal{F}_W$ expressed in $\mathcal{F}_i$.

4.1.1 Camera model

The matrix

$$G_i(t) = \begin{bmatrix} R_i(t)^T & t_i(t) \\ 0 & 1 \end{bmatrix}$$

is an element of the matrix group $SE(3)$ [9].

In this work we consider the pinhole camera model for each agent i, which is defined by the transformation

$$h : \mathbb{R}^3 \times SE(3) \to \{x \in \mathbb{R}^3 : (0,0,1)x = 1\}.$$

The transformation h maps the point $p \in \mathbb{R}^3$ to the point $h(p, G_i(t)) \in \{x \in \mathbb{R}^3 : (0,0,1)x = 1\}$ as follows

$$h(p, G_i(t)) =$$
$$\frac{1}{\lambda}\begin{bmatrix} f_i s_{i,x} & f s_{i,\theta} & o_{i,x} \\ 0 & f_i s_{i,y} & o_{i,y} \\ 0 & 0 & 1 \end{bmatrix} \begin{bmatrix} 1 & 0 & 0 & 0 \\ 0 & 1 & 0 & 0 \\ 0 & 0 & 1 & 0 \end{bmatrix} \begin{bmatrix} R_i(t)^T & t_i(t) \\ & \\ 0 & 1 \end{bmatrix} \begin{bmatrix} p \\ \\ 1 \end{bmatrix}.$$

The point p is represented in the world frame $\mathcal{F}_W$, and the point $h(p, G_i(t))$ is represented in the camera frame $\mathcal{F}_i$. The constant matrix

$$K_i = \begin{bmatrix} f_i s_{i,x} & f_i s_{i,\theta} & o_{i,x} \\ 0 & f_i s_{i,y} & o_{i,y} \\ 0 & 0 & 1 \end{bmatrix}$$

is the intrinsic parameter matrix or the camera calibration matrix, and it is upper triangular with positive diagonal elements, λ is the depth scale. The parameters in this matrix K_i are: f_i, which is the focal length, $s_{i,x}, s_{i,y}$ which determine the size of the pixels, $s_{i,\theta}$, which is the skew factor and is henceforth assumed to be zero, $o_{i,x}$ and $o_{i,y}$, which are the offsets. Now, since $s_{i,\theta}$ is assumed to be zero, which is a reasonable assumption for most applications, we redefine the matrix K_i as

$$K_i = \begin{bmatrix} a_i & 0 & b_i \\ 0 & c_i & d_i \\ 0 & 0 & 1 \end{bmatrix}, \tag{4.1}$$

where a_i and b_i are positive. Thus, K_i is invertible. In some cases one might assume that the principal point is known, in which case $b_i = d_i = 0$, but in general this is the structure we assume.

4.1.2 Distorted rotations and conjugate rotations

Distorted rotations or distorted rotation matrices are matrices on the following form

$$C_i(t) = K_i R_i^T(t) K_i^{-1}, \tag{4.2}$$

$$C_{ij}(t) = K_i R_{ij}^T(t) K_j^{-1}. \tag{4.3}$$

Each agent can compute C_i and transmit this matrix to its neighbors $\mathcal{N}_i$. The matrix C_{ij} is obtained by agent i if agent j is a neighbor of agent i. The matrix C_i is referred to as the conjugate rotation and it is shown in [11] that it has seven degrees of freedom. However in this work, by assuming that $s_{i,\theta} = 0$, we limit the degrees of freedom to six.

In order for the agents to be able to measure C_i and C_{ij} we assume the following setting. The positions of the agents in $\mathbb{R}^3$ are static, *i.e.*, the movements are purely rotational. At time 0 all the cameras are initially rotated in the same way. We can without loss of generality assume that this rotation coincides with the identity matrix in $\mathcal{F}_W$, *i.e.*, $R_i(0) = I$ for all i. In this initial configuration, each camera takes an image of some common reference object that can be seen by all the cameras. The reference object contains a set of local feature points on its surface which can be detected in the images by all the cameras. We assume that there is a ball $B_q(I)$ in $SO(3)$, such that a sufficiently large subset of the feature points on the object are visible in the image plane by the camera of any agent i with rotation R_i contained in the ball $B_q(I)$.

At the initial time $t_0 > 0$ (the time 0 is not regarded as the initial time but rather as the time when the reference images are taken) we assume $R_i(t_0) \in B_q(I)$ for all i. Let us denote the image of the camera i at time t by $\mathcal{I}_i(t)$, which is a rectangular subset of the plane $\{x : x^T(0,0,1)^T = 1\}$ in $\mathcal{F}_i$. Our approach is geometric, so we do not involve any intensity function in the definition of an image. A point correspondence between $\mathcal{I}_i(t_1)$ and $\mathcal{I}_j(t_2)$ is a pair (p_1, p_1), where $p_1 \in \mathcal{I}_i(t_1)$ and $p_2 \in \mathcal{I}_j(t_2)$, for which there is a feature point $p \in \mathcal{F}_W$ such that $p_1 = h(p, G_i(t_1))$ and $p_2 = h(p, G_j(t_2))$.

At time t, given at least four different point correspondences between the images $\mathcal{I}(0)$ and $\mathcal{I}(t)$, $C_i(t)$ can be calculated by means of a homography see [10] or Chapter 6.4.4. in [9]. Regarding $C_{ij}(t)$, it is a bit more challenging since there is a nonzero translation between any pair of cameras. If C_{ij} is calculated we assume that all the camera calibration matrices for the agents are the same, we will come back to this subject. In order to calculate C_{ij}, in general we have to use more than four point correspondences, calculate the fundamental matrix and perform an affine reconstruction, see Chapter 6 in [9] for an introduction on this subject. However, there is a benefit of using $C_{ij}(t)$, since then we do not have to have an initial image $\mathcal{I}_i(0)$, but instead it is enough to use the images $\mathcal{I}_i(t)$ and $\mathcal{I}_j(t)$ at each time t. Furthermore, one could assume a nonzero translational velocity in this case.

The main point here is that in order to calculate R_i (or R_{ij}), often we first calculate C_i (or C_{ij}), and here we provide a way of constructing control laws directly from C_i and C_{ij}, without calculating R_i or R_{ij}.

4.1.3 Local distorted representations

Given a rotation matrix R_i, as described in Chapter 3, there are local representations or parameterizations of this matrix. These are coordinates in a chart covering a portion of $SO(3)$. In this section we show that for some of the most commonly used representations, namely the representations described in Chapter 3, there is a corresponding representation for the conjugate matrix C_i. If y_i denotes a local representation for R_i we denote the distorted local representation for C_i as $\tilde{y}_i$. For all the local representations y_i we consider,

$$\tilde{y}_i = T_i y_i, \text{ where } T_i = \begin{bmatrix} \frac{1}{c_i} & 0 & 0 \\ 0 & \frac{1}{a_i} & 0 \\ 0 & \frac{-d_i}{a_i} & \frac{c_i}{a_i} \end{bmatrix}.$$

The mapping

$$y_i \mapsto \tilde{y}_i$$

is a linear transformation which is a function of the intrinsic camera parameters, and this mapping is the same for any of the local representations we consider.

The local representations are on the same form as in Chapter 3, *i.e.*,

$$y_i = \frac{g(\|x_i\|)}{\|x_i\|} x_i, \text{ where } x_i = (\mathrm{Log}(R_i))^{\vee}.$$

As described in Chapter 3, r is the radius of injectivety for the local representation at hand, whereas $r' = \lim_{\rho \uparrow r} g(\rho)$.

In order to understand the choice and structure of T_i, let us first consider the distorted representation of x_i, *i.e.*, $\tilde{x}_i$. It is easy to verify that the principal logarithm of C_i for $R_i \in B_\pi(I)$ is given by

$$\mathrm{Log}(C_i) = K_i \mathrm{Log}(R_i^T) K_i^{-1} = -K_i \widehat{x}_i K_i^{-1}$$

and if we expand this expression we get that

$$\begin{aligned}
K_i\widehat{x}_iK_i^{-1} &= \begin{bmatrix} c_{11} & c_{12} & c_{13} \\ c_{21} & c_{22} & c_{23} \\ c_{31} & c_{32} & c_{33} \end{bmatrix} \\
&= \begin{bmatrix} a_i & 0 & b_i \\ 0 & c_i & d_i \\ 0 & 0 & 1 \end{bmatrix} \begin{bmatrix} 0 & -x_3 & x_2 \\ x_3 & 0 & -x_1 \\ -x_2 & x_1 & 0 \end{bmatrix} \begin{bmatrix} \frac{1}{a_i} & 0 & -\frac{b_i}{a_i} \\ 0 & \frac{1}{c_i} & -\frac{d_i}{c_i} \\ 0 & 0 & 1 \end{bmatrix} \\
&= \begin{bmatrix} \frac{-b_ix_2}{a_i} & \frac{b_ix_1-a_ix_3}{c_i} & \frac{b_i^2x_2}{a_i} + \frac{(a_ix_3-b_ix_1)d_i}{c_i} + a_ix_2 \\ \frac{c_ix_3-d_ix_2}{a_i} & \frac{d_ix_1}{c_i} & \frac{(d_ix_2-c_ix_3)b_i}{a_i} - \frac{d_i^2x_1}{c_i} - c_ix_1 \\ \frac{-x_2}{a_i} & \frac{x_1}{c_i} & \frac{b_ix_2}{a_i} - \frac{d_ix_1}{c_i} \end{bmatrix}.
\end{aligned}$$

We define the distorted representation $\tilde{x}_i$ as $\tilde{x}_i = (c_{32}, -c_{31}, c_{21})^T$, which also can be written as

$$\tilde{x}_i = \begin{bmatrix} \frac{1}{c_i} & 0 & 0 \\ 0 & \frac{1}{a_i} & 0 \\ 0 & \frac{-d_i}{a_i} & \frac{c_i}{a_i} \end{bmatrix} x_i.$$

Now we define the operator $(\cdot)^{\sqcup}$ as follows. For a matrix

$$A = \begin{bmatrix} q_{11} & q_{12} & q_{13} \\ q_{21} & q_{22} & q_{23} \\ q_{31} & q_{32} & q_{33} \end{bmatrix} \in \mathbb{R}^{3\times 3},$$

$A^{\sqcup} = (q_{32}, -q_{31}, q_{21})^T$. Note that if A is skew-symmetric, $(A)^{\vee} = (A)^{\sqcup}$.

In the Rodrigues Parameter vector, $g(\|x_i\|) = \tan(\|x_i\|/2)$, and this representation is obtained through the Cayley transform as $y_i = f(R_i) = -((I - R_i)(I + R_i)^{-1})^{\vee}$, and

$$\tilde{y}_i = -f(C_i) = \left(K_i f(R_i^T)K_i^{-1}\right)^{\sqcup} = (K_i\widehat{y}_iK_i^{-1})^{\sqcup} = T_iy_i.$$

Another choice is the map $y_i = f(R_i) = \left(\frac{R_i - R_i^{-1}}{2}\right)^{\vee}$, where $g(\|x_i\|) = \sin(\|x_i\|)$, and

$$\tilde{y}_i = -f(C_i) = \left(K_i \left(\frac{R_i - R_i^{-1}}{2}\right) K_i^{-1}\right)^{\sqcup} = (K_i\widehat{y}_iK_i^{-1})^{\sqcup} = T_iy_i.$$

The relationship between distorted representations and undistorted representations are illustrated in Figure 4.1. Given the conjugate rotation C_i, without knowing the rotation matrix R_i and the calibration matrix K_i, it is possible to calculate distorted local representations of C_i using the map 4. Another procedure is to calculate the calibration matrix in order to obtain the rotation matrix (map 1), then calculate the local representation (map 2) and finally the distorted local representation is calculated (map 3).

The matrix T_i has positive diagonal elements, since by assumption a_i and c_i are positive for all i, but its symmetric part is not necessarily positive definite. However, due to the

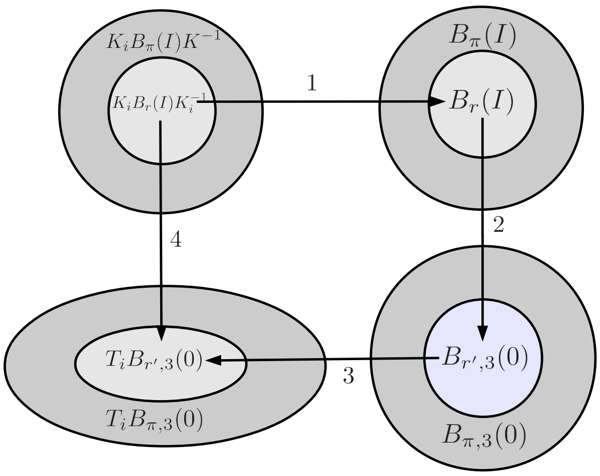

Figure 4.1: The relationship between the representations.

structure of it, there is $\beta_i' > 0$ such that if $P_i' = \text{diag}(1, \beta_i', 1)$, then the matrix $P_i'T_i$ is positive definite. Any matrix P_iT_i is also positive definite if $P_i = \text{diag}(\alpha_i, \beta_i, 1)$ where $\beta_i \geq \beta_i'$ and $\alpha_i > 0$ is arbitrary.

Regarding the distorted representation $\tilde{y}_{ij}$ corresponding to the representation y_{ij}, it is defined in the analogous way, $\tilde{y}_{ij} = T_iy_{ij}$ if $T_i = T_j$ for all i, j. In order for this definition to make sense, all the agents must have the same camera matrices. Henceforth, whenever we are using the distorted local representations for the relative rotations, we are always assuming that all the camera calibration matrices in the system are the same, whereas if we are only using the distorted local representations for the absolute rotations, we in general assume that the camera matrices might differ between the agents. This means that all types of distorted rotations we consider are conjugate rotations.

4.1.4 Kinematics

We recall from Chapter 3 that each agent has a constant position in $\mathcal{F}_i$ for all $t \geq 0$. The kinematics for the rotations is given by

$$\dot{R}_i = R_i\widehat{\omega}_i \quad \text{or} \quad \dot{x}_i = L_{x_i}\omega_i,$$

where $R_i\widehat{\omega}_i$ is an element of the tangent space $T_{R_i}SO(3)$ and L_{x_i} is the Jacobian matrix. The vector $\omega_i \in \mathbb{R}^3$ is the angular velocity of agent i defined in $\mathcal{F}_i$ and comprises our control signal. We are aware of the fact that in practice the actual control is performed on a dynamic level, but the dynamical equations are platform dependent, and the framework presented in this work can be extended to the case of second order systems by using a suitable nonlinear control design technique such as backstepping.

In this chapter we write $x^{\text{abs}} = x = (x_1, \ldots, x_n)^T \in (B_{\pi,3}(0))^n$ and $x^{\text{rel}} = (x_{11}, \ldots, x_{nn})^T \in (B_{\pi,3}(0))^{\sum_{j \in \mathcal{N}_i} |\mathcal{N}_i|}$. We also use the analogous notation for y^{abs} and y^{rel}. For the distorted representations we write $\tilde{y}^{\text{abs}}$ and $\tilde{y}^{\text{rel}}$ respectively.

Let us also introduce the consensus or agreement sets

$$\mathcal{A}^{\text{abs}} = \{x^{\text{abs}} : x_1 = \ldots = x_n\},$$

and

$$\mathcal{A}^{\text{rel}} = \{x^{\text{rel}} : x_{ij} = 0, j \in \mathcal{N}_i, i \in \mathcal{V}\}.$$

Note that $\mathcal{A}^{\text{rel}}$ is actually just the point zero. The purpose of any control strategy proposed in this work is to guarantee that the solution $x^{\text{abs}}(t)$ or $x^{\text{rel}}(t)$ of the closed loop dynamics satisfies $x^{\text{abs}}(t) \to \mathcal{A}^{\text{abs}}$ or $x^{\text{rel}}(t) \to \mathcal{A}^{\text{rel}}$ as $t \to \infty$. We may also say that $x^{\text{abs}}(t)$ ($x^{\text{rel}}(t)$) approaches $\mathcal{A}^{\text{abs}}$ ($\mathcal{A}^{\text{rel}}$).

4.2 Control design and results

We start with the topic of stability and then proceed to the main topic which is consensus.

4.2.1 Stability

Suppose each agent wants to rotate R_i to the identity matrix in the frame $\mathcal{F}_W$. In order to fulfill this task we present the following control law.

$$\omega_i = -P_i \tilde{y}_i, \tag{4.4}$$

where P_i is a matrix such that (the symmetric part of) the matrix $P_i T_i$ is positive definite. We can for example choose $P_i = \text{diag}(1, \beta_i, 1)$, and then $P_i T_i$ is positive definite if β_i is sufficiently large. If the principal point is known, *i.e.*, if $b_i = d_i = 0$, then P_i can be any positive definite matrix.

Proposition 4.1. *suppose $y_i \in B_{r',3}(0)$ and controller* (4.4) *is used, then $B_{r',3}(0)$ is invariant and $x_i(t) \to 0$ as $t \to \infty$.*

Proof: Let us define the following function

$$V = x_i^T x_i.$$

We have that

$$\begin{aligned} \dot{V} &= -x_i^T (P_i T_i) y_i - y_i^T (P_i T_i)^T x_i \\ &= -\|x_i\| g(\|x_i\|) u_i^T ((P_i T_i) + (P_i T_i)^T) u_i \\ &\leq 0, \end{aligned}$$

where $u_i = x_i / \|x_i\|$. The last inequality is strict unless $x_i = 0$. Thus, the invariance and the convergence has been shown at once. ■

For any representation where the radius of injectivety, r, is equal to π, the identity matrix I is almost globally asymptotically stable relative to $SO(3)$ if (4.4) is used.

4.2.2 Local consensus

Here we present local consensus results that are independent of what distorted representation we choose. Compared to Chapter 3, where we could show invariance for all of our control laws, we are in general not able to show the invariance using similar methods here for the distorted local representations. Thus, we have to settle for smaller regions of convergence. However, by choosing the Rodrigues Parameters as the representation, we show in the next section, that we can achieve almost global consensus. Throughout this chapter we assume that the interconnection graph $\mathcal{G}$ is time-invariant. We begin by presenting two types of control laws.

$$\omega_i = \sum_{j \in \mathcal{N}_i} a_{ij}(\tilde{y}_j - \tilde{y}_i), \tag{4.5}$$

$$\omega_i = P \sum_{j \in \mathcal{N}_i} \tilde{y}_{ij}, \tag{4.6}$$

where P is a positive definite diagonal matrix. Note that the parameterization $\tilde{y}^{\text{abs}}$ or $\tilde{y}^{\text{rel}}$ is arbitrary within the class we consider, meaning that it could either be the Axis-Angle Representation, the Rodrigues Parameters etc.

Now we present some results regarding the stability and convergence of the closed loop dynamics when (4.5) and (4.6) are used respectively.

Proposition 4.2. *Suppose $K_i = K_j$ and K_i is a diagonal matrix for all i, j. If the interconnection graph $\mathcal{G}$ is strongly connected and the control law* (4.5) *is used, the point* 0 *is stable for the closed loop dynamics of x^{abs}. Furthermore, if $x^{\text{abs}}(t_0)$ is sufficiently close to* 0*, $x^{\text{abs}}(t)$ approaches $\mathcal{A}$.*

Proposition 4.3. *Suppose $K_i = K_j$ for all i, j and P is such that the symmetric part of PT_i is positive definite for all agents i. If the interconnection graph $\mathcal{G}$ is strongly connected and undirected and the control law* (4.6) *is used, $\mathcal{A}^{\text{rel}}$ is asymptotically stable for the closed loop dynamics of x^{rel}.*

Now we proceed with the introduction of three additional control laws

$$\omega_i = \sum_{j \in \mathcal{N}_i} a_{ij} \text{diag}(1,\ 0,\ 0)(\tilde{y}_j - \tilde{y}_i), \tag{4.7}$$

$$\omega_i = \sum_{j \in \mathcal{N}_i} a_{ij} \text{diag}(0,\ 1,\ 0)(\tilde{y}_j - \tilde{y}_i), \tag{4.8}$$

$$\omega_i = \sum_{j \in \mathcal{N}_i} a_{ij} \text{diag}(0,\ 0,\ 1)(\tilde{y}_j - \tilde{y}_i). \tag{4.9}$$

These control laws are equivalent, up to which of the three elements in the control vector that is allowed to be nonzero.

Proposition 4.4. *Suppose the interconnection graph $\mathcal{G}$ is strongly connected.*

(i) If either one of the control laws (4.7-4.8) is used, the point 0 *is stable for the closed loop dynamics of* x^{abs}*. Furthermore, if* $x^{\text{abs}}(t_0)$ *is sufficiently close to* 0 *and controller (4.7) is used* $y_{i,1}(t) - y_{j,1}(t) \to 0$ *as* $t \to \infty$*, where* $y_{i,k}$ *denotes the* k*-th element of the vector* y_i*. The analogous result holds for controller* (4.8).

(ii) Suppose $y_{i,k_2}(t_0) = y_{i,k_3}(t_0) = 0$ *for all* i *and* $\{k_1, k_2, k_3\} = \{1, 2, 3\}$*. If* $k_1 = 1$ *and controller (4.7) is used, or if* $k_1 = 2$ *and controller (4.8) is used, or if* $k_1 = 3$ *and controller (4.9) is used, it holds that the point* 0 *is stable for the closed loop dynamics of* x^{abs}*. Furthermore, if* $x^{\text{abs}}(t_0)$ *is sufficiently close to* 0*, then* $x^{\text{abs}}(t) \to \mathcal{A}^{abs}$ *as* $t \to \infty$*.*

There are a couple of trade offs between the propositions. Compared to the other two propositions, in Proposition 4.4, the system is allowed to be heterogeneous, *i.e.*, the camera matrices are allowed to be different for the agents. Unfortunately, consensus cannot be reached in general by means of a continuous control input, and *(i)* does only guarantee consensus for some element of y^{abs}.

The strength of Proposition 4.4 lies instead in the second part *(ii)*. This result is useful when the cameras are located in a plane, and are only rotating around the same axis in the global frame F_W. Compared to the results in [4, 5], where the epipoles were used and all the cameras were assumed to have the same camera calibration matrix, we consider a more general scenario for the calibration matrix here.

In Proposition 4.2 we have the assumption that the principal point is known and all the camera calibration matrices are the same. In Proposition 4.3 we assume that graph is undirected and that all the camera calibration matrices are equal. The benefits of these propositions is that they guarantee consensus in local regions of $SO(3)$ of nonzero measure compared to Proposition 4.4 which only guarantees consensus in a region equivalent to a local region of $SO(2)$. If the principal point is known, the common gain matrix P can be set to the identity matrix in Proposition 4.3.

As already mentioned, the control laws differ in what information they use and now we define two scenarios of how to use them. The control law (4.5) and the control laws (4.7-4.8) would be suitable in the following scenario. Suppose that all the rotations at time 0 are the same which we assume without loss of generality is equal to the identity matrix. At time 0 the reference images $\mathcal{I}_i(0)$ are taken for all agents i. During the time period $[0, t_0)$ the agents get some other missions and each camera rotates in a small region close to I. At time t_0 the cameras get the instruction to reach consensus, and the control law is used.

The control law (4.6) would be suitable in the following scenario. Suppose the rotations are sufficiently close to each other, at time t_0, at which time the system get the instruction to reach consensus and (4.5) is used.

Let us now turn to the proofs of the propositions 4.2, 4.3 and 4.4.

Proof of Proposition 4.2: We use the following fact. There is a positive vector $\xi = (\xi_1, \ldots, \xi_n)^T \in \mathbb{R}^n$ such that $L' = \text{diag}(\xi)L(\mathcal{G}, A)$ is the Graph Laplacian matrix of a balanced graph $\mathcal{G}'$, where L is the graph Laplacian matrix of the graph $\mathcal{G}$ with adjacency matrix A, see Lemma 3.7. Let us define the following function

$$\gamma(x^{\text{abs}}) = \sum_{i=1}^{n} \xi_i \int_0^{\|x_i\|} g(s)ds. \tag{4.10}$$

We calculate the time derivate of $\gamma(x^{\text{abs}}(t))$.

$$\begin{aligned}
\dot{\gamma} &= \sum_{i=1}^{n} \xi_i g(\|x_i\|)\dot{\|x_i\|} = \sum_{i=1}^{n} \xi_i y_i^T \omega_i \\
&= \sum_{i=1}^{n} \xi_i y_i^T \sum_{j\in\mathcal{N}_i} a_{ij}(\tilde{y}_j - \tilde{y}_i) \\
&= \sum_{i=1}^{n} \xi_i y_i^T T \sum_{j\in\mathcal{N}_i} a_{ij}(y_j - y_i) \\
&= \sum_{i=1}^{n} \xi_i \bar{y}_i^T \sum_{j\in\mathcal{N}_i} a_{ij}(\bar{y}_j - \bar{y}_i) \\
&= -\bar{y}^{\text{abs}T}(L' \otimes I)\bar{y}^{\text{abs}},
\end{aligned}$$

where $T = T_i$ for all i, $\bar{y}_i = T^{\frac{1}{2}} y_i$, $\bar{y}^{\text{abs}} = (\bar{y}_1, \ldots, \bar{y}_n)^T$, the symbol $\otimes$ denotes the Kronecker product and I is the identity matrix in $\mathbb{R}^3$. It is easy to see that $\dot{\gamma} \leq 0$ and it is equal to zero if and only if $\bar{y}_1 = \ldots = \bar{y}_n$ which implies that $x^{\text{abs}} \in \mathcal{A}^{\text{abs}}$. ∎

Before we proceed with the proof of Proposition 4.3 we state the following lemma which is being used in the proof.

Lemma 4.5. *If $\mathcal{G}$ is quasi-strongly connected and $y^{\text{abs}} \in (B_{r'/2,3})^n$ it holds that $x^{\text{abs}} \in \mathcal{A}^{\text{abs}}$ if and only if*

$$\sum_{j\in\mathcal{N}_i} a_{ij} y_{ij} = 0 \quad \forall\, i, \tag{4.11}$$

where $a_{ij} > 0$ for all pairs (i, j).

Proof: **If**: This is a consequence of (3.7) and the fact that $\mathcal{G}$ is quasi-strongly connected.

Only if: We note that since R_i is invertible, it holds that

$$\sum_{j\in\mathcal{N}_i} a_{ij} y_{ij} = 0 \quad \forall\, i, \quad \Longleftrightarrow \quad R_i \sum_{j\in\mathcal{N}_i} a_{ij} \widehat{y}_{ij} = 0 \quad \forall\, i.$$

According to Theorem 3.4 it holds that

$$R_i \sum_{j\in\mathcal{N}_i} a_{ij} \widehat{y}_{ij} = 0 \quad \forall\, i, \quad \Longleftrightarrow \quad \sum_{j\in\mathcal{N}_i} a_{ij} h_{ij}(z_1, z_j)(z_j - z_i) = 0 \quad \forall\, i,$$

where $h_{ij}(z_1, z_j) \geq 0$ and $h_{ij}(z_1, z_j) = 0$ if and only if $z_i = z_j$. The variable z_i is the Rodrigues Parameter vector of the rotation R_i, see Theorem 3.4.

Now, suppose that $z \notin \{z : z_1 = \ldots = z_n\}$. We define the constants

$$b_{ij} = \begin{cases} a_{ij}h_{ij}(z_i, z_j) & \text{if } z_i \neq z_j, \\ a_{ij} & \text{if } z_i = z_j, \end{cases}.$$

Now we see that

$$a_{ij}h_{ij}(z_1, z_j)(z_j - z_i) = b_{ij}(z_j - z_i).$$

This means that

$$L(\mathcal{G}, [b_{ij}])z = 0,$$

where $L(\mathcal{G}, [b_{ij}])$ is the graph Laplacian matrix for a quasi-strongly connected graph. But this implies that $z \in \{z : z_1 = \ldots = z_n\}$, which is a contradiction. Hence $z \in \{z : z_1 = \ldots = z_n\}$, which implies that $x^{\text{abs}} \in \mathcal{A}^{\text{abs}}$. ■

Remark 4.1. There is an other technique that can be used in order to prove Lemma 4.5, which applies to a wider context than $SO(3)$. One can utilize that

$$\sum_{j \in \mathcal{N}_i} a_{ij}y_{ij} = 0$$

if and only if the rotation R_i is positioned in certain L^2-mean of the rotations $\{R_j\}_{j \in \mathcal{N}_i}$. This means that the rotation is contained in the relative interior of the geodesic convex hull of the neighboring rotations $\{R_j\}_{j \in \mathcal{N}_i}$, see Theorem 3.11 in [14]. If all the rotations are in the relative interior of the hull of the neighboring rotations, provided the graph is quasi-strongly connected, all the rotations are the same.

Proof of Proposition 4.3: Let us define the following function

$$\gamma(x^{\text{rel}}) = \sum_{i \in \mathcal{V}} \sum_{j \in \mathcal{N}_i} \int_0^{\|x_{ij}\|} g(s)ds.$$

We calculate the time derivate of $\gamma(x^{\text{rel}}(t))$.

$$\begin{aligned} \dot{\gamma} &= \sum_{i \in \mathcal{V}} \sum_{j \in \mathcal{N}_i} g_i(\|x_{ij}\|)\|\dot{x_{ij}}\| \\ &= \sum_{i \in \mathcal{V}} \sum_{j \in \mathcal{N}_i} y_{ij}^T(\omega_j - \omega_i) \\ &= \sum_{i \in \mathcal{V}} \sum_{j \in \mathcal{N}_i} y_{ij}^T \left(P \sum_{k \in \mathcal{N}_j} y_{jk} - P \sum_{l \in \mathcal{N}_i} y_{il} \right) \\ &= -y^{\text{rel}T} B^T \text{diag}(P, \ldots, P) B y^{\text{rel}}, \end{aligned}$$

where B is the incidence matrix, see Section 3.5. Now by LaSalle's invariance theorem, x^{rel} converges to the largest invariant set contained in $\dot{\gamma} = 0$. This invariant set is a subset of $\{x^{\text{rel}} : y^{\text{rel}}(x^{\text{rel}}) \in \ker(B)\}$. If we look at the structure of B, we see that $y^{\text{rel}} \in \ker(B(\mathcal{G}))$ implies

$$\sum_{j \in \mathcal{N}_i} y_{ij} = 0 \quad \text{for all } i, \tag{4.12}$$

where we have used the fact that $y_{ij} = -y_{ji}$. According to Lemma 4.5 this implies that $x^{\text{abs}} \in \mathcal{A}^{\text{abs}}$ if the rotations are sufficiently close the identity in $\mathcal{F}_W$. But, since only information is being used in the control law that is independent of $\mathcal{F}_W$, if the rotations are sufficiently close to each other we can choose $\mathcal{F}_W$ as a frame where all the rotations are contained $B_{r/2}(I)$. ■

Proof of Proposition 4.4: (i) Let us consider controller (4.7), the proof when using (4.8) is equivalent and hence omitted. Similar to the proof of Proposition 4.2 we use the fact that there is a positive vector $\xi = (\xi_1, \ldots, \xi_n)^T \in \mathbb{R}^n$ such that $L' = \text{diag}(\xi)L$ is the graph Laplacian matrix of a balanced graph $\mathcal{G}'$.

We define the following function

$$\gamma(x^{\text{abs}}) = \sum_{i=1}^{n} \frac{1}{c_i} \xi_i \int_0^{\|x_i\|} g(s) ds, \tag{4.13}$$

where $1/c_i$ is the first element in the diagonal of T_i. We calculate the time derivate of $\gamma(x^{\text{abs}}(t))$.

$$\begin{aligned}
\dot{\gamma} &= \sum_{i=1}^{n} \frac{1}{c_i} \xi_i g(\|x_i\|) \dot{\|x_i\|} = \sum_{i=1}^{n} \frac{1}{c_i} \xi_i y_i^T \omega_i \\
&= \sum_{i=1}^{n} \frac{1}{c_i} \xi_i y_i^T \sum_{j \in \mathcal{N}_i} a_{ij} \text{diag}(1,\ 0,\ 0)(\tilde{y}_j - \tilde{y}_i) \\
&= -\tilde{y}^{\text{abs}T} \left(L' \otimes \text{diag}(1,\ 0,\ 0) \right) \tilde{y}^{\text{abs}}. \qquad (4.14)
\end{aligned}$$

The expression (4.14) is zero if and only if $\tilde{y}_{i,1} = \tilde{y}_{j,1}$ for all i, j,

(ii) The same procedure holds as in *(i)*, however the consequence of the procedure is different. Now (4.14) is zero if and only if $\tilde{y}_i = \tilde{y}_j$ for all i, j, which is equivalent to the statement that $x^{\text{abs}} \in \mathcal{A}$. This is an implication of the fact that if all the agents have the same rotational axis, this axis will remain as the rotational axis. To see this we simply note that the axis lies in the nullspace of the nonlinear parts of the expression of the Jacobian matrix L_{x_i}. ■

Remark 4.2. In the proofs of propositions 4.2, 4.3 and 4.4

$$\lim_{\|x_i\|\to 0} g(\|x_i\|)\|\dot{x_i}\| = 0 \text{ and}$$
$$\lim_{\|x_{ij}\|\to 0} g(\|x_{ij}\|)\|\dot{x_{ij}}\| = 0.$$

When $\|x_i\| = \|x_{ij}\| = 0$, the expressions shall be interpreted in the sense of their limits.

4.2.3 Almost global consensus

The Rodrigues Parameters play an important role as a parametrization. It has the property that $r' = \infty$, *i.e.*,

$$g(\|x_i\|) = \tan(\|x_i\|/2) \to \infty \text{ as } \|x_i\| \to \pi,$$

and this property can be used to show almost global consensus when (4.5) is used and consensus for convex balls in $SO(3)$ when controller (4.6) is used. We recall that the distorted Rodrigues Parameters are obtained from the Cayley transform as

$$\tilde{y}_i = ((I - C_i)(I + C_i)^{-1})^{\sqcup},$$
$$\tilde{y}_{ij} = ((I - C_{ij})(I + C_{ij})^{-1})^{\sqcup}.$$

Proposition 4.6. *Suppose that the local representations are chosen as the Rodrigues Parameters.*

(i) In Proposition 4.2 and Proposition 4.4 part (ii), if all the initial rotations at time t_0 are contained in $B_\pi(I)$, then there is $q < \pi$, where q is a function of $x^{\text{abs}}(t_0)$, such that $R_i(t) \in \bar{B}_q(I)$ for all $i, t > t_0$ and

$$x^{\text{abs}} \to \mathcal{A}^{\text{abs}} \textit{ as } t \to \infty.$$

(ii) If (4.6) *is used, the graph $\mathcal{G}$ is undirected and a spanning tree and*

$$\max_{(i,j)\in\mathcal{V}\times\mathcal{V}} d(R_i(t_0), R_j(t_0)) < \pi,$$

then there is $q < \pi$, where q is a function of $x^{\text{rel}}(t_0)$, such that

$$\max_{(i,j)\in\mathcal{V}\times\mathcal{V}} d(R_i(t), R_j(t)) \leq q$$

for all $(i,j), t > t_0$ and

$$x^{\text{rel}} \to \mathcal{A}^{\text{rel}} \textit{ as } t \to \infty.$$

Proof of Proposition 4.6: Let us start with (i). It suffices to show invariance. We consider only Proposition 4.2, the proof of Proposition 4.4 part (ii) is similar and omitted. We note that

$$\gamma\left(x^{\text{abs}}\right) = \sum_{i=1}^{n} \int_0^{\|x_i\|} g(s)ds = \sum_{i=1}^{n} \left(-2\log\left(\cos\left(\frac{\|x_i\|}{2}\right)\right)\right).$$

Thus,

$$\gamma\left(x^{\text{abs}}\right) \to \infty \text{ as } \left(\max_{i\in\mathcal{V}} \|x_i\|\right) \to \pi.$$

But from the proof of Proposition 4.4 and 4.2 we know that $\gamma\left(x^{\text{abs}}\right)$ is decreasing, and hence there is q on the desired form.

In the case of (ii), in order to show invariance the procedure is similar. We note that

$$\begin{aligned}\gamma\left(x^{\text{rel}}\right) &= \sum_{i\in\mathcal{V}}\sum_{j\in\mathcal{N}_i}\int_0^{\|x_{ij}\|} g(s)ds \\ &= \sum_{i\in\mathcal{V}}\sum_{j\in\mathcal{N}_i}\left(-2\log\left(\cos\left(\frac{\|x_{ij}\|}{2}\right)\right)\right).\end{aligned}$$

Hence,

$$\gamma\left(x^{\text{abs}}\right) \to \infty \text{ as } \left(\max_{(i,j)\in\mathcal{V}\times\mathcal{V}} \|x_{ij}\|\right) \to \pi.$$

But from the proof of propositions 4.3 we know that $\gamma(x^{\text{rel}})$ is decreasing, hence there is q on the desired form.

Now, from the proof of Proposition 4.3 we get that x^{rel} converges to the set

$$\{x^{\text{rel}} : \sum_{j\in\mathcal{N}_i} a_{ij}y_{ij} = 0, i \in \mathcal{V}\}.$$

Since the rotations are not guaranteed to be contained in a strictly convex set as in Proposition 4.3, we cannot use Lemma 4.5 in order to show that the system has reached consensus, instead the consensus follows as a consequence of the fact that the graph $\mathcal{G}$ is a spanning tree. ■

Remark 4.3. We are aware of the fact that the physical constraints imposed by the actual camera, such as field of view and resolution, makes it practically challenging to consider rotations in large regions around the identity matrix in $SO(3)$.

4.3 Bibliography

[1] R. Tron and R. Vidal. Distributed 3-D localization in camera networks. In *Conference on Decision and Control*. Citeseer, 2009.

[2] J. H. Manton. A globally convergent numerical algorithm for computing the centre of mass on compact Lie groups. In *IEEE int. Conf. on Control, Automation, Robotics and Vision*, pages 2211–2216, 2005.

[3] V. M. Govindu. Lie-algebraic averaging for globally consistent motion estimation. In *IEEE Computer Society Conference on Computer Vision and Pattern Recognition*, volume 1, pages 689–691, 2004.

[4] E. Montijano, J. Thunberg, X. Hu and C. Sagues. Epipolar visual servoing for multi-robot distributed consensus. *IEEE Transactions on Robotics*, 29(5):1212–1225, 2013.

[5] E. Montijano, J. Thunberg, X. Hu and C. Sagues. Multi-robot distributed visual consensus using epipoles. In *IEEE Conference on Decision and Control and European Control Conference (CDC-ECC)*, pages 2750–2755. IEEE, 2011.

[6] R. Hartley and A. Zisserman. *Multiple view geometry in computer vision*, volume 2. Cambridge Univ Press, 2000.

[7] D. Nistér. An efficient solution to the five-point relative pose problem. *IEEE Transactions on Pattern Analysis and Machine Intelligence*, 26(6):756–770, 2004.

[8] K. Kanatani and Y. Sugaya. Compact fundamental matrix computation. In *Advances in Image and Video Technology*, pages 179–190. Springer, 2009.

[9] Y. Ma, S. Soatto, J. Kosecka, and S. Sastry. *An invitation to 3-D vision*. Springer, 2004.

[10] R. Hartley. Self-calibration from multiple views with a rotating camera. *Computer VisionECCV'94*, 800:471–478, 1994.

[11] K. Koser, C. Beder and R. Koch. Conjugate rotation: Parameterization and estimation from an affine feature correspondence. In *IEEE Conference on Computer Vision and Pattern Recognition*, 2008.

[12] F. Chaumette and S. Hutchinson. Visual servo control. I. Basic approaches. *IEEE Robotics & Automation Magazine*, 13(4):82–90, 2006.

[13] F. Chaumette and S. Hutchinson. Visual servo control. II. Advanced approaches. *IEEE Robotics & Automation Magazine*, 14(1):109–118, 2007.

[14] B. Afsari. Riemannian Lp center of mass: Existence, uniqueness and convexity. In *Proc. Amer. Math. Soc*, volume 139, pages 655–673, 2011.

Chapter 5

Optimal output consensus control for systems of agents with continuous linear dynamics

In this chapter we study the output consensus problem for a homogeneous system of agents with linear dynamics, both in finite time and in the asymptotic case (as the time tends to infinity). In the finite time case, the outputs for all the agents shall be the same at some predefined time. It is easy to show that for homogeneous systems of agents with linear dynamics, it is not possible to construct a linear, time-invariant feedback control law based on relative information such that the agents reach consensus in their states in finite time. With relative information in this context, we are referring to pairwise differences between the states of the agents.

Regarding the output consensus problem, using a decomposition of the state space, we show that if the dynamics for the agents is output controllable and the nullspace of the matrix which maps the state to the output satisfies a certain invariance condition, there cannot exist a linear Lipschitz continuous in state, time-invariant feedback control law that solves the problem while using only relative output information in the form of pairwise differences between the outputs of the agents. The output controllability is a standing assumption in order to guarantee consensus from arbitrary initial conditions. If only relative information is used, the control laws need to be either time-varying or non-Lipschitz in order to solve the finite time consensus problem.

In [1], an optimal linear consensus problem is addressed for systems of mobile agents with single-integrator dynamics. In this setting the authors constrain the agents to use only relative information in their controllers, *i.e.*, the controller of each agent consists of a weighted sum of the differences between its state and the states of its neighbors. In this setting the authors show that the graph Laplacian matrix used in the optimal controller for the system corresponds to a complete directed graph.

We formulate the consensus problem as an optimal control problem, where there are no restrictions on the controllers except that the agents shall reach consensus at some predefined time. By solving this problem, it turns out that the optimal controller is linear in state, time-varying and uses only relative information. Moreover, the connectivity graph needs to be completely connected. This implies that for any other topology between the agents than the complete graph, any controller constructed will be suboptimal. The provided control laws are given in closed form and are bounded and continuous. The input and output dimensions are arbitrary.

Not surprisingly, the optimal controller requires the measurement of state errors in general. We identify cases where the optimal controller is only based on the output errors. We also show that in the asymptotic case, there is a corresponding observer based controller, that is only based on the output errors.

The objective function in the optimization problem is a weighted sum of the squared Euclidean norms of the agents' control signals. Formulated from a physical perspective, we want to minimize the energy it takes for the agents to reach consensus in their outputs. The motivation for this problem is the rendezvous problem for mobile robots where all robots in a group shall meet at some position, while using only relative information. We want to solve this problem when the agents have linear dynamics, while minimizing the agents fuel consumption.

Regarding the theoretical contribution of this work, we use linear vector space optimization methods in order to solve the consensus problems. We show that the problem can be posed as a certain minimum norm problem in a Hilbert space [2]. In this framework the finite time consensus problem can be viewed as a solution of an optimization problem. For more references on finite time distributed consensus, see *e.g.*, [3, 4].

5.1 Preliminaries

We consider a system of N agents, where each agent i in the system has the dynamics

$$\begin{aligned} \dot{x}_i &= Ax_i(t) + Bu_i(t), \\ y_i &= Cx_i. \end{aligned}$$

The variable $x_i(t_0) = x_0$, $x_i(t) : \mathbb{R} \to \mathbb{R}^n$, $u_i(t) : \mathbb{R} \to \mathbb{R}^m$ and $y_i(t) : \mathbb{R} \to \mathbb{R}^p$, $A \in \mathbb{R}^{n \times n}$, $B \in \mathbb{R}^{n \times m}$ and $C \in \mathbb{R}^{p \times n}$. Note that compared to chapters 2-4, n now denotes the dimension of the state space and m the dimension of the control vector. It is assumed that B and C are full rank matrices and that the system is output controllable. Let us define

$$\begin{aligned} x(t) &= (x_1(t), x_2(t), \ldots, x_N(t))^T \in \mathbb{R}^{nN}, \\ u(t) &= (u_1(t), u_2(t), \ldots, u_N(t))^T \in \mathbb{R}^{mN}, \\ y(t) &= (y_1(t), y_2(t), \ldots, y_N(t))^T \in \mathbb{R}^{pN}, \end{aligned}$$

and the the vector

$$a = (a_1, a_2, ..., a_N)^T.$$

The matrix

$$L(a) = -\left(\sum_{i=1}^{N} a_i\right)^{-1} \left(1_N a^T - \sum_{i=1}^{N} a_i \mathrm{diag}([1, \ldots, 1]^T\right), \tag{5.1}$$

plays an important role in this chapter as one of the building blocks of the proposed control laws. The vector 1_N is a vector of dimension N with all entries equal to one. The matrix $L(a) \in \mathbb{R}^{N\times N}$ has one eigenvalue 0 and has $N-1$ eigenvalues equal, positive and real. The matrix $L(1_N)$ is the graph Laplacian matrix for the complete graph with edge weights equal to 1.

We now define the matrices

$$\begin{aligned}
V_1(a) &= \left[\frac{1}{a_1}1_{N-1}, -\mathrm{diag}\left(\left[\frac{1}{a_2}, \frac{1}{a_3}, ..., \frac{1}{a_N}\right]^T\right)\right],\\
V_2(a) &= \mathrm{diag}\left(\left[\frac{1}{a_2}, \frac{1}{a_3}, ..., \frac{1}{a_N}\right]^T\right) + \frac{1}{a_1}1_{N-1}1_{N-1}^T,\\
V_3 &= \left[-1_{N-1}, I_{N-1}\right],
\end{aligned}$$

and formulate the following lemma.

Lemma 5.1. $L(a) = -V_1(a)^T V_2(a)^{-1} V_3$.

Proof: The main difficulty is to calculate $V_2(a)^{-1}$, so we limit the proof to the determination of this matrix. Let us define $P \in \mathbb{R}^{N-1\times N-1}$, where the entries are

$$\begin{aligned}
p_{ii} &= a_{i+1}\sum_{j\neq i+1} a_j \left(\sum_k a_k\right)^{-1},\\
p_{ij} &= -a_{i+1}a_{j+1}\left(\sum_k a_k\right)^{-1} \quad i \neq j.
\end{aligned}$$

We prove that $P = V_2(a)^{-1}$. Let $v_i \in \mathbb{R}^{N-1}, i = 1, ..., N-1$, be the transposed row vectors of $V_2(a)$. Let $p_i \in \mathbb{R}^{N-1}, i = 1, ..., N-1$, be the column vectors of P. Now let $\langle\, ,\rangle$ denote the inner product in $\mathbb{R}^{N-1}$. We have that

$$\langle v_i, p_i\rangle = \left(\sum_{i=1}^{N} a_i\right)^{-1}\left(\left(\frac{a_{i+1}}{a_1}+1\right)\sum_{j\neq i+1} a_j - \frac{a_{i+1}}{a_1}\sum_{j\neq 1, i+1} a_j\right) = 1.$$

Now suppose $i \neq j$, then

$$\langle v_i, p_j \rangle \quad = \quad \left(\sum_{i=1}^{N} a_i\right)^{-1} \left(\frac{a_{j+1}}{a_1} \sum_{k \neq j+1} a_k - a_{j+1} - \frac{a_{j+1}}{a_1} \sum_{k \neq 1, j+1} a_k\right) = 0.$$

By using the structure $V_2(a)^{-1}$, it follows by calculation that $-L(a) = V_1(a)^T V_2(a)^{-1} V_3$. ■

Lemma 5.2. *Assume that $C \in \mathbb{R}^{p \times n}$ has full row rank, $P \in \mathbb{R}^{n \times n}$ is nonsingular and ker(C) is P-invariant, then*

$$P^T C^T (CPWP^T C^T)^{-1} CP = C^T (CWC^T)^{-1} C.$$

Proof: We start by noting that since C has full rank, P is invertible and ker(C) is P-invariant, the matrix $CP^T C^T$ is invertible. Now, if ker(C) is P-invariant there exists a K such that

$$P^T C^T = C^T K.$$

Since C is a full rank matrix, it follows that

$$K = (CC^T)^{-1} CP^T C^T,$$

from which it it follows that

$$\begin{aligned} P^T C^T &= C^T (CC^T)^{-1} CP^T C^T \implies \\ CPWP^T C^T &= CPC^T (CC^T)^{-1} CWC^T (CC^T)^{-1} CP^T C^T \implies \\ (CPWP^T C^T)^{-1} &= (CP^T C^T)^{-1} (CC^T)(CWC^T)^{-1} (CC^T)(CPC^T)^{-1}. \end{aligned}$$

If we show that

$$P^T C^T (CPC^T)^{-1} (CC^T) = C^T,$$

we are done. But this indeed true since

$$P^T C^T (CPC^T)^{-1} (CC^T) = C^T K K^{-1} = C^T.$$

■

Let us define

$$W(t, T) = \int_t^T Ce^{A(T-s)} BB^T e^{A^T (T-s)} C^T ds. \tag{5.2}$$

The matrix $W(t, T)$ is the output controllability Gramian, and since the system is assumed to be output controllable, this matrix is nonsingular (for $t < T$). Let us also define the related matrix

$$G(t_0, T) = \int_0^{T-t} Ce^{-Ar} BB^T e^{-A^T r} C^T dr. \tag{5.3}$$

Beware of the difference between the transpose operator $(\cdot)^T$ and the time T.

The approach we use in this work relies to a large extent on the projection theorem in Hilbert spaces. We recall the following version of the projection theorem where inner product constraints are present.

Theorem 5.3 ([2]). *Let H be a Hilbert space and $\{z_1, z_2, \ldots, z_N\}$ a set of linearly independent vectors in H. Among all vectors $w \in H$ satisfying*

$$\begin{aligned}\langle w, z_1 \rangle &= c_1, \\ \langle w, z_2 \rangle &= c_2, \\ &\vdots \\ \langle w, z_M \rangle &= c_M,\end{aligned}$$

let z_0 have minimum norm. Then

$$z_0 = \sum_{i=1}^{n} \beta_i z_i,$$

where the coefficients β_i satisfy the equations

$$\begin{gathered}\langle z_1, z_1 \rangle \beta_1 + \langle z_2, z_1 \rangle \beta_2 + \cdots + \langle z_N, z_1 \rangle \beta_N = c_1, \\ \langle z_1, z_2 \rangle \beta_1 + \langle z_2, z_2 \rangle \beta_2 + \cdots + \langle z_N, z_2 \rangle \beta_N = c_2, \\ \vdots \\ \langle z_1, z_M \rangle \beta_1 + \langle z_2, z_M \rangle \beta_2 + \cdots + \langle z_N, z_M \rangle \beta_N = c_M.\end{gathered}$$

In Theorem 5.3 $\langle \cdot, \cdot \rangle$ denotes the inner product.

5.2 Finite time consensus

In this section we consider the following problem.

Problem 5.1. *For any finite $T > t_0$, construct a control law $u(t)$ for the system of agents such that the agents reach consensus in their outputs at time T, i.e.,*

$$y_i(T) = y_j(T) \;\; \forall i \neq j,$$

while minimizing the following cost functional

$$\int_{t_0}^{T} \sum_{i=1}^{N} a_i u_i^T u_i dt, \tag{5.4}$$

where $a_i \in \mathbb{R}^+$, $i = 1, 2, ..., N$.

Note that the criterion in Problem 5.1 only regards the time T and does not impose any constraints on $y(t)$ when $t > T$. When we say that a control law u for the system is based on only relative information, we mean that

$$u_i = g(y_1 - y_i, \ldots, y_N - y_i), \quad \forall i, t \geq t_0$$

for some function g. An interesting question to answer, is under what circumstances it is possible to construct a control law that solves Problem 5.1 using only relative information. The following lemma provides a first step on the path to the answer of this question.

Lemma 5.4. *Suppose* ker(C) *is* A*-invariant and* u *is based on only relative information, then there is no locally Lipschitz continuous in state, time-invariant feedback control law* u *that solves Problem 5.1 and for which* $g(0, \ldots, 0) = 0$*.*

Proof of Lemma 5.4: Let us introduce the invertible matrix

$$P = \begin{bmatrix} C^T & C_{\text{ker}}^T \end{bmatrix},$$

where C_{ker} has full row rank and the columns of C_{ker}^T span ker(C). Let us now define $\tilde{x}_i = (x_{i,1}, x_{i,2})^T$ through the following relation

$$x_i = P\tilde{x}_i,$$

for all i. The dynamics for $\tilde{x}$ is given by

$$\dot{\tilde{x}}_i = \tilde{A}\tilde{x}_i + \tilde{B}u_i, \quad y_i = \tilde{C}\tilde{x}_i,$$

where

$$\tilde{A} = \begin{bmatrix} A_{11} & 0 \\ A_{21} & A_{22} \end{bmatrix}, \tilde{B} = \begin{bmatrix} B_1 \\ B_2 \end{bmatrix} \text{ and } \tilde{C} = \begin{bmatrix} C_1 & 0 \end{bmatrix}.$$

The structure of $\tilde{A}$ is a consequence of the fact that ker(C) is A-invariant.

Suppose there is a linear time-invariant feedback control law u that solves the Problem 5.1. We note that

$$y_i = CC^T x_{i,1}.$$

We define $y_{1j} = y_1 - y_j$ for all $j > 1$. The control law u has the following form

$$u = f(y_{12}, \ldots, y_{1N}),$$

but $y_{1j} = CC^T x_{1j,1}$, where $x_{1j,1} = x_{1,1} - x_{j,1}$, so u can be written as

$$u = f(x_{12,1}, \ldots, x_{1N,1}).$$

Since CC^T is invertible it follows that $y_{1j} = 0$ for all $j > 1$ if and only if $x_{1j,1} = 0$ for all $j > 1$. But, by the structure of f and $\tilde{A}$ it follows that $(x_{12,1}, \ldots, x_{1N,1})^T = 0$ is an equilibrium for the dynamics of $(x_{12,1}, \ldots, x_{1N,1})^T$. Since the right-hand side of this dynamics is locally Lipschitz continuous, $(x_{12,1}, \ldots, x_{1N,1})^T$ cannot have reached the point 0 in finite time. This is a contradiction. ■

We now provide the solution to Problem 5.1.

Theorem 5.5. *For $T < \infty$ the solution to Problem 5.1 is*

$$u(t) = -L(a) \otimes \left(B^T e^{A^T(T-t)} C^T W(t_0, T)^{-1} C e^{A(T-t_0)} \right) x_0, \text{ or} \tag{5.5}$$

$$u(x,t) = -L(a) \otimes \left(B^T e^{A^T(T-t)} C^T W(t, T)^{-1} C e^{A(T-t)} \right) x. \tag{5.6}$$

Furthermore, if $ker(C)$ is A-invariant, the solution to Problem 5.1 is

$$u(y,t) = -L(a) \otimes B^T C^T G(t_0, T)^{-1} y. \tag{5.7}$$

All the control laws (5.5-5.7) are equivalent but expressed in different ways. The control law (5.5) is the open loop controller and (5.6) is the closed loop version of (5.5). The matrix $W(t,T)$ is invertible due to the assumption of output controllability. We take the liberty of denoting all the controllers (5.5-5.7) by u. Provided u is used during $[t_0, T)$, at the time T we have that

$$\lim_{t \uparrow T} u(x(t), t) = \lim_{t \uparrow T} u(y(t), t) = u(T).$$

Even though the feedback controllers in (5.6) and (5.7) are bounded and continuous for $t \in [t_0, T)$ (see the open loop version of u in (5.5)), computational difficulties arise as $t \to T$ when (5.5) and (5.6) are used, since $W(T)$ is not invertible.

Proof of Theorem 5.5: Problem 1 is formally stated as follows

$$\text{minimize } \int_{t_0}^{T} \sum_{i=1}^{N} a_i u_i^T u_i dt \quad a_i \in \mathbb{R}^+ \;\; i = 1, 2, ..., N,$$

when

$$y_i(t) = Ce^{A(t-t_0)} x_i(t_0) + \int_{t_0}^{t} Ce^{A(t-s)} B u_i ds, \text{ for all } i,$$

and

$$\int_{t_0}^{T} Ce^{A(T-s)} B \left(u_1 - u_i\right) ds = -Ce^{A(T-t_0)} \left(x_1(t_0) - x_i(t_0)\right), \tag{5.8}$$

for $i \in \{2, ..., N\}$. Here we have without loss of generality assumed that the outputs of the agents at time T, $y_i(T)$, shall be equal to the output of agent 1 at time T, $y_1(T)$.

We notice that this problem is a minimum norm problem in the Hilbert space of all functions

$$f = (f_1(t), f_2(t), ..., f_N(t))^T : \mathbb{R} \to \mathbb{R}^{mN},$$

such that the Lebesgue integral

$$\int_{t_0}^{T} \sum_{i=1}^{N} a_i f_i^2(t) dt \tag{5.9}$$

converges. Here $f_i : \mathbb{R} \to \mathbb{R}^m$. We denote this space H, and the norm is given by the square root of (5.9).

Now we continue along the lines of Theorem 5.3 and reformulate the constraints (5.8) into inner product constraints in H.

$$\begin{aligned}\int_{t_0}^{T} Ce^{A(T-s)}B(u_1(s)-u_i(s))ds &= \\ \left\langle \left[\frac{Ce^{A(T-s)}B}{a_1}, 0, ..., 0, -\frac{Ce^{A(T-s)}B}{a_i}, 0, ..., 0\right]^T, \right. & \\ \left. \left[u_1^T, 0, ..., 0, u_i^T, 0, ..., 0\right]^T \right\rangle &= \\ -Ce^{A(T-t_0)}\left(x_1(t_0)-x_i(t_0)\right). &\end{aligned}$$

Depending on context the symbol $\langle \cdot, \cdot \rangle$ shall be interpreted as follows. If f and g belongs to H, $\langle f, g\rangle$ denotes the inner product between these two elements. If $f(t)$ and $g(t)$ are matrices of proper dimensions, then $\langle f, g\rangle$ is a matrix inner product where each element in the matrix is an inner product between a column in f and a column in g.

To simplify the notation we define

$$p_i = \left[\frac{Ce^{A(T-s)}B}{a_1}, 0, ..., 0, -\frac{Ce^{A(T-s)}B}{a_i}, 0, ..., 0\right]^T.$$

Since this is a minimum norm problem and all the columns of all the p_i are independent, by Theorem 5.3 we get that the optimal controller $u(t)$ is given by

$$u(t) = [p_2, ..., p_N]\beta, \tag{5.10}$$

where β is the solution to

$$Q\beta = V_3 \otimes Ce^{A(t-t_0)}x_0, \tag{5.11}$$

where

$$Q = \begin{bmatrix} \langle p_2, p_2\rangle & \langle p_3, p_2\rangle & \cdots & \langle p_N, p_2\rangle \\ \langle p_2, p_3\rangle & \langle p_3, p_3\rangle & \cdots & \langle p_N, p_3\rangle \\ \vdots & \vdots & \ddots & \vdots \\ \langle p_2, p_N\rangle & \langle p_3, p_N\rangle & \cdots & \langle p_N, p_N\rangle \end{bmatrix}. \tag{5.12}$$

From (5.10 - 5.12) we get that $\beta = Q^{-1}V_3 \otimes Ce^{A(t-t_0)}x_0$ and $u = [p_1, p_2, ..., p_N]Q^{-1}V_3 \otimes Ce^{A(t-t_0)}x_0$. Now we have that $[p_1, p_2, ..., p_N] = V_1(a)^T \otimes (B^T e^{A^T(T-t)}C^T)$.

Since

$$\langle p_i, p_j\rangle = \begin{cases} \frac{1}{a_1}W(t_0, T) & \text{if } i \neq j, \\ \left(\frac{1}{a_1} + \frac{1}{a_{i+1}}\right)W(t_0, T) & \text{if } i = j, \end{cases}$$

where $W(t_0,T) = \int_{t_0}^{T} Ce^{A(T-s)}BB^Te^{A^T(T-s)}C^T ds$, we have that

$$Q = V_2(a) \otimes W(t_0,T).$$

$$\begin{aligned}
u(t) &= V_1(a)^T \otimes (B^Te^{A^T(T-t)}C^T)V_2(a)^{-1} \otimes W(t_0,T)^{-1}V_3 \otimes Ce^{A(T-t_0)}x_0 \\
&= (V_1(a)^TV_2(a)^{-1}V_3) \otimes (B^Te^{A^T(T-t)}C^TW(t_0,T)^{-1}Ce^{A(T-t_0)})x_0 \qquad (5.13) \\
&= -L(a) \otimes (B^Te^{A^T(T-t)}C^TW(t_0,T)^{-1}Ce^{A(T-t_0)})x_0, \qquad (5.14)
\end{aligned}$$

where (5.13) follows from the mixed-product property of the Kronecker product and (5.14) follows from Lemma 5.1. By Bellman's Principle we get that

$$u(x,t) = -L(a) \otimes \left(B^Te^{A^T(T-t)}C^TW(t,T)^{-1}Ce^{A(T-t)}\right)x(t). \tag{5.15}$$

Now, suppose ker(C) is P-invariant. It holds that

$$\begin{aligned}
e^{A^T(T-t)}C^TW(t,T)^{-1}Ce^{A(T-t)} &= \\
e^{A^T(T-t)}C^T\left(\int_t^T Ce^{A(T-s)}BB^Te^{A^T(T-s)}C^T ds\right)^{-1}Ce^{A(T-t)} &= \\
e^{A^T(T-t)}C^T\left(\int_0^{T-t} Ce^{A(T-t)}e^{-Ar}BB^Te^{-A^Tr}e^{A^T(T-t)}C^T dr\right)^{-1}Ce^{A(T-t)} &= \\
e^{A^T(T-t)}C^T\left(Ce^{A(T-t)}(\int_0^{T-t} e^{-Ar}BB^Te^{-A^Tr}dr)e^{A^T(T-t)}C^T\right)^{-1}Ce^{A(T-t)} &= \\
\{\text{by using Lemma 5.2 }\} &= \\
C^T\left(C\int_0^{T-t} e^{-Ar}BB^Te^{-A^Tr}drC^T\right)^{-1}C &= \\
C^T\left(\int_0^{T-t} Ce^{-Ar}BB^Te^{-A^Tr}C^Tdr\right)^{-1}C &= \\
C^TG(t_0,T)C&,
\end{aligned}$$

from which we get that

$$u(y,t) = -L(a) \otimes B^TC^TG(t_0,T)^{-1}y.$$

■

Corollary 5.6. *The controllers (5.6-5.7) use only relative information, i.e. differences of the states (outputs) of the agents.*

Proof:

$$u_i(t,y) = B^T e^{A^T(T-t)} C^T W(t,T)^{-1} C e^{A(T-t)} \left(\sum_{i=1}^{n} a_i \right)^{-1} \sum_{j=1}^{n} a_j (y_j - y_i), \quad (5.16)$$

$$u_i(t,y) = B^T C^T G(t_0,T)^{-1} \left(\sum_{i=1}^{n} a_i \right)^{-1} \sum_{j=1}^{n} a_j (y_j - y_i). \quad (5.17)$$

■

Let us define $y_c = \frac{1}{\sum_{i=1}^{N} a_i} \sum_{i=1}^{N} a_i y_i$,and $\bar{y}_c = (y_c, \ldots, y_c)^T \in \mathbb{R}^{pN}$.

Lemma 5.7. *Suppose that A has not full rank and $x_i(0) = x_0 \in ker(A)$ for all $i = 1, ..., N$, then the consensus point for the system of agents using the controller* (5.6) *or* (5.7) *is $y_c(0)$.*

Proof: We use (5.14), from which we get that

$$y(T) = I_N \otimes Ce^{A(T-t_0)} x_0 + \int_{t_0}^{T} \left(I_N \otimes Ce^{A(T-t)} B \right) \cdot$$
$$\left(-L(a) \otimes B^T e^{A^T(T-t)} C^T W(t_0,T)^{-1} C e^{A(T-t_0)} \right) x_0 dt =$$
$$y_0 + \int_{t_0}^{T} \left(-L(a) \otimes Ce^{A(T-t)} B B^T e^{A^T(T-t)} C^T W(t_0,T)^{-1} \right) y_0 dt = \bar{y}_c(t_0).$$

■

5.3 Extension to the asymptotic consensus problem

We now examine the asymptotic case, *i.e.*, we want the system to asymptotically reach consensus while minimizing the cost functional. The problem is formally stated as follows.

Problem 5.2. *Construct a control law $u(t)$ for the system of agents such that the agents asymptotically reach consensus in the outputs,* i.e.,

$$\lim_{t\to\infty} (y_i(t) - y_j(t)) = 0 \ \textit{ for all } i, j \textit{ such that } i \neq j,$$

while minimizing the following cost functional

$$\int_{t_0}^{\infty} \sum_{i=1}^{N} a_i u_i^T(t) u_i(t) dt \quad (5.18)$$

where $a_i \in \mathbb{R}^+$ for $i = 1, 2, ..., N$.

In order to solve Problem 5.2, we start by defining the matrix

$$P(t) = e^{A^T(T-t)}C^T W(t,T)^{-1} C e^{A(T-t)}$$

which satisfies the following differential Riccati equation

$$\dot{P} = -A^T P - PA + PBB^T P. \tag{5.19}$$

The matrix $P(t)$ is an essential part of the control laws that were presented in the last section, and here we see that this matrix is provided as the solution to a differential matrix Riccati equation. It is well known that (5.19) has a positive semidefinite limit P_0 as $T-t \to \infty$ if (A, B) is stabilizable and A does not have any eigenvalue on the imaginary axis. In order to see this we consider the following problem

$$\begin{aligned} &\min \int_0^\infty \|u\|^2 dt \\ &s.t.\ \dot{x} = Ax + Bu. \end{aligned} \tag{5.20}$$

If (A, B) is stabilizable and A does not have any eigenvalue on the imaginary axis,

$$u = -B^T P_0 x$$

is the optimal control law that solves (5.20), where P_0 is the positive semi-definite solution to

$$-A^T P_0 - P_0 A + P_0 BB^T P_0 = 0.$$

This Algebraic Riccati equation is obtained by letting the left-hand side of (5.19) be equal to zero.

The problem (5.20) is not a consensus problem, and the question is, except for the fact the same matrix P_0 is used in the optimal control law, how it is related to our consensus problem. It turns out that the control law, except for being the solution of the consensus problem, is also the solution of N problems on the form (5.20). In order to show this we introduce

$$x_c = \frac{1}{\sum_{i=1}^N a_i} \sum_{i=1}^N a_i x_i, \text{ and } \delta_i = x_i - x_c.$$

The dynamics of x_c and δ_i are given by

$$\dot{x}_c = Ax_c \quad \text{and} \quad \dot{\delta}_i = A\delta_i + Bu_i.$$

Now each control law $u_i(t)$ contained in the vector

$$u(t) = -L(a) \otimes (B^T P_0)x,$$

can be written as

$$u_i = B^T P_0 \delta_i$$

and u_i solves the problem

$$\begin{aligned} &\min \int_0^\infty \|u\|^2 dt \\ &s.t.\ \dot{x} = A\delta_i + Bu_i. \end{aligned} \tag{5.21}$$

By using K in Lemma 5.2, provided ker(C) is A-invariant, it is possible to express the control law u as follows

$$u = -L(a) \otimes (B^T C^T (CC^T)^{-1} C P_0 C^T (C^T C)^{-1} y. \tag{5.22}$$

Thus, by introducing $G_0 = (CC^T)^{-1} C P_0 C^T (C^T C)^{-1}$, (5.22) can be written as

$$u = -L(a) \otimes (B^T C^T G_0) y.$$

Proposition 5.8. *If A is stabilizable with no eigenvalues on the imaginary axis. Then P_0 exists, is positive semidefinite and the optimal control law that solves Problem 5.2 is*

$$u = -L(a) \otimes (B^T P_0) x.$$

Furthermore, if ker(C) is also A-invariant then

$$u = -L(a) \otimes (B^T C^T G_0) y.$$

When only the output $y_i = Cx_i$ is available for control action, and ker(C) is not necessarily $P - invariant$, an observer can be designed.

$$\dot{\hat{\delta}}_i = (A - BB^T P_0)\hat{\delta}_i - Q\left(\frac{1}{\sum_{i=1}^N a_i}\sum_{j=1}^N a_j(y_i - y_j) - C\hat{\delta}_i\right).$$

Under the assumption that (A, C) is detectable and A does not have any eigenvalue on the imaginary axis we have that

$$\dot{\hat{\delta}} = A\hat{\delta} - BB^T P_0 \hat{x} - Q((y_i - y_c) - C\hat{\delta}),$$

where

$$AQ + QA^T = -QC^T CQ.$$

We summarize our results in this case in the following theorem.

Proposition 5.9. *Suppose (A, B) is stabilizable and (A, C) is detectable, and A has no eigenvalue on the imaginary axis. Then, if the following dynamic output control law is used,*

$$\begin{aligned} u_i &= -B^T P_0 \hat{\delta}_i, \\ \dot{\hat{\delta}}_i &= (A - BB^T P_0)\hat{\delta}_i - Q\left(\frac{1}{\sum_{i=1}^N a_i}\sum_{j=1}^N a_j(y_i - y_j) - C\hat{\delta}_i\right), \end{aligned}$$

the system reaches asymptotic consensus in the outputs.

5.4 Bibliography

[1] W. Ren and Y. Cao. LQR-based optimal linear consensus algorithms *IEEE American Control Conference*, 2009.

[2] D.G. Luenberger. *Optimization by vector space methods*. John Wiley & Sons, Inc., 1997.

[3] F. Xiao and L. Wang. Finite-time consensus problems for networks of dynamic agents. *IEEE Transactions on Automatic Control*, 55(5):950–955, 2010.

[4] C.N. Hadjicostis and S. Sundram. Finite-time distributed consensus in graphs with time-invariant topologies. American Control Conference, 2007.

Chapter 6

A mixed integer linear programming approach to pursuit-evasion problems with optional connectivity constraints

In this chapter we solve the visibility pursuit-evasion problem by using the tools of Mixed Integer Linear Programming (MILP) and Receding Horizon Control (RHC). These tools were applied to UAV path planning in [1], where MILP was used to find detailed trajectories over a short planning horizon. The MILP computations were then iterated in a RHC fashion where each trajectory ended closer to goal than the previous one. The polygonal pursuit-evasion problem is quite different from the UAV problem studied in [1], but share the properties of a complex short term planning step and a long term goal. In the pursuit-evasion problem we let the size of the cleared area be a measure of how far we are from completing the search, and encode the motion of the pursuers and the evolution of the cleared area into a MILP problem that is iteratively solved. The proposed approach is implemented in MATLAB/CPLEX and illustrated by a number of solved examples. To the knowledge of the author, he and Petter Ögren where the first ones to solve the visibility based pursuit-evasion problem, by formulating it as a MILP.

A complete solution to the one-pursuer case was proposed by Guibas et al. [2] where it was also pointed out that the extension of that same approach presented considerable challenges in the multi-pursuer case. The two pursuer case was addressed in [3], but since Guibas et al. also showed that the general problem is indeed NP-hard, solving problems with additional pursuers in reasonable time will be very hard. The concepts of [2] were built upon in [4], where a field of view limitation was incorporated into the problem. The one-pursuer case was successfully treated, but once again, the multi-pursuer case turned out to be computationally intractable. Additional aspects of the problem have also been addressed, such as curved environments [5] and bounded speed evaders [6].

As optimal deterministic strategies with guaranteed capture are hard to find, the option of using randomized strategies was explored in [7]. It was shown that a single pursuer can locate an evader in any simply connected environment with high probability. Randomized approaches such as these are clearly an option for the multi-pursuer problem, but will not be investigated in this thesis. An interesting approach, focusing on the discrete time evolution of the cleared and contaminated parts of the environment was presented in [8].

A problem that is closely related to the visibility based pursuit-evasion problem is the one where the evader and pursuers are constrained to move in a graph. All instances of the former can be more or less conservatively discretized into the latter, [9]. One version of the graph search problem is called graph-clear, and was studied in [10]. In the graph-clear problem, each vertex corresponds to a room, and each edge corresponds to a door. Each vertex and edge furthermore has a number assigned to it, corresponding to how many pursuers are needed to clear the vertex (room), or block the edge (door). The problem is now to deploy pursuers to the edges and vertices in such a way that the whole graph is cleared. It is easy to see that most polygonal environments can be divided into rooms and doors in many different ways. The rooms could either be very small, and trivially clearable by a single pursuer, or quite big, making the room clearing a non-trivial subproblem. The potential drawback of making the rooms very small is that the quality of the solution might be reduced since pursuers can not see from one room to another. Therefore, one could imagine a hierarchical approach with a global graph-clear problem and a polygonal pursuit-evasion problem for each room. The latter can be solved by e.g., the approach presented here, to find how many pursuers are needed to clear each room.

The proposed approach in this chapter can be seen as a lying in between the exact approaches and the graph based ones in the following sense. The visibility properties of the different areas is captured by the MILP in a way that is more conservative than the exact approaches [2, 3], but less conservative than the graph based ones [9].

6.1 Problem formulation

Following Guibas et al. [2], the pursuers and evader are modeled as points moving in the polygonal free space, F. Let $e(\tau)$ denote the position of the evader at time $\tau \geq 0$. It is assumed that $e : [0, \infty) \to F$ is continuous, and the evader is able to move arbitrarily fast. The initial position $e(0)$ and path e is not known to the pursuers. At each time instant, F is partitioned into two subsets, the cleared and the contaminated, where the latter might contain the evader and the former might not. Given N pursuers, let $p_i(\tau) : [0, \infty) \to F$ denote the position of the i:th pursuer, and $P = \{p_1, \dots, p_N\}$ be the *motion strategy* of the whole group of pursuers.

Let $V(q)$ denote the set of all points that are visible from $q \subset F$, i.e., the line segment joining q and any point in $V(q)$ is contained in F.

Problem 6.1 (Pursuit Evasion)**.** *Given an evader, a set of N pursuers and a polygonal free space F, find a solution strategy P such that for every continuos function $e : [0, \infty) \to F$*

there exists a time τ and an i such that $e(\tau) \in V(p_i(\tau))$, i.e., the pursuer will always be seen by some evader, regardless of its path.

It was shown in [2] that computing the minimal number of pursuers needed to solve Problem 6.1 is NP-hard. Hence it is also NP-hard to determine if a solution exists for a given number of pursuers. To find efficient solutions in reasonable time one must thus sacrifice optimality. This can be done by exploring randomized approaches [7], or by relaxing the problem and applying other optimization schemes.

In the following section we will first relax Problem 6.1 by discretizing it, and then apply a combination of Mixed Integer Linear Programming (MILP) and Receding Horizon Control (RHC). These tools have proved to be very useful when addressing other hard path planning problems [1] and we will argue that they are applicable to Problem 6.1 as well.

6.2 Proposed solution

In the proposed solution, we first discretize Problem 6.1 by partitioning the polygonal free space F into a set of *convex* regions, $F = \cup_{i \in J} F_i$, $J = \{1, \ldots, K\}$. The relations between those regions are then described by $M_j \subset J$ and $N_j \subset J$, where M_j is the index set of other regions that are neighbors to F_j, and N_j is the index set of regions that are visible from F_j. Then, a MILP is formulated, capturing what regions are occupied by pursuers at what times, and when the regions are cleared or contaminated over time. By maximizing the cleared area at the end time of the MILP, the continuous pursuer trajectories $p_i(\tau)$ can be constructed from the discrete MILP output.

6.2.1 Discretization of the free space environment

The first step of the discretization of Problem 6.1, i.e., the partitioning $F = \cup_i F_i$, is illustrated in Figure 6.1. As can be seen, all straight obstacle boundaries are extended until they reach another obstacle, or the perimeter of F. From these extended boundaries the partition $F = \cup_i F_i$ is formed.

Lemma 6.1. *In the partition there are at most $O(n^2)$ regions, where n is the number of straight boundaries of the obstacle polygons and the perimeter.*

Proof: In the partitioning, each extended straight obstacle boundary intersects a number of other extended boundaries. There are less than $n(n-1)/2$ such intersections and there are less than n^2 line-segments that form the boundaries of the regions in F. For each such line-segment there are two regions that share the line-segment as part of their boundaries. Thus the number of regions k, satisfy $k \leq 2n^2$. ■

The second step of the discretization of Problem 6.1 deals with the motion, $p_i(\tau)$, of the pursuers. These are now discretized into moving between the regions F_i. A pursuer standing in F_i can in the next, discretized, time instant occupy any region with index in the set $\mathcal{M}_i$, i.e., any neighboring region. This is illustrated in Figure 6.2 (a).

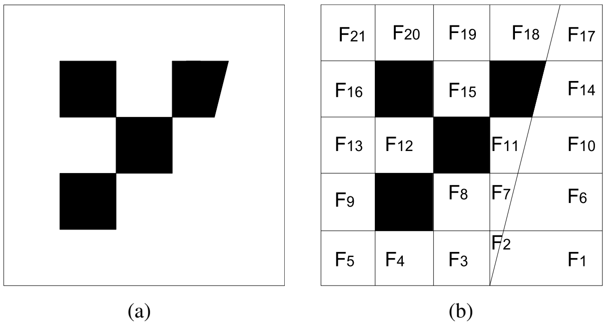

Figure 6.1: An example environment with one irregularly shaped obstacle (a), and the corresponding partition of the free space F into convex polygons $F_1 \ldots F_{21}$ (b).

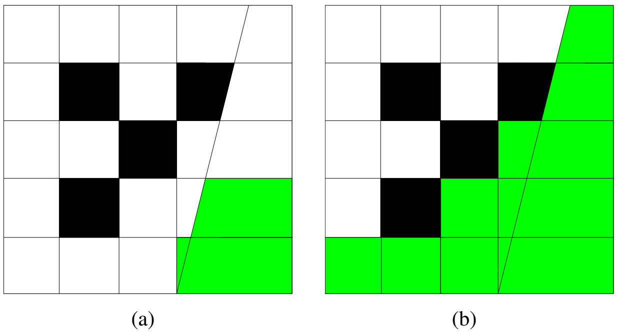

Figure 6.2: The neighborhood that can be moved to, M_1 (a) and the neighborhood that can be seen, N_1 (b), from area F_1, see Figure 6.1.

The third step in discretizing Problem 6.1 involves the visible set $V(\cdot)$. Let $\mathcal{N}_i$ be the index set of regions such that $F_j \subset V(x)$ for all $j \in \mathcal{N}_i$ and all $x \in F_i$. Note that visibility is symmetric, i.e. $j \in \mathcal{N}_i$ implies $i \in N_j$.

Remark 6.1. Note that the discretization of $V(\cdot)$ is conservative, since regions F_j that are partially visible are considered not visible at all. In some approaches, such as [2, 4], this is not the case, but in others, such as the graph search approaches [9], an even more conservative discretization is needed to address open areas.

The final step of discretizing Problem 6.1 is to capture the regions being clear, or contaminated during the search in terms of a MILP.

6.2.2 MILP formulation

As described above, a pursuer located in region i sees the regions with index in the set $\mathcal{N}_i$ and can move to regions with index in the set $\mathcal{M}_i$.

During the search we keep track of where the pursuers are, and which regions are cleared and which are contaminated. In order to do so, we introduce the following binary variables $\lambda_{it}, \sigma_{it}, \theta_{it} \in \{0, 1\}$, where $i \in J$ and $t \in \{1, 2, ..., T\}$. Let $\lambda_{it} = 1$ if and only if a pursuer is *located* in region i at time t. Let furthermore $\sigma_{it} = 1$ if and only if region i is *seen* at time t and $\theta_{it} = 1$ if and only if region i is *cleared but unseen* at time t.

Before formulating the MILP we define four different search-states that each region F_i can be in. Theoretically, there are eight combinations of the three binary variables $\lambda_{it}, \sigma_{it}, \theta_{it}$, but given the meanings we assign to them, only four of those eight combinations are possible, and we denote them S_1, S_2, S_3, S_4. These four states will help us capture the time evolution of the search in the MILP formalism. We differentiate between three different *cleared* states, S_1, S_2, S_3 and one *contaminated* state, S_4.

S_1 The region is seen by a pursuer and contains a pursuer, i.e., $\lambda_{it} = 1,\ \sigma_{it} = 1$ and $\theta_{it} = 0$.

S_2 The region is seen by a pursuer, but does not contain a pursuer, i.e., $\lambda_{it} = 0,\ \sigma_{it} = 1$ and $\theta_{it} = 0$.

S_3 The region is not seen by a pursuer, but can not contain the evader, i.e., $\lambda_{it} = 0,\ \sigma_{it} = 0$ and $\theta_{it} = 1$.

S_4 The region might contain the evader, i.e., $\lambda_{it} = 0,\ \sigma_{it} = 0$ and $\theta_{it} = 0$.

We now state the MILP formulation and then show, in Lemma 6.2, that a feasible solution does indeed correspond to traversable pursuer paths $p_i(\tau)$ and an expanding cleared region $\{i : \theta_{it} = 1\}$. Note that the proof of Lemma 6.2, as a side effect, gives motivations for all the constraints (6.2)-(6.12).

Problem 6.2 (MILP). *Given a $T \in \mathbb{Z}^+$ solve the following integer linear program.*

$$\textit{maximize } Z = \alpha \sum_{i \in J} \theta_{iT} + (1 - \alpha) \sum_{i \in J} \sigma_{iT} \tag{6.1}$$

subject to

$$\textit{State } S_1 \textit{ constraints}:$$

$$\sum_{j\in\mathcal{M}_i} \lambda_{jt} - \lambda_{i(t-1)} \geq 0 \tag{6.2}$$

$$N-(N-1)\lambda_{it} - \sum_{j\in\mathcal{M}_i} \lambda_{jt} \geq 0 \tag{6.3}$$

$$2-\sum_{j\in\mathcal{M}_i} \lambda_{j(t-1)} - \lambda_{it} \geq 0 \tag{6.4}$$

$$2-\sum_{j\in\mathcal{M}_i} \lambda_{jt} \geq 0 \tag{6.5}$$

$$\sum_{i\in J} \lambda_{it} - N = 0 \tag{6.6}$$

$$\textit{State } S_2 \textit{ constraints}:$$

$$\sum_{j\in\mathcal{N}_i} \lambda_{jt} - \sigma_{it} \geq 0, \tag{6.7}$$

$$\sigma_{it} - \lambda_{jt} \geq 0 \quad \forall j \in \mathcal{N}_i \tag{6.8}$$

$$\textit{State } S_3 \textit{ constraints}:$$

$$\sigma_{jt} + \theta_{jt} - \theta_{it} \geq 0, \quad \forall j \in \mathcal{M}_i - \{i\}, \tag{6.9}$$

$$\sigma_{i(t-1)} + \theta_{i(t-1)} - \theta_{it} \geq 0, \tag{6.10}$$

$$1 - \sigma_{it} - \theta_{it} \geq 0, \tag{6.11}$$

$$\theta_{i1} = 0, \tag{6.12}$$

where $\alpha \in [0,1]$, $i \in J$ *and* $t \in \{2,3,...,T\}$ *in* (6.2), (6.4) *and* (6.10) *and* $t \in \{1,2,...,T\}$ *in the other constraints.*

Note that $\alpha = 1$ corresponds to maximizing the cleared but unseen region (S_3), $\alpha = 0$ corresponds to maximizing the visible region (S_1 or S_2), while $\alpha = 0.5$ corresponds to maximizing the cleared region (S_1, S_2 or S_3) at the final time T. In Section 6.6 below we will see that $\alpha = 1$ is actually the best measure of progress for the clearing task. Note also that constraint (6.6) imply that pursuers never occupy the same region. This restriction is somewhat conservative, as it is not present in Problem 6.1.

Lemma 6.2. *A feasible solution to Problem 6.2 can be used to generate pursuer paths* $p_i(\tau), \tau \in [0,T']$, $i \in \{1,...,N\}$, *guaranteeing the following. If* $e(\tau) \notin V(p_i(\tau))$ *for all* i *and* $\tau \in [0,T']$, *then* $e(T') \in F_i$ *such that* F_i *is in state* S_4 *at discrete time T, i.e., if the evader has not been seen up till time* T', *then it must be in the contaminated area. Above,* T' *is the continuous final time corresponding to the discrete final time* T.

Proof: We first prove that N valid pursuer paths can be generated from a feasible solution. In (6.6) it is guaranteed that there are exactly N pursuers at each time t. In (6.2) it is guaranteed that there must must be a pursuer in the move neighbourhood of region i at time $t+1$ if there is a pursuer at the region i at time t. Constraints (6.3), (6.4) and (6.5) together guarantee that a pursuer move between adjacent regions in consecutive time steps. Now, pursuer paths $p_i(\tau)$ can be created from λ_{it} where all pursuers cross borders between the F_i at the same time. Finally, a mapping between continuous time τ and discrete time t can be created to accommodate the pursuer velocity bounds.

To see that the right regions are denoted as seen, $\sigma_{it} = 1$, we note that in (6.7) and (6.8) the variable σ_{it} is set to 1 if and only if there is a $j \in \mathcal{N}_i$ such that $\lambda_{jt} = 1$.

To see that the cleared area, $\theta_{it} = 1$, evolves correctly note the following. In (6.9) it is verified that the region i cannot be in state S_3 at time t if any of the $\mathcal{M}_i$-neighbours are in state S_4, and in (6.10) it is verified that the region i cannot be in state S_3 at time t if it was in state S_4 at time $t-1$. In (6.11) it is verified that region i cannot be in state S_3 if it is in state S_1 or state S_2 at time t and (6.12) verifies that that no region is in state S_3 when the search starts.

To conclude we note that evader $e(\tau)$ can not start in the cleared area S_3 and that the cleared area is always separated from the contaminated S_4 by seen or occupied areas S_1, S_2. Thus, if it is not seen, it must be in the contaminated area. ■

Lemma 6.3. *A feasible solution strategy P to Problem 6.2 with N pursuers ending with an empty contaminated area, i.e.,*

$$\sum_{i \in J} (\sigma_{iT} + \theta_{iT}) = |J|, \tag{6.13}$$

is a solution to Problem 6.1.

Proof: A straightforward application of Lemma 6.2 above. ■

Remark 6.2 (Backwards). Given a solution strategy P of Problem 6.1, a new solution can be created by running the pursuer trajectories $p_i(\tau)$ backwards. To see this note that the cleared unseen area (S_3) is always separated from the contaminated area (S_4), and we start with an empty cleared unseen area and finish with an empty contaminated area. Running the trajectories backwards would thus result in exchanging the labels cleared unseen and contaminated, i.e. switching states S_3 and S_4.

Remark 6.3 (Number of pursuers). In the proposed MILP formulation, the number of variables or the number of constraints will not increase with the number of pursuers, *i.e.*, the size of the problem does not grow with the number of pursuers. However, the number of constraints does grow linearly with the number of regions.

6.3 Reducing the computation times using RHC and relaxation

In this section we will describe how the computation times for solving Problem 6.1 can be reduced using RHC and by relaxing some of the integer constraints in the MILP.

6.3.1 An RHC solution to the pursuit-evasion problem

Depending on the problem size, large time horizons T might be needed to find a solution to Problem 6.2 with empty contaminated area. Large time horizons T often result in long computation times. A classical way to balance performance with computational resources is RHC, where an optimization problem over a shorter time horizon is iteratively solved instead of solving it once and for all over a longer time horizon. In our setting the RHC concept might be implemented as follows.

Algorithm 6.1.

1. *Solve the MILP with* $\alpha = 1$ *or* $\alpha = 0.5$ *and some given horizon length* T.
2. *If the final states* σ_{iT} *and* θ_{iT} *satisfies*

$$\sum_{i \in J} (\sigma_{iT} + \theta_{iT}) = |J|, \tag{6.14}$$

   the whole area is cleared, and the algorithm terminates.

3. *Else, if there was no increase in* $\sum_{i \in J} (\sigma_{iT} + \theta_{iT})$ *increase either the horizon length* T *or the number of pursuers* N.
4. *Prepare a new RHC iteration by removing constraint* (6.12) *and adding constraints setting the initial states of the next iteration* $\theta_{i1}, \lambda_{i1}, \sigma_{i1}$ *equal to the terminal states* $\theta_{iT}, \lambda_{iT}, \sigma_{iT}$ *of the current iteration.*
5. *Goto 1.*

Remark 6.4. In step (3) of Algorithm 6.1, the choice depends on the situation at hand. If pursuers are scarce, the horizon length is increased. If, on the other hand, computational time is critical, the number of pursuers is increased. If none of the above solves the problem, decompositioning, as described in Algorithm 6.2, can be used.

Lemma 6.4. *If Algorithm 6.1 terminates, a solution to Problem 6.1 is found.*

Proof: A straightforward application of Lemma 6.3 above. ■

6.3.2 Relaxation of the MILP problem

To increase the computational efficiency when solving Problem 6.2 we note that some of the integer constraints can be relaxed.

Problem 6.3 (Relaxation)**.** *The variables* σ_{it} *and* θ_{it} *in Problem 6.2 are relaxed such that they are no longer binary variables but belong to* $[0, 1]$, i.e

$$0 \leq \sigma_{it} \leq 1, \tag{6.15}$$

$$0 \leq \theta_{it} \leq 1. \tag{6.16}$$

Using CPLEX 10.2, Problem 6.3 is as much as 20 times faster than the original formulation in some scenarios.

Lemma 6.5. *The pursuer paths λ_{it} in the solution to Problem 6.3 are also pursuer paths in an optimal solution to Problem 6.2.*

Proof: Note that if there is a j such that $\lambda_{jt} = 1$, $j \in \mathcal{N}_i$ then $\sigma_{it} = 1$ by (6.8), also if $\lambda_{jt} = 0, \forall j \in \mathcal{N}_i$ then $\sigma_{it} = 0$ by (6.7), thus σ_{it} is binary. Now let (λ, σ, θ^b) be a solution to to Problem 6.2 in which only θ^b differs from the solution of problem 6.3. Let Z_2 and Z_3 be the cost of the solutions to Problem 6.2 and 6.3 respectively. From (6.9), (6.10) and (6.11) we get that that for each $\theta_{it} \in (0, 1]$, $\theta^b_{it} = 1$. This implies that $Z_3 \leq Z_2$, but since problem 6.3 is a relaxation of problem 6.2 this implies that $Z_2 \leq Z_3$. Thus $Z_2 = Z_3$. ■

6.4 Decomposition of large environments

One way of reducing the complexity of large problem instances is to use a hierarchical decomposition with a graph-clear problem at the top and instances of Problem 6.1 at the lower level. Another option is to decrease the problem size and complexity by placing stationary pursuers at positions where they cover large areas, and then solve instances of Problem 6.1 in the remaining unseen parts of F. This approach is described below.

Algorithm 6.2.

1. *Solve the MILP with k pursuers and one time step with $\alpha = 0$. This corresponds to maximizing the number of seen regions by k pursuers, i.e., solving an Art Gallery Problem [11].*
2. *Remove all regions that are in state S_1 or S_2 from F, leaving a possibly disconnected F.*
3. *Apply Algorithm 6.1 to each connected component of F and let q be the maximal number of pursuers needed.*
4. *The number of pursuers needed to clear the original F is now $k + q$.*

What we mean by *connected component* in Algorithm 6.2 is that it is possible to go between neighboring regions between two regions that are in state S_3 or S_4 without entering a region that is in state S_1 or S_2.

6.5 Connectivity constrained search

An area receiving an increasing amount of interest is communication aware motion planning, [12, 13]. In this section we will show how the proposed MILP framework can be extended to handle one such problem, namely the problem where the whole group of pursuers shall be connected in a line-of-sight graph at a given time instant t'. We will present two sets of constraints. The first set corresponds to a general line-of-sight graph, while the second set corresponds to a special case, a star shaped line-of-sight graph, where one of the pursuers sees all others.

For the general case we extend Problem 6.2 with a set of binary variables u_{ij}, where $i \in J$ and $j \in \{1, 2, ..., N\} = J_P$, and the following constraints

$$\lambda_{it'} - u_{ij} \geq 0, \quad \forall i \in J, \quad j \in J_P, \tag{6.17}$$

$$\sum_{j \in J_p} u_{ij} \leq 1, \quad \forall i \in J, \tag{6.18}$$

$$\sum_{i \in J} u_{ij} = 1, \quad \forall j \in J_P, \tag{6.19}$$

$$\sum_{l=1}^{j-1} \sum_{k \in \mathcal{N}_i} u_{kl} - u_{ij} \geq 0, \quad \forall i \in J,\ j \in J_P - \{1\}. \tag{6.20}$$

Equation (6.17) states that u_{ij} can be equal to 1 only if $\lambda_{it'}$ is equal to 1. Equations (6.18) and (6.19) together guarantee that there is one and only one unique $u_{ij} = 1$ for each $\lambda_{it'} = 1$. Equation (6.20) states that u_{ij} where $i \in J$ and $j \in \{2, 3, ..., N\}$ can only be equal to 1 if there is at least one one pair (k, l), where $k \in \mathcal{N}_i$ and $l \in \{1, 2, ..., j-1\}$, such that $u_{k,l} = 1$. Given equations (6.17)-(6.19), equation (6.20) guarantees the existence of a line-of-sight graph.

Remark 6.5. If these constraints are used at all time steps, the entire search is performed with the group of pursuers connected in a line-of-sight graph.

An alternative to the general case above, is the problem of creating a line-of-sight graph where one single vertex is connected to all others. This results in a smaller set of binary variables u_i. The topology of the connected visibility graph is defined by the first constraints below, whereas the last constraint, with the sum of all u_j:s, implies that there must exist such a graph.

$$\lambda_{it'} + \sum_{j \in \mathcal{N}_i} \lambda_{jt'} - (N+1)u_i \geq 0, \quad i \in J \tag{6.21}$$

$$\sum_{j \in J} u_j \geq 1. \tag{6.22}$$

Both of these sets of constraints will result in a connected graph independently of the number of pursuers.

6.6 Simulation examples

When running Algorithm 6.1, it turns out that the best results are found using $\alpha = 1$. A drawback of the more intuitive $\alpha = 1/2$ is that the pursuers might get stuck at positions

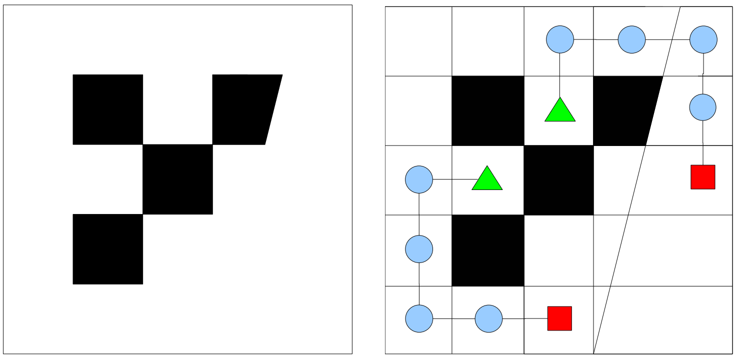

(a) (b)

Figure 6.3: The results of running Algorithm 6.1 with a six step planning horizon (b) in the environment in (a). A green triangle denotes the start of a pursuer path, and a red square denotes the end of a pursuer path, blue discs denote intermediate steps.

where they see a large area, *e.g.*, looking down a corridor, but any motion results in a reduction of this area. Thus we use $\alpha = 1$ in all but one of the examples below. The simulations were done on a Intel Xeon CPU X5450, 3.00GHz, running the MILP software CPLEX 10.2 [14]. Furthermore, all results were found using the relaxed version, Problem 6.3, as it was found to be on average twice as fast as the non-relaxed formulation. Finally, we note that the proposed approach is not directly suitable for very large problems. Such problems can be decomposed into smaller ones, either by applying Algorithm 6.2 or using a graph-clear formulation. The performance and limitations of the approach can be seen from the examples below.

The first problem instance is depicted in Figure 6.3(a) with the corresponding solution in Figure 6.3(b). With a time horizon of $T = 6$, and $\alpha = 1/2$, a single RHC iteration was needed, and found in four seconds.

The second problem instance is shown in Figure 6.4, with corresponding solution in Figure 6.5 (a-c). The problem was first solved in 3 RHC iterations using a total number 10 time steps. The computational time was about 3 seconds for each iteration resulting in a computational time of 9 seconds in total. Note that the first two RHC iterations achieved progress with $T = 3$, while the third iteration needed $T = 4$ to remove the last S_4 region. Figure 6.5 (d) shows the result of the alternative failed iteration with three time steps. This problem was also solved in a single iteration using a time horizon of $T = 6$, with a corresponding computation time of 110 seconds, see Figure 6.6(a).

The third problem instance is shown in Figure 6.6(b) with corresponding solution in Figure 6.7. The solution involves three RHC iterations with 2 pursuers, followed by one iteration with three pursuers. The computational time was about 5 seconds for the three first iterations and 15 seconds for the last iteration. In order to find a two-pursuer solution we

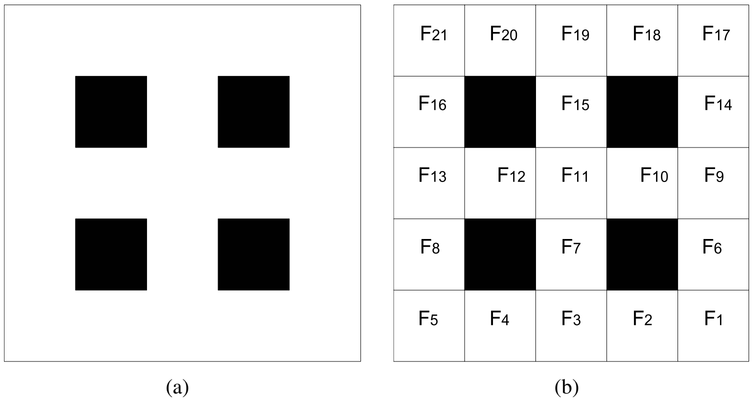

Figure 6.4: The partition (b) of a Manhattan grid with four obstacles (a).

run the algorithm with 2 pursuers and 10 time steps in the first iteration, after 45 minutes, the algorithm had not finished.

The solution of the fourth problem is shown in Figure 6.8. The environment is the same as the third problem, but the solution is found using decomposition, i.e., Algorithm 2, as presented in Section 6.4. Step 1 of the algorithm was solved in two seconds with $k = 1$, *i.e.* one stationary pursuer was used. The position of this pursuer is shown in Figure 6.8 (a). The search of the remaining unseen parts of F, in this case five disconnected regions, took two seconds each and is shown in Figure 6.8 (b). Thus the problem was solved in a total of twelve seconds, using 2 pursuers.

The fifth problem illustrates the connectivity constraints. The Manhattan grid in Figure 6.4 was solved with the algorithm in two iterations with 4 and 5 time steps respectively, see Figure 6.9. The additional connectivity constraints (6.21) and (6.22) were active at the final time of each iteration. In the figure one can see that the two pursuers are indeed connected by a fee line of sight at the final time of each iteration.

The sixth problem is a single pursuer problem, where a problem is solved that requires so-called recontamination, Figure 6.11. The problem is taken from [2], where it was shown that some problems require a linear (in edges) number of recontaminations, i.e., some areas need to change back and forth between being contaminated and cleared a number of times, before finally being cleared. In this problem, the recontaminated area is at the very top, and the recontamination is shown in Figure 6.11(b).

In the seventh problem, we want to illustrate how the computational time grows with the problem size. In Figure 6.10 we have a subset of one of the scenarios in the classic arcade game Pac-Man. We run Algorithm 1 with $\alpha = 1$ and time horizon $T = 3$ on four different sub-regions of the Pac-Man scenario. In Figure 6.10 the four regions are defined as follows. Region 1 is defined as A. Region 2 is defined as the union of A and B. Region 3 is defined as the union of A, B and C and region 4 is defined as the union of the regions

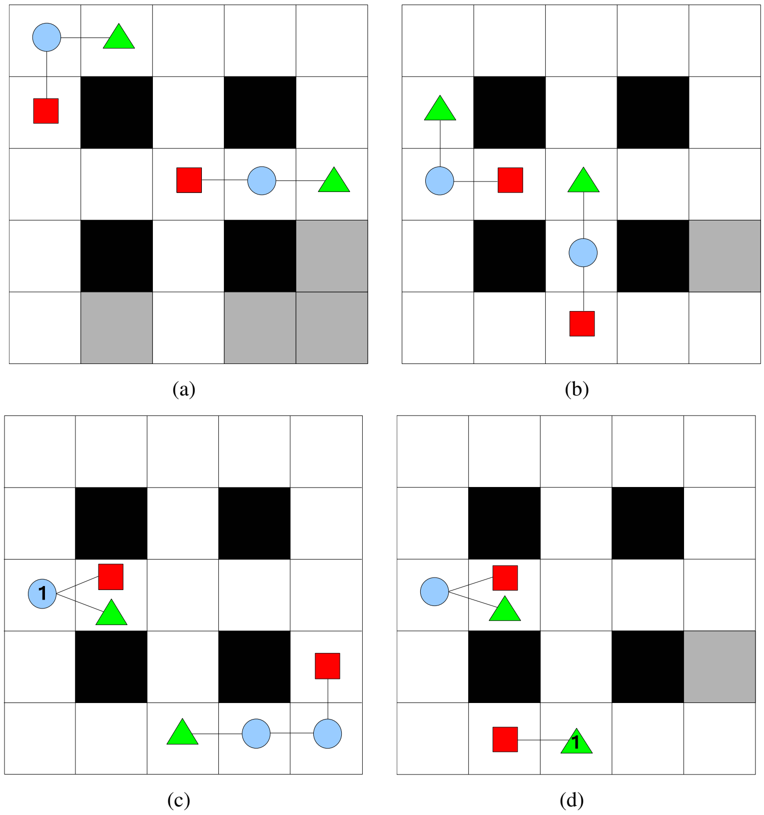

Figure 6.5: The results of running Algorithm 6.1 on a Manhattan grid with four obstacles. The search problem is solved with two pursuers in three iterations where the results of iteration 1, 2 and 3 are shown in (a), (b) and (c) respectively. Note that four time steps were necessary in iteration 3, the result of the third iteration with three time steps is shown in (d). White regions are in states S_1, S_2 or S_3, whereas grey regions are in state S_4. A green triangle denotes the start of a pursuer path, and a red square denotes the stop of a pursuer path, blue discs denote intermediate steps. A number i inside a triangle, disc or square indicates that the pursuer waits an additional i time steps in the region.

A, B, C and D.

The computational times for different amount of pursuers are shown for each scenario in Table 6.1. In this table the computational time of running Algorithm 1 with $\alpha = 1$ and time horizon $T = 3$ is shown as a function of the number of pursuers and the Region. The computational time is measured in seconds. Each element in the leftmost column constitute

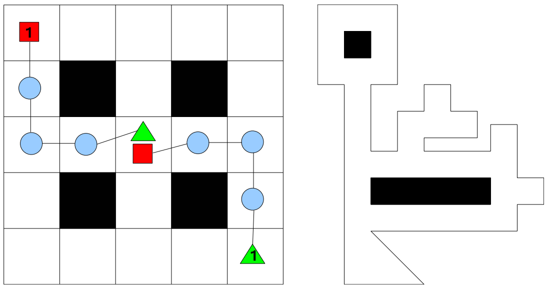

Figure 6.6: (a) The solution when running Algorithm 6.1 on the environment in Figure 6.4 with two pursuers for six time steps. The color coding of the regions are as in Figure 6.5. (b) A complex environment with fewer loops.

	Region 1	Region 2	Region 3	Region 4
2	0	7	timeout	timeout
3	0	26	timeout	timeout
4	0	0	timeout	timeout
5	0	8	timeout	timeout
6	0	0	timeout	timeout
7	0	13	timeout	timeout
8	0	0	timeout	timeout
9	0	13	timeout	timeout
10	0	1	21	timeout
11	infeasible	0	2	timeout
12	infeasible	0	39	timeout
13	infeasible	72	38	0
14	infeasible	0	0	18
15	infeasible	infeasible	0	10

Table 6.1

the number of pursuers, where this number goes between 2 and 15. The elements in the top row denote the regions 1-4. If a cell contains the words infeasible or timeout, this indicates that the it was not possible to find feasible initial positions and that the computational time exceeded 1700s. If the computational time exceeded 1700s, the execution was aborted, and this is denoted as ”timeout”. If it was not possible to find initial positions for the pursuers, this is denoted as ”infeasible”. One can observe that the computational time in general decreases with the number of pursuers.

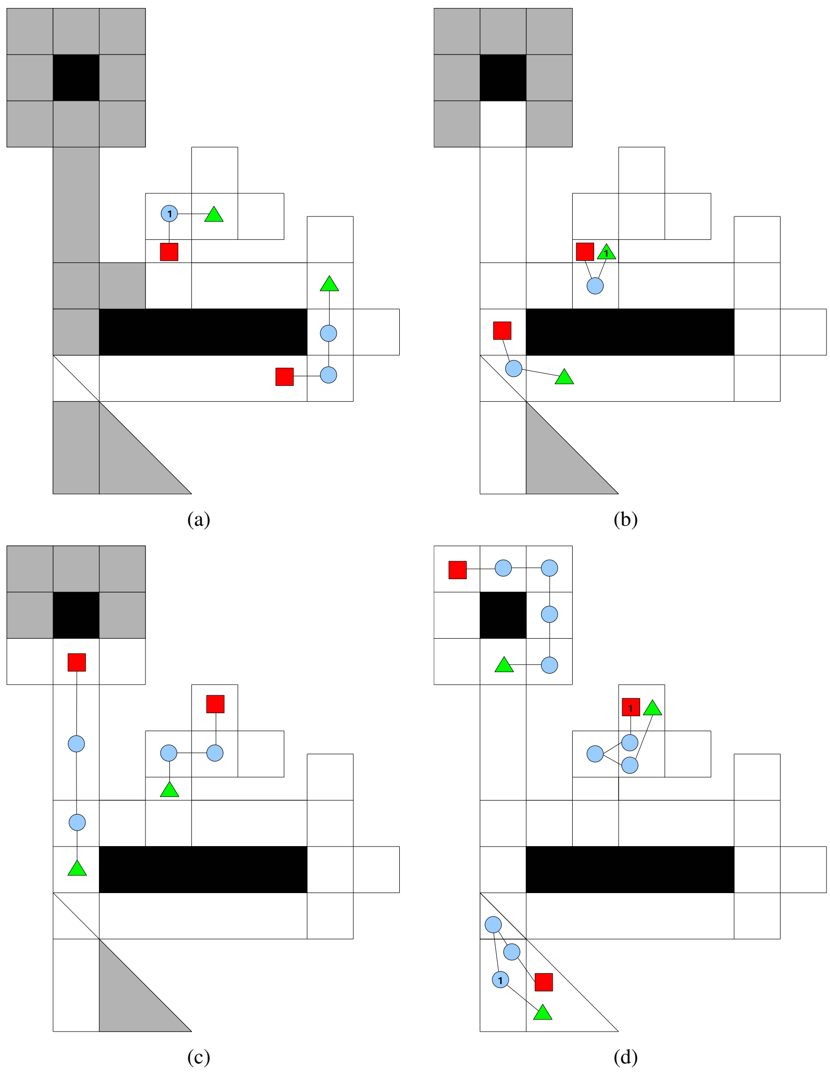

Figure 6.7: The results of running Algorithm 6.1 on the environment in Figure 6.6(b). The search problem is solved with three pursuers in four iterations where the results of iteration 1, 2, 3 and 4 are shown in (a), (b), (c) and (d) respectively. After iteration 3, no improvement is achieved with 2 pursuers, thus one more pursuer is added in iteration 4. The number of time steps was also increased. The color coding of the regions are the same as in Figure 6.5.

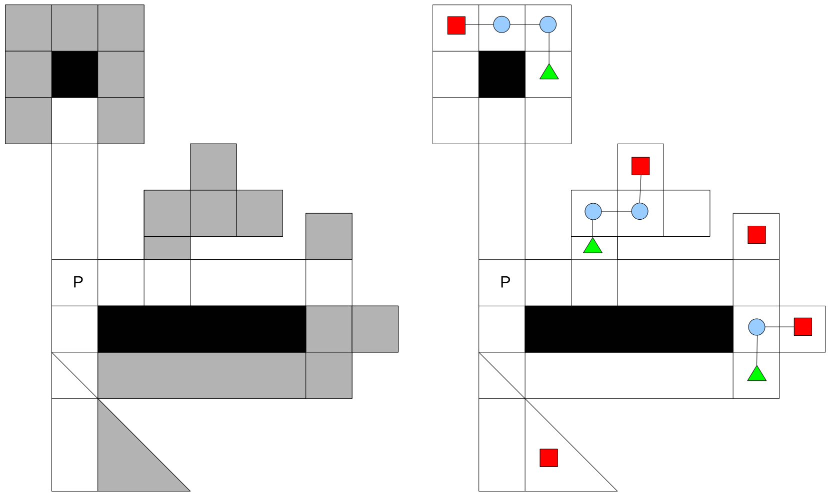

(a) (b)

Figure 6.8: The results or running Algorithm 6.2 with two pursuers on the environment in Figure 6.6(b). In step 1, we use $k = 1$, i.e., one pursuer is used to cover as much of the area as possible, and the resulting position is shown in (a) denoted by P. Then the remaining five connected components of F are searched one after the other with one pursuer, (b). The color coding of the regions are as in Figure 6.5.

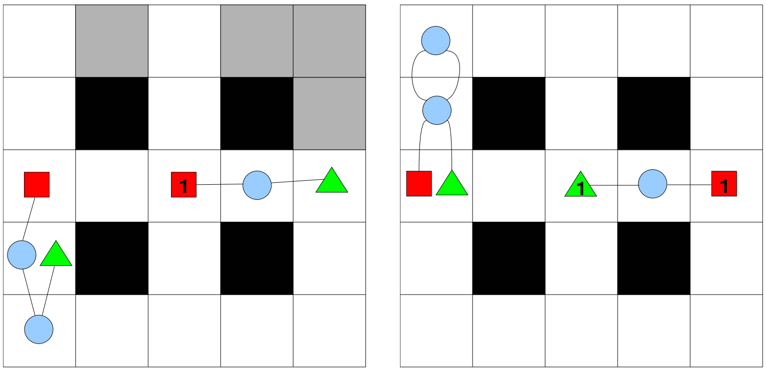

(a) (b)

Figure 6.9: The result of running Algorithm 6.1 on the Manhattan grid with the additional connectivity constraints (6.21) and (6.22) active at the final time of each iteration. The problem was solved in two iterations using 4 and 5 time steps respectively, and one can verify that the pursuers can see each other at the final time of each iteration.

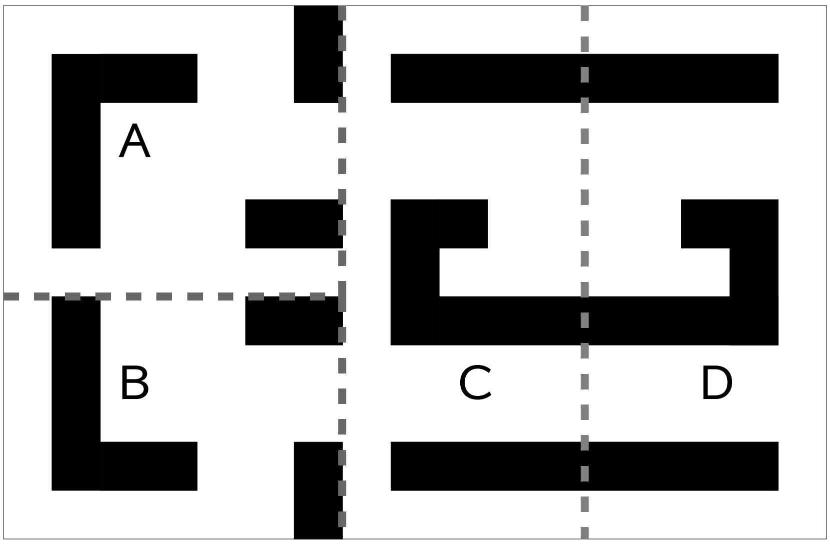

Figure 6.10: In this figure four different regions are defined; A, B, C and D.

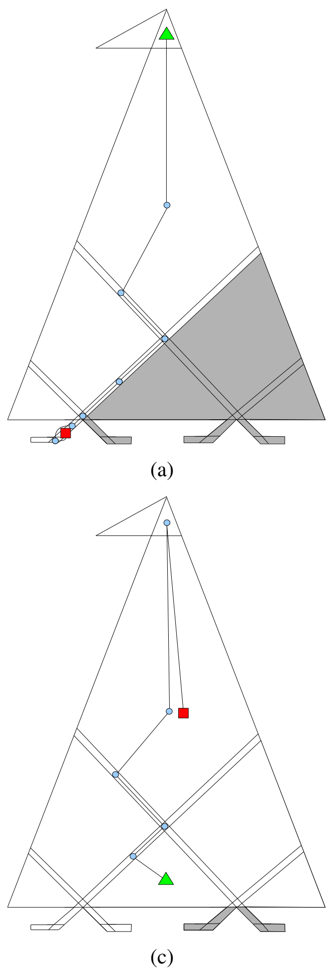

Figure 6.11: The results of running Algorithm 6.1 on a problem requiring recontamination. Note that the upper part of the area is first cleared, then contaminated and finally cleared once again, and that recontamination is necessary when clearing the whole area with one pursuer.

6.7 Bibliography

[1] B. Mettler and E. Bachelder. Combining on-and offline optimization techniques for efficient autonomous vehicle's trajectory planning. In *Proc. of the AIAA Guidance, Navigation, and Control Conference and Exhibit, San Francisco, CA, USA*, 2005.

[2] L.J. Guibas, J.C. Latombe, S.M. LaValle, D. Lin and R. Motwani. A visibility-based pursuit-evasion problem. *International Journal of Computational Geometry and Applications*, 1999.

[3] B.H. Simov, G. Slutzki and S.M. LaValle. Clearing a polygon with two 1-searchers. *International Journal of Computational Geometry and Applications*, 19(1):59–92, 2009.

[4] B.P. Gerkey, S. Thrun and G. Gordon. Visibility-based pursuit-evasion with limited field of view. *The International Journal of Robotics Research*, 25(4):299, 2006.

[5] S.M. LaValle and J.E. Hinrichsen. Visibility-based pursuit-evasion: The case of curved environments. *Robotics and Automation, IEEE Transactions on*, 17(2):196–202, 2002.

[6] B. Tovar and S. LaValle. Visibility-based pursuit-evasion with bounded speed. *Algorithmic Foundation of Robotics VII*, pages 475–489, 2008.

[7] V. Isler, S. Kannan and S. Khanna. Randomized pursuit-evasion in a polygonal environment. *IEEE Transactions on Robotics*, 21(5):875–884, 2005.

[8] J. Yu and S.M. LaValle. Tracking hidden agents through shadow information spaces. In *Robotics and Automation, 2008. ICRA 2008. IEEE International Conference on*, pages 2331–2338. IEEE, 2008.

[9] G. Hollinger, S. Singh and A. Kehagias. Improving the efficiency of clearing with multi-agent teams. *International Journal of Robotics Research*, 29(8):1088–1105, 2010.

[10] A. Kolling and S. Carpin. The GRAPH-CLEAR problem: definition, theoretical properties and its connections to multirobot aided surveillance. In *Proceedings of the IEEE/RSJ International Conference on Intelligent Robots and Systems*, pages 1003–1008, 2007.

[11] J. Urrutia. Art gallery and illumination problems. *Handbook of Computational Geometry*, pages 973–1027, 2000.

[12] D.A. Anisi, P. Ögren and X. Hu. Cooperative minimum time surveillance with multiple ground vehicles. *IEEE Transactions on Automatic Control*, To appear.

[13] M. Lindhe and K.H. Johansson. Communication-aware trajectory tracking. In *IEEE International Conference on Robotics and Automation, ICRA*, pages 1519–1524, 2008.

[14] *ILOG CPLEX 10.0 User's Manual*. 2006.